Equilibrium and Transport Properties of the Noble Gases and Their Mixtures at Low Density

J. Kestin, K. Knierim, E. A. Mason, B. Najafi, S. T. Ro, and M. Waldman

Division of Engineering, Brown University, Providence, Rhode Island 02912

The report contains a set of easy-to-program expressions for the calculation of the thermodynamic and transport properties of the five noble gases (He, Ne, Ar, Kr, Xe) and of the 26 binary and multicomponent mixtures that can be formed with them. The properties in question are second virial coefficient B, viscosity η, thermal conductivity λ, self-diffusion and binary diffusion coefficient D, and thermal diffusion factor α_T. The calculation of properties is restricted to low densities ($\rho \ll B/C$) but covers the full range of compositions and a temperature interval extending from absolute zero to the onset of ionization. Owing to the careful theoretical basis on which the algorithm has been erected, all properties are thermodynamically consistent with each other. Reference to a selected set of critically evaluated measurements provides a basis for the estimation of uncertainties. The report contains 54 abbreviated tables of numerical data and 86 deviation plots. It is asserted that the results are comparable to the best measurements that could be performed at present.

Key words: argon; corresponding states; helium; krypton; mixtures, noble gases; neon; noble gases, equilibrium properties; noble gases, mixtures; noble gases, transport properties; xenon.

Contents

List of Tables of Numerical Outputs

List of Deviation Plots

List of Symbols

A^*	ratio of collision integrals, Eq. (C2)
B	second virial coefficient
B^*	reduced second virial coefficient, Eq. (C11); ratio of collision integrals, Eq. (C5)
B_l^*	reduced second virial coefficient in Wigner–Kirkwood expansion, Eq. (15), $l = 0,1,...$
B^*_{perfect}	reduced second virial coefficient of perfect-gas contribution, Eq. (16)
C	third virial coefficient
C^*	ratio of collision integrals, Eq. (C4)
C_6	long-range dispersion coefficient
C_6^*	low-temperature scaling parameter, Eq. (12)
C_p°	ideal-gas specific heat at constant pressure
C_v°	ideal-gas specific heat at constant volume
D	binary or self-diffusion coefficient
E^*	ratio of collision integrals, Eq. (C3)
F^*	ratio of collision integrals, Eq. (C7)
f_D	higher order correction factor for self-diffusion coefficient, Eq. (C9)
f_η	higher order correction factor for viscosity, Eq. (C8)
f_λ	higher order correction factor for thermal conductivity, Eq. (C10)
h	Planck constant
k	Boltzmann constant
M	atomic weight
m	mass of an atom
N_A	Avogadro constant
P	pressure
R	universal gas constant
r	atom separation in pair potential
s	nuclear spin
T	temperature
T^*	reduced temperature, Eq. (5)
V	intermolecular force potential
V_o	short-range energy parameter, Eq. (13)
V_o^*	high-temperature scaling parameter, Eq. (14a)
x	mole fraction
α_0	isotopic thermal diffusion factor, Eq. (17)
α_R	reduced thermal diffusion factor, Eq. (C23a)
α_T	thermal diffusion factor
Δ	higher order correction factor for binary diffusion coefficient, Eq. (C22a)
δ	tolerance limit of density, Eq. (3b)
ϵ	energy scaling parameter
η	viscosity
κ_o	higher order correction for isotopic thermal diffusion factor, Eq. (C15a)
κ_2	higher order correction for thermal diffusion factor, Eq. (C23)
Λ^*	reduced de Broglie wavelength, Eq. (9)
λ	thermal conductivity
ρ	density; short-range length parameter, Eq. (13)
ρ^*	high-temperature scaling parameter, Eq. (14b)
σ	length scaling parameter
$\Omega^{(l,s)^*}$	reduced collision integral

1. Introduction

It is not often that correlators succeed in producing a thermodynamically consistent representation of the equilibrium as well as of the transport properties of a system. The low-density properties of the noble gases (He, Ne, Ar, Kr, Xe) and of the 26 different mixtures that can be formed with them constitute a rare exception. This is due to the fact that we are in possession of a secure theoretical basis in Boltzmann's equation and in its solution derived by the independent work of Sydney Chapman and David Enskog, since clarified, amplified, and extended by a number of successor investigators. These results supplied a firm foundation for the extended law of corresponding states due to J. Kestin, S. T. Ro, and W. A. Wakeham,[1] later modified and improved by B. Najafi, E. A. Mason, and J. Kestin.[2] In addition to these theoretical results, there existed a very large body of direct and indirect measurements of the equilibrium and transport properties of the systems under consideration, even though they covered but a small fraction of the desired range of compositions and temperatures. Nevertheless, it was possible to create a complete synthesis which is made use of in this report.

The purpose of this report is to provide a comprehensive and thermodynamically consistent synthesis and tabulation of the low-density equilibrium and transport properties of all systems that can be formed with the five noble gases: He, Ne, Ar, Kr, Xe. The set of systems consists of five pure components, ten binary mixtures, ten ternary mixtures, five quaternary mixtures, and one five-component mixture, or a total of 31.

The correlations which result from the synthesis are restricted to low densities, i.e., to regimes in which properties are determined by binary collisions. In these circumstances, all properties of interest are functions of temperature only, apart from composition. The synthesis is valid over the whole temperature span, stretching from absolute zero to the onset of ionization.

The report contains easy-to-program expressions for the various integrals of 15 pair potentials which govern the low-density properties (B, η, λ, D, α_T) of our 31 systems as functions of temperature and composition. Each pair potential is characterized by five material constants which have been accurately determined by a complex numerical fit to a selected body of experimental data with a considerable additional input from theory, mainly of quantum-mechanical character. Thus, all properties can be calculated over the whole range of temperatures from absolute zero to the onset of ionization and over the complete composition range of any one of the binary and multicomponent mixtures. Such a calculation goes a long way beyond the ranges covered by direct measurements, but the secure theoretical foundation on which the correlation is based makes such an extrapolation both possible and reliable. The authors venture the statement that the results of the calculations on the basis of the algorithm presented in this report are comparable to the best measurements that could be performed with the aid of present-day techniques.

Even though definite forms of the pair potentials are implied in this work, the task of retrieving them from the collision integrals has not been undertaken.

The report contains 54 abbreviated tables of properties and a bibliography of 112 selected entries, in addition to 32 literature references and 86 deviation plots.

The algorithm presented in this report is intended as a contribution to the work of the Subcommittee on Transport Properties of Commission I.2 (Thermodynamics) of the International Union of Pure and Applied Chemistry.

Thermodynamic consistency is safeguarded by the fact that all formulas are based on the exact solutions of the Boltzmann equation by the Chapman–Enskog method.[3–6] The extension to include transport properties of multicomponent mixtures was first derived by J. O. Hirschfelder, C. F. Curtiss, and C. Muckenfuss[7,8] (see also Refs. 3–6). Furthermore, all functionals of intermolecular pair potentials, i.e., the integral for the second virial coefficient B and for the collision integrals $\Omega^{(l,s)*}$, satisfy the recursion relations imposed on them by theory.

The report contains a brief explanation of the methods used, a listing of all optimized constants which characterize the binary collisions, as well as a listing of the relevant formulas. In view of the ease of programing, we included only a limited number of tables. Even so, there are 54 of them, because of the very large number of systems, and hence data, covered by this correlation. The tables employ the SI system of units throughout. Temperatures below the ice point are given in Kelvins (K), and those above it in degrees Celsius (°C).

The properties listed are

second virial coefficient	B (m³/kmol)
viscosity	η (μPa s)
thermal conductivity	λ (mW/m K)
diffusion or self-diffusion coefficient	D (m²/s)
thermal diffusion factor	α_T.

Quantum corrections were introduced for the second virial coefficients of all systems. Quantum corrections for the transport properties are less important, and were introduced only for ^{3}He, ^{4}He, and their mixtures in the cryogenic range 0–100 K.

In order to calculate all equilibrium properties of the systems listed here, it suffices to know only the second virial coefficient $B(T)$ and to recall that all noble gases have constant specific heats

$$C_p^\circ = \tfrac{5}{2}R \quad \text{and} \quad C_v^\circ = \tfrac{3}{2}R. \tag{1}$$

The universal gas constant $R = 8.314\,41$ kJ/kmol K. In the range determined by binary collisions, the equation of state is

$$P = \rho RT\{1 + B(T)\rho\}, \tag{2}$$

which is valid for densities for which

$$\rho \ll B/C, \tag{3a}$$

or more precisely, for which

$$\left|1 - \frac{B}{C\rho}\right| = \delta; \tag{3b}$$

here δ is the required fractional accuracy in ρ, and C is the third virial coefficient.

The combination of Eqs. (1) and (2) is equivalent to a fundamental equation[9] from which all thermodynamic properties can be derived directly. The transport properties are calculated with the aid of the appropriate equations using the same atomic constants. Consequently, consistency with equilibrium properties is automatically guaranteed.

2. Two-Parameter Principle of Corresponding States

The numerical data in the tables of this report and the correlations are based on an extended principle of corresponding states, and specifically do not make use of a parametrized form of the pair potential (e.g., Lennard-Jones n-6, etc.). The adoption of such a potential is replaced by the hypothesis that the 15 pair potentials can be made congruent by a judicious choice of scaling parameters. In the first approximation, employed in Ref. 1, it was assumed that two such scaling parameters are adequate to secure congruence. These were selected as a length scaling factor σ (which may be chosen as the distance of zero energy), and an energy scaling factor ϵ (which may correspond to the energy minimum). The latter is usually expressed in the form of a reference temperature ϵ/k, where k is Boltzmann's constant.

The preceding hypothesis is translated into the statement that all pair potentials, being centrally symmetric, must be of the form

$$V(r) = \epsilon\, \mathrm{f}(r/\sigma), \tag{4}$$

in which f is a universal function. These statements have as their immediate consequence the assertion that all properties of the respective gases can be uniquely reduced to a dimensionless form, and that they depend on the single reduced temperature

$$T^* = kT/\epsilon. \tag{5}$$

For example, the reduced second virial coefficient becomes

$$B^*(T^*) = B(T)/(\tfrac{2}{3}\pi N_A \sigma^3), \tag{6}$$

and is a universal function of T^*. Here $B(T)$ is the second virial coefficient measured at temperature T, and N_A is Avogadro's constant. Complete expressions for the other properties are given in Appendix C. The essence of the method consists in the fact that the universal functionals of the potential $V(r)$, such as $B^*(T^*)$, are determined with reference to critically evaluated measurements.

It is evident that in the case of binary mixtures the resulting principle of corresponding states does not refer to the properties measured on the mixtures directly. All formulas for mixtures, such as, for example,

$$B(T) = x_i^2 B_{ii}(T) + 2x_i x_j B_{ij}(T) + x_j^2 B_{jj}(T), \tag{7}$$

exhibit an explicit dependence on the mole fractions x_i and x_j and contain the functionals B_{ii}, B_{jj} of the pair potential for like collisions and of the pair potential B_{ij} for unlike collisions. Evidently, the three reduced functionals $B_{ii}^*(T_{ii}^*)$, $B_{jj}^*(T_{jj}^*)$, and $B_{ij}^*(T_{ij}^*)$ must separately satisfy the universal relation of the type of Eq. (6). The reduced property of the mixture [such as a reduced form of $B(T)$] is not a universal function of any reduced temperature.

In the case of multicomponent mixtures, in the low-density regime discussed here, only functionals of binary-collision pair potentials enter the analogs of Eq. (7). Thus, apart from the fact that such a mixture is described by more

than three characteristic temperatures ϵ_{ij}/k and an equal number of interaction functionals (such as B_{ij}), the method of calculation remains unchanged.

The two-parameter law of corresponding states has proved very useful in the correlation of many measurements on the noble gases.[10–15] On closer examination, it turned out that the two-parameter principle of corresponding states leads to a universal set of functionals which are valid in the middle range of the temperature interval

$$1.0 < T^* < 25, \tag{8}$$

and show signs of breaking down at very low and very high temperatures. B. Najafi, E. A. Mason, and J. Kestin[2] succeeded in improving the principle so that its validity now extends to the whole temperature range of interest, namely from 0 K to the onset of ionization. This was achieved at the cost of increasing the number of binary-interaction parameters to five (σ, ϵ/k, $C_6^* = C_6/\epsilon\sigma^6$, $\rho^* = \rho/\sigma$, and $V_o^* = V_o/\epsilon$). Note that the symbol ρ was earlier used for density. Here ρ and V_o are scaling factors for the repulsive wall of the potential, Eq. (13).

The tables of numerical data in this report are based on this improved principle of corresponding states with the further introduction of quantum corrections for second virial coefficients in the cryogenic range. In this range, a sixth scaling parameter, de Boer's reduced de Broglie wavelength

$$\Lambda_{ij}^* = h/\sigma_{ij}(m_{ij}\epsilon_{ij})^{1/2}, \tag{9}$$

intervenes. Here

$$m_{ij} = 2m_i m_j/(m_i + m_j), \tag{10}$$

and m_i, m_j denote the masses of the respective atoms.

3. Improved Principle of Corresponding States

The improved principle of corresponding states retains the basic assumption of similarity expressed in Eq. (4), but admits the possibility that the function f may contain additional material parameters. It was found necessary to add three parameters (C_6^*, ρ^*, and V_o^*) to the previous two, and to put

$$V(r) = \epsilon\, \mathrm{f}(r/\sigma, C_6^*, \rho^*, V_o^*). \tag{11}$$

The additional parameters arise from the following considerations:

(1) Accurate values of the coefficients of the long-range dispersion energy became available through a combination of quantum theory with dielectric and optical data.[16] It has been found necessary to include only the term $-C_6/r^6$, thus introducing the one dimensionless parameter

$$C_6^* = C_6/\epsilon_{ij}\sigma_{ij}^6. \tag{12}$$

The availability of these reliable values makes it possible to determine the low-temperature asymptotic behavior of all functionals of interest.[2] The forms given in Appendix B incorporate the results of such calculations.[17–19]

(2) Accurate data on the scattering of beams of noble gases, largely by Y. T. Lee,[20] make it possible to supplement correlations with direct information concerning the pair potentials.

Similar, albeit indirect information is supplied by pair potentials obtained by the direct numerical methods of inversion developed by E. B. Smith, G. C. Maitland, and coworkers.[21,22]

(3) Accurate information on high-energy beam scattering and approximate theoretical calculations make it possible to determine the repulsive wall of the potential.[23–27] Since the latter can be accurately represented by the form

$$V(r) = V_o \exp(-r/\rho), \tag{13}$$

it becomes necessary to introduce the additional material parameters

$$V_o^* = V_o/\epsilon_{ij}, \tag{14a}$$

and

$$\rho^* = \rho/\sigma_{ij}. \tag{14b}$$

An integration of the form of $V(r)$ in Eq. (13) enables us to derive analytic expressions for the asymptotic behavior of all functionals needed for the correlation.[2] Those cited later in Appendix B possess that proper form.

The resulting functionals for the classical second virial coefficient $B_0(T^*)$ and the collision integral $\Omega^{(2,2)*}(T^*)$ are depicted in Figs. 1 and 2. Here $B_0(T^*)$ denotes the first term in the expansion of the second virial coefficient in powers of the de Boer parameter Λ^*, i.e., without quantum corrections, and the same is true of $\Omega^{(2,2)*}$ in Fig. 2.

The two diagrams clearly show that the two-parameter representation provides us with an excellent correlation in the middle temperature range

$$1.2 \leqslant T^* \leqslant 10.$$

In the cryogenic range,

$$0 \leqslant T^* \leqslant 1.2,$$

it is necessary to invoke the material constant C_6^* (as well as quantum corrections). In the high-temperature range,

$$T^* \geqslant 10,$$

the two material constants V_o^* and ρ^* must be added to σ and ϵ.

All material constants assume fixed values for each bi-

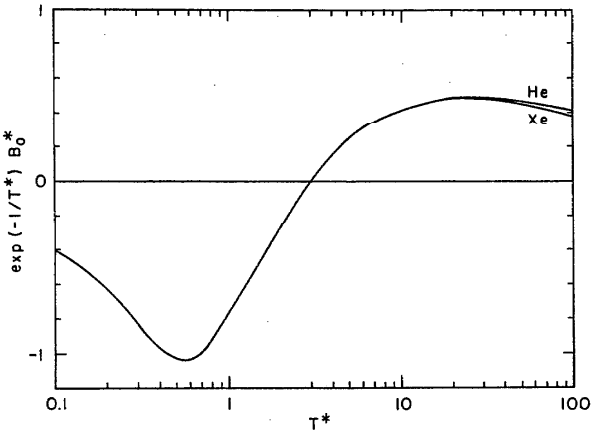

FIG. 1. Correlation curves for B_o^*, the classical portion of the second virial coefficient. The single curve at low and intermediate temperatures is correlated by the parameters σ, ϵ. At higher temperatures the repulsion parameters ρ^*, V_o^* are also needed.

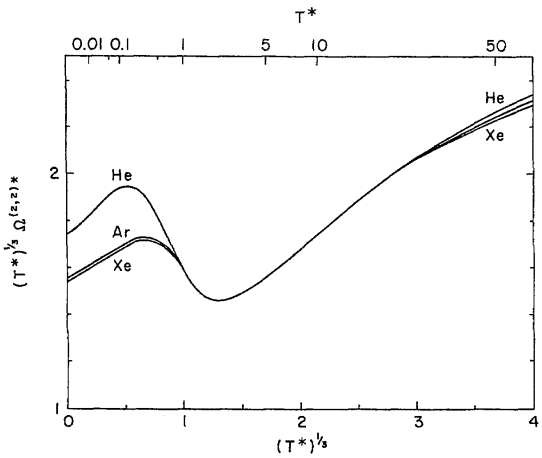

FIG. 2. Correlation curves for $\Omega^{(2,2)*}$, the reduced collision integral for viscosity. The single curve at intermediate T^* is the region of the two-parameter (σ,ϵ) correlation. At low temperatures, the parameter C_6^* is also needed, and at high temperatures the parameters ρ^*, V_0^* are needed.

nary interaction. We have refrained from adding subscripts i,j to them for the sake of economy. The empirically fitted forms of the above two (as well as other) functionals given piecewise in Appendix B are continuous, and possess continuous first and second derivatives at $T^* = 1.1$ or $T^* = 1.2$ as the case may be, and at $T^* = 10$.

4. Quantum Corrections

Quantum corrections have been introduced in the calculation of the second virial coefficients. For most systems, this could be done through the truncated semiclassical, Wigner–Kirkwood expansion

$$B^* = B_0^* + (\Lambda^*)^2 B_1^* + (\Lambda^*)^4 B_2^* + (\Lambda^*)^6 B_3^* + (\Lambda^*)^3 B_{\text{perfect}}^* , \tag{15}$$

with

$$B_{\text{perfect}}^* \begin{bmatrix} \text{BE} \\ \text{FD} \end{bmatrix} = \pm \frac{1}{2s+1} \frac{1}{(4\pi)^{5/2}} \left(\frac{1}{T^*} \right)^{3/2} , \tag{16}$$

where s is the nuclear spin. This term is significant only for ^{3}He ($s = \frac{1}{2}$, FD) and ^{4}He ($s = 0$, BE).

The range of convergence of Eq. (15) is discussed in Ref. 2 where it is shown that the expression fails for ^{3}He, ^{4}He, and their mixtures in the cryogenic temperature range, approximately $T < 50$ K. For these systems, the results of a full quantum-mechanical calculation were used.

Even though analogous results hold for the transport properties, it was not possible to include all of them. The relevant and rather complicated calculations corresponding to the Wigner–Kirkwood expression have never been carried out, but it is reasonably certain that the corrections introduced by them are not important for our present purposes.[2] The systems ^{3}He, ^{4}He, and their mixtures are an exception, for which the results of a full quantum-mechanical calculation were used.

5. Functionals and Scaling Factors

The recommended forms of the functionals for B_0^*, B_1^*, B_2^*, B_3^*, $\Omega^{(2,2)*}$, $\Omega^{(1,1)*}$ together with the consistent values of the four material constants σ, ϵ/k, V_0^*, and ρ^* have been derived by a complicated iterative method. The functional B_{perfect}^* and the values of C_6 have been taken directly from theory.

The expressions for these functionals are given in Appendix B.

Table A1 contains values of the universal constants employed in this work,[28] and Table A2 lists the values of the atomic masses of the pure gases as well as the reduced masses for mixtures in accordance with Eq. (10) and in conformity with the recommendations of the Commission on Atomic Weights of the International Union of Pure and Applied Chemistry.[29] The optimum values of the material constants are given in Tables A3–A6. The latter have been normalized with respect to argon for which we assume

$$\sigma = 0.3350 \text{ nm}, \quad \epsilon/k = 141.5 \text{ K}.$$

These were determined by R. A. Aziz and H. H. Chen[30] on the basis of a realistic Ar–Ar potential.

The optimum parameters arrange themselves in the form of quite regular periodic tables.

The lengthy iterative procedure which resulted in the above optimal, internally consistent set of functionals-cum-constants was based on the theoretical data discussed in Sec. 3 and on a critically reviewed set of experimentally determined numerical data. More specifically, the algebraic forms of the functionals possess the correct asymptotic behavior (at $T \to 0$ and at $T \to \infty$), as mentioned earlier and derived in Ref. 2. The total synthesis was, finally, validated with respect to a wider data set. This aspect is discussed in Secs. 6 and 7.

Appendix B contains also convenient expressions for B_{perfect}^* and $F^* = \Omega^{(3,3)*}/\Omega^{(1,1)*}$. Appendix C lists standard formulas which are needed for programing.

6. Experimental Data

The experimental data considered in this work were contained in over 2000 references. These were based on a computer output supplied to us by the Purdue University Center for Information and Numerical Data Analysis and Synthesis (CINDAS), supplemented with citations from our own collection. All these references were scrutinized and their number reduced to about 400. In turn, these were read, critically evaluated, and divided into three classes.

The division into three classes was based on a number of objective and subjective criteria which included (a) a subjective assessment of the reliability of the data, guided by an examination of internal consistency of error analysis and reproducibility; (b) the authors' statement of precision and accuracy; (c) a direct intercomparison of results from different laboratories and of results obtained by different methods; (d) an evaluation of the capability of the method used and of the correctness of the theory of the instrument; and (e) a scrutiny of the consistency between the measurement of different properties imposed by theory.

TABLE a. Estimate of accuracy of fit in the temperature range 50–1000 K

System	B (10^{-3} m^3/kmol)	η (%)	λ (%)	D (%)	α_T (%)
He	±0.5	±0.3	±0.7	±1.0	±5.0
Ne	±0.7	±0.3	±0.7	±0.7	±5.0
Ar	±0.5	±0.3	±0.7	±0.7	±5.0
Kr	±0.7	±0.3	±0.5	±1.0	±3.0
Xe	±1.0	±0.3	±0.5	±0.5	±3.0
He–Ne	±0.5	±0.5	±0.7	±1.0	±8.0
He–Ar	±0.7	±0.4	±0.7	±1.0	±3.0
He–Kr	±0.5	±0.4	*(±0.7)	±1.5	±5.0
He–Xe	±2.0	±0.3	*(±0.7)	±1.2	±4.0
Ne–Ar	±0.7	±0.3	±0.5	±0.7	±5.0
Ne–Kr	±1.0	±0.3	*(±0.7)	±1.0	±3.0
Ne–Xe	±0.7	±0.3	*(±0.7)	±2.0	±5.0
Ar–Kr	±1.0	±0.4	±0.5	±2.0	±4.0
Ar–Xe	±1.0	±0.3	*(±0.7)	±0.8	±6.0
Kr–Xe	±1.0	±0.3	*(±0.7)	±0.7	±3.0
He–Ne–Kr	*(±1.0)	±0.3	*(±0.7)		
He–Ar–Kr	*(±1.0)	±0.3	*(±0.7)		
Ne–Ar–Kr	*(±1.0)	±0.3	*(±0.7)		
He–Ne–Ar					
He–Ne–Xe					
He–Ar–Xe					
He–Kr–Xe					
Ne–Ar–Xe					
Ne–Kr–Xe					
Ar–Kr–Xe					
He–Ne–Ar–Kr	*(±1.0)	*(±0.3)	*(±0.7)		
He–Ne–Ar–Xe					
He–Ne–Kr–Xe					
He–Ar–Kr–Xe					
Ne–Ar–Kr–Xe					
He–Ne–Ar–Kr–Xe					

Note: The open literature contains no experimental data for the properties and systems distinguished by an asterisk. The respective uncertainties have been determined by analogy.

Class 1 contain primary data which were used in the iterative schemata for correlation. Class 2 contains secondary data used in validation. Classes 1 and 2 together embrace references listed in the bibliography of Appendix E. Papers of Class 1 are distinguished by an asterisk. Some papers in this bibliography contain a mixture of data of Classes 1 and 2. They are also provided with an asterisk. Papers of Class 3, left out of our correlation and validation as a result of our earlier critical review, could not be included in this report owing to their great bulk. A list has been deposited with AIP's Physics Auxiliary Publication Service (PAPS) of the American Institute of Physics.[a]

7. Validation, Deviation Plots, and Accuracy

The validation of our synthesis, that is of the resulting computational algorithm, is represented in 86 deviation plots reproduced here as Appendix D. All diagrams testify to the fact that the algorithm represents the primary data very accurately, and that it is validated by the secondary data which have not been employed in the iterative procedure. Naturally, the degree of concordance varies with the system, property, temperature range, and (also) quality of the respective measurements.

The deviation plots can be used as a basis of an estimate of accuracy. The numbers in brackets in the captions refer to the Bibliography of Appendix E. The result of our interpretations is summarized in Table a. For the following systems: He–Ne–Ar, He–Ne–Xe, He–Ar–Xe, He–Kr–Xe, Ne–Ar–Xe, Ne–Kr–Xe, Ar–Kr–Xe, He–Ne–Ar–Kr, He–Ne–Ar–Xe, He–Ne–Kr–Xe, He–Ar–Kr–Xe, Ne–Ar–Kr–Xe, and He–Ne–Ar–Kr–Xe, as well as for the properties in the above table which are distinguished by an asterisk (*), the open literature contains no experimental data of either Class 1 or Class 2. For this reason, the estimate of accuracy cannot be made by a direct comparison of the correlation with measurement. The estimates indicated have been made by analogy.

8. Description of the Tables

The tables of numerical data are not meant to be exhaustive and have not been designed for linear interpolation They are convenient extracts only, because the entire algorithm can be programed without difficulty, thus making it possible easily to interpolate both for temperature and composition (in the case of mixtures). A more extensive tabulation would be prohibitive in its volume.

The 54 tables of numerical data naturally fall into four groups. In the first group, we tabulate the following properties for the pure components:

second virial coefficient	B in 10^{-3} m^3/kmol
viscosity	η in μPa s
thermal conductivity	λ in mW/m K
diffusion coefficient at $P = 1.013\,25$ bar	D in 10^{-4} m^2/s
thermal diffusion factor	α_T (dimensionless).

In all cases, except for helium, it is sufficient to indicate a single value of the the thermal diffusion factor because it is virtually independent of isotopic composition, although it depends on the isotopic mass ratio in a simple way. The latter dependence is removed by defining an isotopic thermal diffusion factor α_o as

$$\alpha_T = \alpha_o\left(\frac{m_1 - m_2}{m_1 + m_2}\right), \quad (m_1 > m_2). \tag{17}$$

As far as helium is concerned, we listed the two extreme values for a mixture of ^{4}He and ^{3}He. Interpolation can easily be performed, because $1/\alpha_T$ is a linear function of composition.[2] The temperature interval chosen, 0 K to 3000 °C is subdivided into two ranges. Below the ice point (0 °C = 273.15 K), temperatures are given in Kelvins at 50 K intervals. Above the ice point, the steps are 20 °C for 0 °C < T < 100 °C, 50 °C for 100 °C < T < 500 °C, 100 °C for 500 °C < T < 1000 °C, and 500 °C for 1000 °C < T < 3000 °C.

The number of significant figures exceeds that which would be justified by the analysis of Sec. 7. The choice was governed more by aesthetic considerations than determined by an assessment of accuracy.

[a] See AIP document no. PAPS JPCRD-13-229-200 for 200 pages of data tables. Order by PAPS number and journal reference from the American Institute of Physics, Physics Auxiliary Publication Service, 335 East 45th Street, New York, N.Y. 10017. The price is $1.50 for a microfiche or $5.00 for a photocopy. Airmail is additional. Make checks payable to the American Institute of Physics.

Table A7 in Appendix A lists the ionization limit for the pure gases. The onset of ionization was calculated from the Saha equation with the first ionization potential taken from Ref. 31 and for a 1% mol fraction of ionized atoms.

The second group of tables contains values for binary mixtures. The steps and ranges are the same as for the first group. In all cases, we tabulate three molar compositions: 25%–75%, 50%–50%, and 75%–25%.

The third group of tables lists values for the ternary, quaternary, and five-component mixtures, limiting entries to a single, equimolar composition. No data for diffusion or thermal diffusion are given here for the sake of simplicity.

A fourth group contains tables for ^{3}He, ^{4}He and an equimolar mixture of them. The properties listed are B, η, λ, D, and α_T for the mixture. The temperature range covered is $0.1\ \mathrm{K} \leqslant T \leqslant 100\ \mathrm{K}$ in steps varying from 0.1 K at the low end to 10 K at the upper end of the scale. All data listed in these tables are based on quantum-mechanical calculations of second virial coefficients and collision integrals.[32] We are grateful to Drs. W. L. Taylor and G. T. McConville for supplying numerical tables of their results, which were reported only graphically in Ref. 32.

9. Tables

Table 1. Properties of helium as a function of temperature

T K or °C	B 10^{-3}m^3/kmol	η μPa s	λ mW/m K	D(1.013 bar) 10^{-4}m^2/s	α_T $x(^4\mathrm{He})=1$	α_T $x(^4\mathrm{He})=0$
50 K	9.68	6.04	47.17	0.0888	0.0618	0.0655
100	11.35	9.66	75.54	0.2874	0.0717	0.0757
150	11.89	12.61	98.63	0.5669	0.0708	0.0747
200	12.02	15.26	119.32	0.9188	0.0695	0.0733
250	11.94	17.72	138.53	1.3378	0.0683	0.0719
300	11.77	20.04	156.66	1.8200	0.0673	0.0708
0 °C	11.86	18.81	147.04	1.5534	0.0678	0.0714
20	11.79	19.73	154.23	1.7503	0.0674	0.0709
40	11.72	20.63	161.29	1.9569	0.0671	0.0705
60	11.64	21.52	168.22	2.1731	0.0667	0.0702
80	11.55	22.40	175.04	2.3986	0.0664	0.0698
100	11.47	23.25	181.75	2.6333	0.0661	0.0695
150	11.27	25.35	198.11	3.2597	0.0654	0.0687
200	11.07	27.38	213.96	3.9411	0.0648	0.0681
250	10.88	29.35	229.37	4.6761	0.0642	0.0675
300	10.70	31.28	244.39	5.4632	0.0638	0.0670
350	10.53	33.16	259.07	6.3014	0.0633	0.0665
400	10.36	35.00	273.44	7.1895	0.0629	0.0660
450	10.21	36.80	287.54	8.1266	0.0625	0.0656
500	10.07	38.58	301.39	9.1119	0.0622	0.0652
600	9.80	42.04	328.43	11.2242	0.0615	0.0645
700	9.56	45.41	354.70	13.5207	0.0609	0.0639
800	9.34	48.69	380.30	15.9970	0.0604	0.0633
900	9.14	51.90	405.33	18.6491	0.0599	0.0627
1000	8.95	55.04	429.84	21.4733	0.0594	0.0623
1500	8.20	69.96	546.30	38.0791	0.0575	0.0602
2000	7.65	83.94	655.33	58.6286	0.0559	0.0585
2500	7.22	97.24	759.14	82.9239	0.0547	0.0572
3000	6.86	110.04	859.01	110.8216	0.0536	0.0560

Table 2. Properties of neon as a function of temperature

T K or °C	B 10^{-3}m^3/kmol	η μPa s	λ mW/m K	D(1.013 bar) 10^{-4}m^2/s	α_0
50 K	-36.36	7.70	11.89	0.0206	0.0901
100	-5.01	14.39	22.26	0.0766	0.2876
150	4.12	19.72	30.54	0.1589	0.3981
200	8.15	24.29	37.63	0.2627	0.4640
250	10.14	28.36	43.96	0.3851	0.5045
300	11.16	32.10	49.77	0.5245	0.5287
0 °C	10.69	30.13	46.71	0.4476	0.5173
20	11.05	31.60	49.00	0.5045	0.5262
40	11.34	33.04	51.22	0.5639	0.5331
60	11.56	34.43	53.39	0.6258	0.5385
80	11.75	35.80	55.51	0.6901	0.5425
100	11.91	37.13	57.58	0.7570	0.5452
150	12.26	40.35	62.57	0.9345	0.5467
200	12.61	43.42	67.34	1.1268	0.5479
250	12.91	46.38	71.93	1.3328	0.5552
300	13.15	49.25	76.38	1.5518	0.5610
350	13.34	52.03	80.69	1.7835	0.5642
400	13.48	54.74	84.90	2.0277	0.5652
450	13.59	57.39	89.00	2.2842	0.5647
500	13.66	59.99	93.02	2.5527	0.5631
600	13.75	65.02	100.83	3.1256	0.5583
700	13.77	69.89	108.36	3.7451	0.5527
800	13.74	74.60	115.67	4.4100	0.5471
900	13.69	79.19	122.78	5.1194	0.5417
1000	13.62	83.67	129.72	5.8722	0.5368
1500	13.17	104.72	162.33	10.2579	0.5176
2000	12.69	124.15	192.41	15.6205	0.5045
2500	12.26	142.44	220.73	21.8983	0.4946
3000	11.87	159.85	247.69	29.0462	0.4867

Table 3. Properties of argon as a function of temperature

T K or °C	B $10^{-3}m^3$/kmol	η μPa s	λ mW/m K	D(1.013 bar) $10^{-4}m^2$/s	α_o
50 K	-713.46	4.32	3.38	0.0058	0.1990
100	-190.80	7.97	6.22	0.0221	0.0806
150	-85.75	11.94	9.32	0.0489	0.0689
200	-48.48	15.89	12.41	0.0856	0.1362
250	-28.77	19.50	15.23	0.1308	0.2003
300	-16.40	22.83	17.83	0.1839	0.2538
0 °C	-22.41	21.08	16.46	0.1545	0.2263
20	-17.82	22.39	17.49	0.1762	0.2470
40	-13.87	23.66	18.49	0.1991	0.2663
60	-10.45	24.90	19.46	0.2231	0.2843
80	-7.44	26.11	20.41	0.2483	0.3011
100	-4.79	27.29	21.33	0.2745	0.3168
150	0.64	30.11	23.55	0.3444	0.3516
200	4.80	32.79	25.64	0.4204	0.3813
250	8.05	35.34	27.65	0.5022	0.4067
300	10.63	37.78	29.56	0.5895	0.4286
350	12.70	40.12	31.40	0.6820	0.4475
400	14.36	42.39	33.18	0.7796	0.4638
450	15.72	44.57	34.90	0.8821	0.4780
500	16.82	46.70	36.56	0.9892	0.4902
600	18.47	50.77	39.76	1.2172	0.5099
700	19.59	54.65	42.80	1.4626	0.5244
800	20.36	58.36	45.72	1.7250	0.5347
900	20.93	61.94	48.52	2.0037	0.5416
1000	21.37	65.39	51.23	2.2985	0.5457
1500	23.16	81.33	63.73	4.0042	0.5409
2000	24.14	95.84	75.08	6.0781	0.5286
2500	24.51	109.45	85.73	8.4984	0.5172
3000	24.55	122.39	95.86	11.2483	0.5078

Table 4. Properties of krypton as a function of temperature

T K or °C	B $10^{-3}m^3$/kmol	η μPa s	λ mW/m K	D(1.013 bar) $10^{-4}m^2$/s	α_o
50 K	-2216.24	4.97	1.85	0.0032	0.2540
100	-426.27	8.85	3.29	0.0116	0.1418
150	-203.02	12.86	4.78	0.0255	0.0760
200	-114.30	17.15	6.38	0.0448	0.0651
250	-74.14	21.50	8.00	0.0693	0.1054
300	-50.57	25.59	9.52	0.0984	0.1561
0 °C	-61.90	23.43	8.72	0.0822	0.1297
20	-53.22	25.05	9.32	0.0941	0.1495
40	-45.86	26.63	9.91	0.1067	0.1684
60	-39.53	28.16	10.48	0.1200	0.1864
80	-34.03	29.67	11.04	0.1340	0.2034
100	-29.19	31.14	11.59	0.1486	0.2195
150	-19.31	34.67	12.91	0.1878	0.2564
200	-11.72	38.02	14.16	0.2307	0.2889
250	-5.70	41.22	15.36	0.2771	0.3176
300	-0.83	44.28	16.51	0.3268	0.3430
350	3.17	47.23	17.61	0.3797	0.3656
400	6.50	50.07	18.67	0.4356	0.3858
450	9.30	52.81	19.70	0.4945	0.4039
500	11.67	55.47	20.69	0.5562	0.4202
600	15.41	60.57	22.60	0.6878	0.4480
700	18.17	65.41	24.41	0.8297	0.4706
800	20.22	70.03	26.14	0.9814	0.4890
900	21.76	74.46	27.80	1.1427	0.5039
1000	22.92	78.74	29.40	1.3131	0.5159
1500	25.85	98.30	36.72	2.2940	0.5455
2000	27.48	115.79	43.25	3.4784	0.5349
2500	28.63	132.02	49.30	4.8714	0.4918
3000	29.24	147.42	55.05	6.4705	0.4675

Table 5. Properties of xenon as a function of temperature

T K or °C	B $10^{-3}m^3$/kmol	η μPa s	λ mW/m K	D(1.013 bar) $10^{-4}m^2$/s	α_o
50 K	-10637.20	4.77	1.13	0.0019	0.2889
100	-1053.39	8.34	1.98	0.0069	0.2001
150	-476.27	11.81	2.81	0.0149	0.1276
200	-281.64	15.42	3.66	0.0260	0.0809
250	-180.90	19.23	4.57	0.0403	0.0628
300	-126.32	23.16	5.50	0.0576	0.0737
0 °C	-151.47	21.04	5.00	0.0479	0.0643
20	-132.03	22.62	5.37	0.0551	0.0705
40	-116.35	24.19	5.75	0.0627	0.0811
60	-103.16	25.75	6.11	0.0707	0.0951
80	-91.88	27.28	6.48	0.0792	0.1107
100	-82.11	28.77	6.83	0.0880	0.1258
150	-62.57	32.39	7.69	0.1120	0.1613
200	-47.85	35.85	8.52	0.1385	0.1936
250	-36.32	39.16	9.31	0.1673	0.2231
300	-27.03	42.34	10.06	0.1983	0.2499
350	-19.37	45.40	10.79	0.2314	0.2743
400	-12.96	48.36	11.50	0.2666	0.2966
450	-7.52	51.22	12.18	0.3037	0.3170
500	-2.84	53.99	12.84	0.3428	0.3357
600	4.73	59.30	14.11	0.4265	0.3687
700	10.55	64.34	15.31	0.5171	0.3967
800	15.10	69.15	16.46	0.6142	0.4207
900	18.72	73.76	17.56	0.7177	0.4412
1000	21.60	78.19	18.62	0.8272	0.4589
1500	29.60	98.37	23.44	1.4582	0.5167
2000	32.62	116.23	27.70	2.2168	0.5417
2500	34.27	132.57	31.60	3.0935	0.5476
3000	35.71	147.84	35.24	4.0846	0.5372

Table 6. Properties of the binary mixture of helium and neon with x_{He}=0.25 and x_{Ne}=0.75 as a function of temperature

T K or °C	B $10^{-3}m^3$/kmol	η μPa s	λ mW/m K	D(1.013 bar) $10^{-4}m^2$/s	α_T
50 K	-19.98	7.72	16.93	0.0510	0.1607
100	1.32	14.00	29.79	0.1751	0.2420
150	7.24	18.98	40.17	0.3500	0.2696
200	9.76	23.27	49.16	0.5675	0.2749
250	11.07	27.11	57.09	0.8252	0.2810
300	11.77	30.66	64.69	1.1182	0.2861
0 °C	11.45	28.79	60.67	0.9567	0.2841
20	11.70	30.19	63.68	1.0761	0.2858
40	11.89	31.55	66.61	1.2007	0.2866
60	12.04	32.88	69.47	1.3307	0.2867
80	12.16	34.18	72.26	1.4658	0.2864
100	12.25	35.45	74.99	1.6061	0.2858
150	12.45	38.53	81.59	1.9790	0.2835
200	12.63	41.49	87.92	2.3830	0.2807
250	12.76	44.34	94.02	2.8174	0.2781
300	12.86	47.10	99.95	3.2816	0.2755
350	12.92	49.78	105.72	3.7747	0.2732
400	12.96	52.40	111.35	4.2963	0.2712
450	12.97	54.96	116.85	4.8458	0.2693
500	12.97	57.47	122.25	5.4226	0.2675
600	12.92	62.34	132.76	6.6565	0.2645
700	12.84	67.05	142.93	7.9946	0.2620
800	12.75	71.63	152.82	9.4340	0.2597
900	12.64	76.08	162.46	10.9723	0.2578
1000	12.52	80.42	171.87	12.6071	0.2560
1500	11.94	100.89	216.33	22.1668	0.2491
2000	11.41	119.82	257.58	33.9092	0.2441
2500	10.96	137.66	296.55	47.7071	0.2400
3000	10.57	154.67	333.81	63.4673	0.2366

Table 7. Properties of the binary mixture of helium and neon with x_{He}=0.50 and x_{Ne}=0.50 as a function of temperature

T K or °C	B $10^{-3}m^3$/kmol	η μPa s	λ mW/m K	D(1.013 bar) $10^{-4}m^2$/s	α_T
50 K	-6.84	7.59	23.68	0.0508	0.1836
100	6.15	13.27	39.93	0.1739	0.2741
150	9.57	17.78	53.15	0.3471	0.3043
200	10.94	21.69	64.74	0.5627	0.3097
250	11.69	25.22	74.97	0.8178	0.3172
300	12.07	28.50	84.96	1.1079	0.3227
0°C	11.90	26.77	79.66	0.9480	0.3206
20	12.03	28.06	83.63	1.0662	0.3224
40	12.13	29.33	87.49	1.1897	0.3232
60	12.21	30.56	91.27	1.3185	0.3233
80	12.26	31.77	94.97	1.4525	0.3229
100	12.30	32.96	98.59	1.5916	0.3221
150	12.35	35.84	107.37	1.9615	0.3195
200	12.38	38.60	115.82	2.3625	0.3165
250	12.38	41.28	123.99	2.7937	0.3135
300	12.36	43.88	131.93	3.2544	0.3107
350	12.32	46.41	139.67	3.7441	0.3082
400	12.27	48.88	147.24	4.2620	0.3059
450	12.21	51.30	154.66	4.8076	0.3039
500	12.14	53.67	161.93	5.3805	0.3020
600	11.99	58.29	176.10	6.6060	0.2987
700	11.84	62.75	189.85	7.9352	0.2959
800	11.68	67.09	203.23	9.3651	0.2934
900	11.52	71.31	216.28	10.8934	0.2913
1000	11.37	75.44	229.05	12.5178	0.2894
1500	10.70	94.93	289.51	22.0184	0.2819
2000	10.15	113.00	345.82	33.6920	0.2764
2500	9.69	130.07	399.19	47.4122	0.2720
3000	9.30	146.38	450.35	63.0872	0.2682

Table 8. Properties of the binary mixture of helium and neon with x_{He}=0.75 and x_{Ne}=0.25 as a function of temperature

T K or °C	B $10^{-3}m^3$/kmol	η μPa s	λ mW/m K	D(1.013 bar) $10^{-4}m^2$/s	α_T
50 K	3.05	7.14	33.11	0.0507	0.2150
100	9.50	11.97	54.19	0.1726	0.3178
150	11.12	15.83	71.37	0.3439	0.3511
200	11.70	19.22	86.63	0.5573	0.3567
250	11.98	22.31	100.30	0.8095	0.3664
300	12.07	25.20	113.59	1.0964	0.3723
0°C	12.04	23.67	106.54	0.9382	0.3701
20	12.07	24.82	111.81	1.0552	0.3720
40	12.08	25.93	116.97	1.1774	0.3727
60	12.07	27.03	122.03	1.3049	0.3727
80	12.06	28.11	126.99	1.4376	0.3722
100	12.03	29.17	131.86	1.5754	0.3713
150	11.95	31.74	143.70	1.9420	0.3682
200	11.86	34.22	155.13	2.3395	0.3648
250	11.75	36.63	166.20	2.7671	0.3614
300	11.64	38.97	176.99	3.2241	0.3583
350	11.52	41.26	187.51	3.7098	0.3555
400	11.40	43.49	197.81	4.2236	0.3529
450	11.29	45.68	207.91	4.7650	0.3506
500	11.17	47.83	217.82	5.3334	0.3485
600	10.95	52.02	237.16	6.5496	0.3449
700	10.74	56.07	255.93	7.8687	0.3418
800	10.54	60.02	274.21	9.2882	0.3391
900	10.36	63.87	292.07	10.8053	0.3367
1000	10.18	67.64	309.55	12.4181	0.3346
1500	9.45	85.46	392.48	21.8530	0.3263
2000	8.89	102.05	469.94	33.4500	0.3203
2500	8.44	117.77	543.55	47.0840	0.3154
3000	8.07	132.84	614.23	62.6642	0.3112

Table 9. Properties of the binary mixture of helium and argon with x_{He}=0.25 and x_{Ar}=0.75 as a function of temperature

T K or °C	B $10^{-3}m^3$/kmol	η μPa s	λ mW/m K	D(1.013 bar) $10^{-4}m^2$/s	α_T
50 K	-408.93	4.74	7.62	0.0317	0.1109
100	-104.79	8.65	13.43	0.1144	0.2200
150	-42.76	12.66	18.79	0.2343	0.2704
200	-20.71	16.55	23.79	0.3844	0.2963
250	-9.19	20.08	28.39	0.5610	0.3094
300	-1.99	23.33	32.71	0.7619	0.3144
0°C	-5.49	21.62	30.42	0.6511	0.3125
20	-2.82	22.90	32.13	0.7330	0.3141
40	-0.50	24.15	33.66	0.8186	0.3128
60	1.52	25.36	35.16	0.9083	0.3128
80	3.29	26.54	36.67	1.0017	0.3141
100	4.86	27.69	38.18	1.0987	0.3157
150	8.06	30.46	41.86	1.3559	0.3189
200	10.50	33.10	45.38	1.6336	0.3201
250	12.39	35.61	48.76	1.9312	0.3200
300	13.87	38.03	52.02	2.2485	0.3190
350	15.04	40.35	55.16	2.5849	0.3176
400	15.98	42.60	58.21	2.9402	0.3160
450	16.72	44.78	61.18	3.3141	0.3143
500	17.32	46.90	64.07	3.7062	0.3127
600	18.18	50.98	69.67	4.5440	0.3096
700	18.73	54.88	75.05	5.4514	0.3068
800	19.09	58.62	80.25	6.4265	0.3043
900	19.32	62.23	85.30	7.4677	0.3021
1000	19.48	65.73	90.21	8.5733	0.3002
1500	20.08	81.96	113.22	15.0259	0.2925
2000	20.30	96.78	134.44	22.9313	0.2871
2500	20.21	110.71	154.46	32.2006	0.2828
3000	19.99	123.96	173.58	42.7685	0.2792

Table 10. Properties of the binary mixture of helium and argon with x_{He}=0.50 and x_{Ar}=0.50 as a function of temperature

T K or °C	B $10^{-3}m^3$/kmol	η μPa s	λ mW/m K	D(1.013 bar) $10^{-4}m^2$/s	α_T
50 K	-186.90	5.28	14.03	0.0317	0.1391
100	-42.42	9.44	24.06	0.1139	0.2731
150	-12.16	13.43	32.63	0.2325	0.3343
200	-1.37	17.17	40.38	0.3810	0.3656
250	4.13	20.55	47.55	0.5555	0.3810
300	7.51	23.67	54.36	0.7543	0.3865
0°C	5.86	22.02	50.74	0.6447	0.3845
20	7.12	23.25	53.44	0.7257	0.3862
40	8.22	24.45	55.81	0.8105	0.3849
60	9.18	25.62	58.12	0.8992	0.3852
80	10.03	26.75	60.49	0.9916	0.3869
100	10.78	27.86	62.86	1.0875	0.3889
150	12.31	30.54	68.71	1.3419	0.3926
200	13.45	33.09	74.35	1.6167	0.3940
250	14.31	35.54	79.79	1.9115	0.3938
300	14.96	37.90	85.04	2.2257	0.3925
350	15.46	40.18	90.13	2.5590	0.3908
400	15.85	42.39	95.08	2.9112	0.3888
450	16.14	44.54	99.92	3.2817	0.3868
500	16.36	46.64	104.65	3.6705	0.3849
600	16.64	50.69	113.84	4.5011	0.3812
700	16.78	54.58	122.73	5.4010	0.3779
800	16.82	58.33	131.35	6.3681	0.3749
900	16.81	61.96	139.74	7.4009	0.3723
1000	16.78	65.49	147.94	8.4977	0.3699
1500	16.56	81.95	186.63	14.9005	0.3609
2000	16.26	97.07	222.56	22.7477	0.3545
2500	15.90	111.30	256.57	31.9512	0.3494
3000	15.52	124.87	289.14	42.4467	0.3452

Table 11. Properties of the binary mixture of helium and argon with $x_{He}=0.75$ and $x_{Ar}=0.25$ as a function of temperature

T K or °C	B $10^{-3}m^3/kmol$	η μPa s	λ mW/m K	D(1.013 bar) $10^{-4}m^2/s$	α_T
50 K	-47.36	5.90	24.87	0.0316	0.1865
100	-3.71	10.20	41.44	0.1132	0.3601
150	6.06	13.96	55.04	0.2305	0.4382
200	9.54	17.36	67.20	0.3769	0.4778
250	11.17	20.45	78.51	0.5491	0.4967
300	12.10	23.30	89.28	0.7455	0.5026
0°C	11.65	21.79	83.55	0.6371	0.5007
20	11.99	22.92	87.82	0.7172	0.5024
40	12.29	24.02	91.67	0.8011	0.5013
60	12.56	25.10	95.42	0.8886	0.5024
80	12.79	26.15	99.24	0.9798	0.5048
100	12.99	27.18	103.06	1.0744	0.5074
150	13.37	29.67	112.46	1.3256	0.5120
200	13.63	32.06	121.57	1.5971	0.5136
250	13.80	34.37	130.37	1.8884	0.5132
300	13.90	36.61	138.92	2.1991	0.5115
350	13.96	38.78	147.23	2.5289	0.5093
400	13.98	40.90	155.35	2.8773	0.5068
450	13.97	42.96	163.29	3.2441	0.5043
500	13.94	44.99	171.08	3.6289	0.5018
600	13.85	48.91	186.24	4.4513	0.4972
700	13.72	52.70	200.93	5.3424	0.4931
800	13.57	56.38	215.23	6.3003	0.4894
900	13.42	59.95	229.18	7.3233	0.4862
1000	13.27	63.43	242.83	8.4099	0.4833
1500	12.60	79.83	307.50	14.7552	0.4723
2000	12.05	95.00	367.81	22.5350	0.4644
2500	11.57	109.34	425.06	31.6625	0.4582
3000	11.15	123.05	480.00	42.0742	0.4530

Table 12. Properties of the binary mixture of helium and krypton with $x_{He}=0.25$ and $x_{Kr}=0.75$ as a function of temperature

T K or °C	B $10^{-3}m^3/kmol$	η μPa s	λ mW/m K	D(1.013 bar) $10^{-4}m^2/s$	α_T
50 K	-1257.01	5.36	5.59	0.0272	0.1103
100	-237.38	9.51	9.71	0.0987	0.2250
150	-108.10	13.65	13.36	0.2027	0.2786
200	-56.79	17.96	16.83	0.3333	0.3069
250	-33.62	22.26	20.17	0.4868	0.3218
300	-20.06	26.29	23.33	0.6614	0.3284
0°C	-26.58	24.16	21.65	0.5651	0.3257
20	-21.59	25.75	22.91	0.6363	0.3279
40	-17.34	27.31	24.16	0.7106	0.3294
60	-13.67	28.82	25.43	0.7880	0.3305
80	-10.47	30.30	26.62	0.8685	0.3291
100	-7.65	31.74	27.75	0.9521	0.3268
150	-1.91	35.21	30.41	1.1753	0.3210
200	2.49	38.52	32.96	1.4182	0.3168
250	5.95	41.68	35.42	1.6802	0.3141
300	8.74	44.71	37.80	1.9605	0.3125
350	11.00	47.63	40.13	2.2587	0.3115
400	12.88	50.45	42.40	2.5741	0.3108
450	14.43	53.17	44.62	2.9064	0.3103
500	15.74	55.82	46.78	3.2552	0.3100
600	17.77	60.91	50.99	4.0008	0.3094
700	19.23	65.75	55.04	4.8086	0.3089
800	20.29	70.38	58.95	5.6767	0.3083
900	21.05	74.84	62.75	6.6033	0.3076
1000	21.60	79.15	66.45	7.5870	0.3070
1500	22.77	98.95	83.72	13.3233	0.3034
2000	23.29	116.75	99.55	20.3422	0.2999
2500	23.60	133.31	114.42	28.5640	0.2967
3000	23.65	149.04	128.61	37.9301	0.2937

Table 13. Properties of the binary mixture of helium and krypton with $x_{He}=0.50$ and $x_{Kr}=0.50$ as a function of temperature

T K or °C	B $10^{-3}m^3/kmol$	η μPa s	λ mW/m K	D(1.013 bar) $10^{-4}m^2/s$	α_T
50 K	-566.28	5.87	11.48	0.0272	0.1419
100	-101.49	10.35	19.59	0.0982	0.2870
150	-40.64	14.60	26.41	0.2011	0.3543
200	-16.56	18.86	32.64	0.3301	0.3896
250	-5.77	23.02	38.51	0.4818	0.4079
300	0.50	26.90	44.12	0.6544	0.4157
0°C	-2.51	24.85	41.13	0.5592	0.4126
20	-0.20	26.38	43.36	0.6295	0.4151
40	1.77	27.88	45.59	0.7031	0.4168
60	3.48	29.33	47.88	0.7797	0.4175
80	4.98	30.76	50.00	0.8595	0.4155
100	6.30	32.15	52.01	0.9424	0.4126
150	8.99	35.50	56.75	1.1637	0.4053
200	11.03	38.69	61.28	1.4045	0.4001
250	12.60	41.76	65.68	1.6641	0.3968
300	13.85	44.71	69.98	1.9419	0.3948
350	14.84	47.55	74.18	2.2373	0.3936
400	15.64	50.31	78.29	2.5498	0.3928
450	16.30	52.98	82.32	2.8790	0.3922
500	16.83	55.59	86.27	3.2246	0.3918
600	17.62	60.60	93.98	3.9633	0.3911
700	18.15	65.39	101.44	4.7637	0.3905
800	18.49	69.99	108.68	5.6239	0.3898
900	18.71	74.44	115.73	6.5421	0.3890
1000	18.84	78.74	122.62	7.5172	0.3883
1500	18.81	98.66	155.06	13.2041	0.3840
2000	18.59	116.70	185.08	20.1653	0.3797
2500	18.35	133.56	213.44	28.3219	0.3758
3000	18.06	149.60	240.57	37.6162	0.3723

Table 14. Properties of the binary mixture of helium and krypton with $x_{He}=0.75$ and $x_{Kr}=0.25$ as a function of temperature

T K or °C	B $10^{-3}m^3/kmol$	η μPa s	λ mW/m K	D(1.013 bar) $10^{-4}m^2/s$	α_T
50 K	-144.05	6.48	22.10	0.0272	0.1989
100	-18.58	11.22	36.86	0.0976	0.3962
150	-0.65	15.40	48.94	0.1992	0.4864
200	6.38	19.37	59.79	0.3262	0.5334
250	9.42	23.13	69.92	0.4756	0.5572
300	11.11	26.63	79.60	0.6459	0.5664
0°C	10.30	24.78	74.45	0.5519	0.5629
20	10.92	26.16	78.29	0.6214	0.5658
40	11.45	27.51	82.13	0.6940	0.5673
60	11.91	28.82	86.05	0.7697	0.5671
80	12.32	30.11	89.72	0.8486	0.5639
100	12.68	31.37	93.23	0.9307	0.5597
150	13.30	34.42	101.60	1.1497	0.5499
200	13.88	37.34	109.63	1.3879	0.5432
250	14.24	40.15	117.43	1.6448	0.5390
300	14.50	42.88	125.05	1.9195	0.5364
350	14.68	45.51	132.51	2.2117	0.5349
400	14.81	48.08	139.82	2.5207	0.5339
450	14.89	50.58	147.00	2.8463	0.5333
500	14.94	53.02	154.04	3.1880	0.5328
600	14.96	57.75	167.80	3.9186	0.5320
700	14.92	62.30	181.15	4.7102	0.5312
800	14.84	66.70	194.14	5.5611	0.5303
900	14.74	70.96	206.82	6.4695	0.5294
1000	14.62	75.11	219.21	7.4342	0.5285
1500	13.95	94.50	277.90	13.0628	0.5231
2000	13.37	112.29	332.54	19.9557	0.5179
2500	12.89	129.01	384.35	28.0352	0.5130
3000	12.46	144.97	434.02	37.2446	0.5085

Table 15. Properties of the binary mixture of helium and xenon with x_{He}=0.25 and x_{Xe}=0.75 as a function of temperature

T K or °C	B $10^{-3}m^3$/kmol	η μPa s	λ mW/m K	D(1.013 bar) $10^{-4}m^2$/s	α_T
50 K	-5995.57	5.14	4.41	0.0235	0.1202
100	-589.16	9.00	7.61	0.0848	0.2363
150	-260.10	12.65	10.35	0.1739	0.2895
200	-148.98	16.36	12.91	0.2855	0.3169
250	-91.65	20.20	15.39	0.4167	0.3308
300	-60.57	24.14	17.82	0.5658	0.3361
0 °C	-74.91	22.02	16.52	0.4836	0.3342
20	-63.83	23.60	17.50	0.5444	0.3360
40	-54.86	25.17	18.40	0.6080	0.3355
60	-47.30	26.71	19.27	0.6744	0.3353
80	-40.82	28.23	20.15	0.7436	0.3353
100	-35.21	29.71	21.01	0.8155	0.3355
150	-23.99	33.31	23.10	1.0067	0.3357
200	-15.55	36.74	25.12	1.2137	0.3354
250	-8.97	40.02	27.06	1.4360	0.3348
300	-3.70	43.18	28.94	1.6732	0.3340
350	0.63	46.23	30.76	1.9249	0.3331
400	4.23	49.17	32.54	2.1909	0.3322
450	7.27	52.02	34.27	2.4707	0.3313
500	9.87	54.78	35.95	2.7642	0.3304
600	14.04	60.09	39.22	3.3909	0.3286
700	17.20	65.13	42.37	4.0695	0.3269
800	19.65	69.95	45.41	4.7982	0.3254
900	21.55	74.58	48.35	5.5757	0.3240
1000	23.05	79.05	51.22	6.4010	0.3226
1500	26.98	99.44	64.61	11.2090	0.3170
2000	28.19	117.59	76.86	17.0866	0.3126
2500	28.70	134.26	88.34	23.9658	0.3089
3000	29.16	149.88	99.25	31.7968	0.3057

Table 16. Properties of the binary mixture of helium and xenon with x_{He}=0.50 and x_{Xe}=0.50 as a function of temperature

T K or °C	B $10^{-3}m^3$/kmol	η μPa s	λ mW/m K	D(1.013 bar) $10^{-4}m^2$/s	α_T
50 K	-2673.89	5.68	9.74	0.0235	0.1578
100	-256.96	9.90	16.56	0.0844	0.3080
150	-106.68	13.76	22.23	0.1724	0.3764
200	-55.82	17.57	27.39	0.2826	0.4115
250	-29.76	21.44	32.28	0.4122	0.4290
300	-15.63	25.32	37.01	0.5597	0.4353
0 °C	-22.16	23.24	34.49	0.4783	0.4331
20	-17.12	24.79	36.39	0.5385	0.4352
40	-13.02	26.33	38.11	0.6014	0.4346
60	-9.55	27.84	39.79	0.6671	0.4343
80	-6.56	29.33	41.46	0.7356	0.4344
100	-3.98	30.78	43.11	0.8067	0.4346
150	1.18	34.29	47.14	0.9958	0.4348
200	5.03	37.65	51.03	1.2006	0.4345
250	8.01	40.86	54.79	1.4206	0.4337
300	10.37	43.96	58.44	1.6553	0.4327
350	12.28	46.95	61.98	1.9045	0.4316
400	13.85	49.84	65.44	2.1678	0.4304
450	15.16	52.65	68.82	2.4448	0.4292
500	16.26	55.37	72.13	2.7354	0.4281
600	17.99	60.62	78.57	3.3561	0.4259
700	19.25	65.62	84.78	4.0282	0.4238
800	20.20	70.42	90.82	4.7500	0.4219
900	20.90	75.04	96.69	5.5203	0.4201
1000	21.43	79.51	102.42	6.3379	0.4184
1500	22.54	100.04	129.40	11.1031	0.4115
2000	22.55	118.48	154.36	16.9303	0.4060
2500	22.33	135.51	177.91	23.7526	0.4014
3000	22.17	151.53	200.39	31.5207	0.3975

Table 17. Properties of the binary mixture of helium and xenon with x_{He}=0.75 and x_{Xe}=0.25 as a function of temperature

T K or °C	B $10^{-3}m^3$/kmol	η μPa s	λ mW/m K	D(1.013 bar) $10^{-4}m^2$/s	α_T
50 K	-672.14	6.42	19.91	0.0234	0.2296
100	-56.79	11.05	33.17	0.0838	0.4421
150	-16.02	15.08	44.01	0.1707	0.5379
200	-2.15	18.89	53.76	0.2791	0.5865
250	4.77	22.61	62.91	0.4068	0.6100
300	8.48	26.25	71.67	0.5522	0.6175
0 °C	6.76	24.31	67.02	0.4719	0.6152
20	8.08	25.76	70.52	0.5313	0.6175
40	9.17	27.19	73.75	0.5933	0.6167
60	10.10	28.59	76.91	0.6582	0.6165
80	10.89	29.96	80.04	0.7257	0.6167
100	11.58	31.31	83.13	0.7959	0.6169
150	12.93	34.55	90.69	0.9825	0.6172
200	13.91	37.66	98.00	1.1846	0.6167
250	14.62	40.66	105.09	1.4018	0.6156
300	15.17	43.54	111.98	1.6336	0.6143
350	15.58	46.34	118.69	1.8797	0.6128
400	15.89	49.05	125.25	2.1398	0.6112
450	16.14	51.69	131.68	2.4135	0.6096
500	16.32	54.27	137.98	2.7006	0.6081
600	16.57	59.25	150.25	3.3139	0.6051
700	16.71	64.03	162.14	3.9781	0.6024
800	16.76	68.63	173.70	4.6917	0.5999
900	16.76	73.09	184.98	5.4532	0.5975
1000	16.73	77.42	196.01	6.2617	0.5953
1500	16.28	97.54	248.18	10.9751	0.5863
2000	15.70	115.87	296.72	16.7417	0.5791
2500	15.17	132.98	342.72	23.4955	0.5732
3000	14.73	149.18	386.79	31.1880	0.5680

Table 18. Properties of the binary mixture of neon and argon with x_{Ne}=0.25 and x_{Ar}=0.75 as a function of temperature

T K or °C	B $10^{-3}m^3$/kmol	η μPa s	λ mW/m K	D(1.013 bar) $10^{-4}m^2$/s	α_T
50 K	-450.58	4.86	4.66	0.0115	0.0188
100	-119.29	9.19	8.77	0.0444	0.0571
150	-51.17	13.50	12.77	0.0949	0.0962
200	-26.03	17.57	16.52	0.1601	0.1217
250	-12.61	21.25	19.91	0.2380	0.1391
300	-4.26	24.63	23.02	0.3273	0.1515
0 °C	-8.31	22.85	21.38	0.2780	0.1453
20	-5.21	24.19	22.61	0.3144	0.1500
40	-2.57	25.48	23.80	0.3525	0.1541
60	-0.29	26.74	24.96	0.3923	0.1577
80	1.70	27.96	26.09	0.4336	0.1608
100	3.43	29.16	27.19	0.4765	0.1635
150	6.95	32.02	29.85	0.5903	0.1690
200	9.60	34.74	32.37	0.7132	0.1727
250	11.65	37.33	34.78	0.8447	0.1751
300	13.27	39.82	37.10	0.9846	0.1765
350	14.57	42.22	39.33	1.1328	0.1770
400	15.64	44.53	41.46	1.2891	0.1765
450	16.53	46.78	43.53	1.4536	0.1769
500	17.27	48.96	45.55	1.6259	0.1777
600	18.39	53.16	49.48	1.9925	0.1790
700	19.15	57.18	53.23	2.3878	0.1795
800	19.67	61.04	56.85	2.8109	0.1791
900	20.04	64.77	60.34	3.2614	0.1784
1000	20.32	68.39	63.72	3.7387	0.1775
1500	21.28	85.20	79.45	6.5116	0.1724
2000	21.66	100.56	93.83	9.8935	0.1684
2500	21.66	114.99	107.33	13.8466	0.1653
3000	21.48	128.71	120.18	18.3419	0.1629

Table 19. Properties of the binary mixture of neon and argon with x_{Ne}=0.50 and x_{Ar}=0.50 as a function of temperature

T K or °C	B $10^{-3}m^3$/kmol	η μPa s	λ mW/m K	D(1.013 bar) $10^{-4}m^2$/s	α_T
50 K	-250.11	5.55	6.34	0.0115	0.0217
100	-64.49	10.65	12.04	0.0444	0.0654
150	-24.66	15.30	17.13	0.0948	0.1095
200	-9.10	19.51	21.68	0.1597	0.1379
250	-0.75	23.29	25.77	0.2373	0.1573
300	4.38	26.74	29.52	0.3262	0.1710
0°C	1.91	24.92	27.55	0.2771	0.1642
20	3.80	26.28	29.03	0.3134	0.1694
40	5.40	27.60	30.46	0.3513	0.1739
60	6.76	28.88	31.86	0.3908	0.1779
80	7.94	30.13	33.22	0.4319	0.1813
100	8.96	31.35	34.55	0.4746	0.1843
150	10.99	34.28	37.76	0.5877	0.1903
200	12.51	37.07	40.81	0.7099	0.1944
250	13.66	39.73	43.74	0.8406	0.1970
300	14.57	42.29	46.57	0.9798	0.1985
350	15.30	44.77	49.30	1.1273	0.1989
400	15.92	47.16	51.90	1.2828	0.1984
450	16.45	49.49	54.42	1.4465	0.1989
500	16.90	51.76	56.91	1.6178	0.1999
600	17.57	56.14	61.75	1.9825	0.2014
700	18.03	60.35	66.41	2.3757	0.2018
800	18.34	64.42	70.91	2.7968	0.2014
900	18.54	68.35	75.27	3.2452	0.2006
1000	18.68	72.18	79.51	3.7203	0.1995
1500	18.99	90.06	99.31	6.4814	0.1938
2000	18.92	106.47	117.51	9.8498	0.1893
2500	18.66	121.89	134.61	13.7875	0.1858
3000	18.34	136.57	150.89	18.2659	0.1831

Table 20. Properties of the binary mixture of neon and argon with x_{Ne}=0.75 and x_{Ar}=0.25 as a function of temperature

T K or °C	B $10^{-3}m^3$/kmol	η μPa s	λ mW/m K	D(1.013 bar) $10^{-4}m^2$/s	α_T
50 K	-112.03	6.46	8.61	0.0115	0.0256
100	-26.39	12.39	16.34	0.0443	0.0764
150	-6.23	17.39	22.80	0.0947	0.1268
200	2.29	21.75	28.41	0.1594	0.1591
250	6.84	25.65	33.43	0.2366	0.1810
300	9.52	29.20	38.02	0.3249	0.1965
0°C	8.24	27.33	35.60	0.2762	0.1889
20	9.22	28.73	37.41	0.3122	0.1947
40	10.03	30.09	39.17	0.3499	0.1998
60	10.72	31.42	40.89	0.3892	0.2042
80	11.29	32.71	42.56	0.4301	0.2081
100	11.78	33.97	44.19	0.4725	0.2115
150	12.76	37.01	48.13	0.5849	0.2182
200	13.51	39.90	51.89	0.7063	0.2227
250	14.08	42.68	55.51	0.8363	0.2256
300	14.53	45.36	59.01	0.9747	0.2271
350	14.89	47.95	62.40	1.1214	0.2275
400	15.20	50.47	65.65	1.2761	0.2271
450	15.47	52.92	68.81	1.4388	0.2278
500	15.69	55.32	71.93	1.6091	0.2289
600	16.02	59.97	77.99	1.9717	0.2306
700	16.23	64.44	83.85	2.3628	0.2310
800	16.36	68.78	89.52	2.7816	0.2305
900	16.42	72.99	95.03	3.2278	0.2295
1000	16.45	77.09	100.39	3.7006	0.2283
1500	16.28	96.34	125.56	6.4492	0.2217
2000	15.93	114.06	148.75	9.8031	0.2166
2500	15.53	130.74	170.56	13.7245	0.2126
3000	15.14	146.61	191.33	18.1849	0.2095

Table 21. Properties of the binary mixture of neon and krypton with x_{Ne}=0.25 and x_{Kr}=0.75 as a function of temperature

T K or °C	B $10^{-3}m^3$/kmol	η μPa s	λ mW/m K	D(1.013 bar) $10^{-4}m^2$/s	α_T
50 K	-1308.38	5.42	3.08	0.0093	0.0312
100	-255.04	9.94	5.62	0.0361	0.0790
150	-118.55	14.35	8.01	0.0776	0.1378
200	-63.61	18.81	10.32	0.1314	0.1772
250	-38.20	23.19	12.53	0.1960	0.2048
300	-23.23	27.27	14.58	0.2703	0.2248
0°C	-30.42	25.11	13.49	0.2293	0.2149
20	-24.91	26.73	14.31	0.2596	0.2224
40	-20.25	28.30	15.10	0.2913	0.2291
60	-16.25	29.82	15.87	0.3244	0.2351
80	-12.78	31.31	16.62	0.3588	0.2403
100	-9.75	32.77	17.36	0.3946	0.2450
150	-3.60	36.26	19.13	0.4894	0.2544
200	1.07	39.58	20.82	0.5918	0.2614
250	4.73	42.74	22.45	0.7014	0.2663
300	7.67	45.78	24.02	0.8180	0.2696
350	10.08	48.70	25.53	0.9413	0.2715
400	12.11	51.52	27.01	1.0712	0.2724
450	13.83	54.25	28.38	1.2078	0.2716
500	15.29	56.90	29.74	1.3510	0.2716
600	17.63	61.99	32.37	1.6563	0.2718
700	19.34	66.84	34.89	1.9860	0.2715
800	20.61	71.49	37.32	2.3394	0.2709
900	21.55	75.97	39.66	2.7158	0.2699
1000	22.25	80.30	41.93	3.1147	0.2689
1500	23.88	100.27	52.46	5.4326	0.2633
2000	24.61	118.28	62.02	8.2575	0.2587
2500	25.04	135.05	70.94	11.5567	0.2550
3000	25.16	150.98	79.43	15.3059	0.2520

Table 22. Properties of the binary mixture of neon and krypton with x_{Ne}=0.50 and x_{Kr}=0.50 as a function of temperature

T K or °C	B $10^{-3}m^3$/kmol	η μPa s	λ mW/m K	D(1.013 bar) $10^{-4}m^2$/s	α_T
50 K	-642.44	5.99	4.81	0.0093	0.0374
100	-127.76	11.28	8.89	0.0361	0.0950
150	-55.87	16.13	12.51	0.0775	0.1650
200	-26.31	20.74	15.79	0.1310	0.2116
250	-12.18	25.10	18.81	0.1952	0.2440
300	-3.83	29.13	21.60	0.2688	0.2673
0°C	-7.83	27.01	20.13	0.2201	0.2557
20	-4.76	28.60	21.23	0.2582	0.2645
40	-2.17	30.14	22.30	0.2896	0.2723
60	0.03	31.65	23.35	0.3225	0.2792
80	1.93	33.11	24.37	0.3566	0.2852
100	3.58	34.54	25.37	0.3920	0.2906
150	6.89	37.97	27.78	0.4860	0.3015
200	9.38	41.23	30.08	0.5875	0.3094
250	11.31	44.35	32.30	0.6961	0.3149
300	12.84	47.34	34.45	0.8117	0.3185
350	14.09	50.23	36.54	0.9339	0.3205
400	15.14	53.02	38.58	1.0628	0.3213
450	16.05	55.72	40.47	1.1983	0.3204
500	16.84	58.36	42.34	1.3404	0.3203
600	18.09	63.44	45.99	1.6433	0.3204
700	19.00	68.30	49.52	1.9705	0.3201
800	19.66	72.99	52.92	2.3212	0.3192
900	20.14	77.51	56.22	2.6948	0.3180
1000	20.48	81.90	59.43	3.0909	0.3167
1500	21.11	102.31	74.43	5.3927	0.3100
2000	21.19	120.87	88.17	8.1990	0.3045
2500	21.11	138.23	101.06	11.4771	0.3002
3000	20.91	154.74	113.33	15.2029	0.2966

Table 23. Properties of the binary mixture of neon and krypton with x_{Ne}=0.75 and x_{Kr}=0.25 as a function of temperature

T K or °C	B $10^{-3}m^3$/kmol	η μPa s	λ mW/m K	D(1.013 bar) $10^{-4}m^2/s$	α_T
50 K	-218.44	6.74	7.44	0.0093	0.0468
100	-44.42	12.87	13.85	0.0361	0.1193
150	-14.98	18.11	19.25	0.0773	0.2059
200	-2.39	22.80	23.96	0.1305	0.2629
250	3.94	27.07	28.21	0.1942	0.3022
300	7.63	30.99	32.11	0.2672	0.3304
0°C	5.87	28.93	30.05	0.2269	0.3164
20	7.23	30.47	31.59	0.2567	0.3270
40	8.35	31.97	33.09	0.2878	0.3364
60	9.30	33.43	34.55	0.3203	0.3447
80	10.11	34.86	35.97	0.3541	0.3520
100	10.80	36.24	37.36	0.3892	0.3584
150	12.18	39.58	40.73	0.4822	0.3714
200	13.23	42.76	43.96	0.5827	0.3806
250	14.03	45.81	47.07	0.6902	0.3869
300	14.66	48.74	50.08	0.8046	0.3909
350	15.17	51.58	53.02	0.9258	0.3929
400	15.60	54.33	55.90	1.0536	0.3933
450	15.97	57.01	58.59	1.1879	0.3924
500	16.29	59.63	61.25	1.3287	0.3923
600	16.79	64.69	66.45	1.6289	0.3922
700	17.14	69.56	71.48	1.9533	0.3916
800	17.37	74.27	76.35	2.3011	0.3903
900	17.52	78.84	81.09	2.6717	0.3888
1000	17.60	83.29	85.70	3.0646	0.3870
1500	17.54	104.10	107.34	5.3488	0.3786
2000	17.22	123.21	127.27	8.1346	0.3718
2500	16.85	141.15	146.02	11.3896	0.3664
3000	16.47	158.22	163.87	15.0898	0.3620

Table 24. Properties of the binary mixture of neon and xenon with x_{Ne}=0.25 and x_{Xe}=0.75 as a function of temperature

T K or °C	B $10^{-3}m^3$/kmol	η μPa s	λ mW/m K	D(1.013 bar) $10^{-4}m^2/s$	α_T
50 K	-6058.39	5.22	2.26	0.0079	0.0470
100	-611.11	9.42	4.05	0.0305	0.0877
150	-273.27	13.35	5.69	0.0656	0.1524
200	-157.70	17.26	7.23	0.1113	0.1957
250	-97.62	21.23	8.73	0.1661	0.2262
300	-64.84	25.23	10.19	0.2291	0.2482
0°C	-79.98	23.09	9.41	0.1943	0.2372
20	-68.29	24.69	9.99	0.2200	0.2456
40	-58.83	26.28	10.56	0.2470	0.2530
60	-50.87	27.84	11.12	0.2751	0.2596
80	-44.08	29.36	11.67	0.3044	0.2655
100	-38.21	30.86	12.21	0.3347	0.2707
150	-26.51	34.47	13.51	0.4153	0.2813
200	-17.74	37.91	14.76	0.5024	0.2891
250	-10.92	41.20	15.96	0.5955	0.2947
300	-5.45	44.36	17.13	0.6945	0.2986
350	-0.95	47.41	18.26	0.7992	0.3010
400	2.84	50.35	19.35	0.9096	0.3021
450	6.07	53.19	20.26	1.0259	0.2996
500	8.87	55.95	21.22	1.1480	0.3017
600	13.41	61.25	23.16	1.4078	0.3082
700	16.89	66.30	25.06	1.6867	0.3129
800	19.60	71.12	26.88	1.9842	0.3152
900	21.73	75.76	28.62	2.2999	0.3157
1000	23.41	80.23	30.31	2.6335	0.3151
1500	27.93	100.72	38.04	4.5633	0.3070
2000	29.43	119.03	45.01	6.9090	0.2993
2500	30.11	135.89	51.48	9.6460	0.2934
3000	30.67	151.70	57.60	12.7546	0.2889

Table 25. Properties of the binary mixture of neon and xenon with x_{Ne}=0.50 and x_{Xe}=0.50 as a function of temperature

T K or °C	B $10^{-3}m^3$/kmol	η μPa s	λ mW/m K	D(1.013 bar) $10^{-4}m^2/s$	α_T
50 K	-2765.32	5.83	3.92	0.0079	0.0581
100	-288.95	10.83	7.12	0.0305	0.1092
150	-125.54	15.32	9.95	0.0655	0.1893
200	-68.09	19.57	12.48	0.1108	0.2425
250	-38.02	23.71	14.83	0.1652	0.2797
300	-21.44	27.76	17.05	0.2277	0.3065
0°C	-29.13	25.60	15.87	0.1932	0.2932
20	-23.19	27.21	16.75	0.2187	0.3033
40	-18.37	28.80	17.61	0.2454	0.3123
60	-14.33	30.35	18.45	0.2732	0.3203
80	-10.88	31.86	19.27	0.3022	0.3273
100	-7.91	33.34	20.07	0.3322	0.3336
150	-2.01	36.91	22.01	0.4120	0.3463
200	2.37	40.30	23.88	0.4981	0.3555
250	5.75	43.54	25.68	0.5902	0.3621
300	8.44	46.66	27.43	0.6883	0.3665
350	10.64	49.66	29.14	0.7920	0.3691
400	12.51	52.57	30.81	0.9013	0.3701
450	14.12	55.39	32.11	1.0164	0.3679
500	15.52	58.12	33.53	1.1372	0.3706
600	17.80	63.39	36.47	1.3940	0.3785
700	19.53	68.42	39.37	1.6699	0.3839
800	20.86	73.25	42.16	1.9643	0.3865
900	21.89	77.91	44.86	2.2769	0.3869
1000	22.69	82.42	47.47	2.6074	0.3860
1500	24.63	103.25	59.53	4.5210	0.3759
2000	25.04	122.06	70.50	6.8485	0.3664
2500	25.05	139.51	80.77	9.5649	0.3592
3000	25.02	155.97	90.53	12.6507	0.3536

Table 26. Properties of the binary mixture of neon and xenon with x_{Ne}=0.75 and x_{Xe}=0.25 as a function of temperature

T K or °C	B $10^{-3}m^3$/kmol	η μPa s	λ mW/m K	D(1.013 bar) $10^{-4}m^2/s$	α_T
50 K	-757.98	6.67	6.65	0.0079	0.0762
100	-86.92	12.65	12.21	0.0305	0.1447
150	-33.07	17.76	16.92	0.0653	0.2496
200	-12.80	22.33	21.03	0.1104	0.3188
250	-2.10	26.58	24.74	0.1642	0.3668
300	3.90	30.57	28.17	0.2260	0.4012
0°C	1.10	28.46	26.36	0.1919	0.3841
20	3.26	30.04	27.72	0.2171	0.3971
40	5.02	31.59	29.04	0.2435	0.4086
60	6.49	33.09	30.33	0.2710	0.4187
80	7.73	34.56	31.59	0.2997	0.4276
100	8.80	35.99	32.82	0.3293	0.4355
150	10.91	39.44	35.80	0.4081	0.4514
200	12.48	42.72	38.66	0.4932	0.4629
250	13.69	45.87	41.43	0.5842	0.4708
300	14.64	48.90	44.12	0.6811	0.4758
350	15.41	51.82	46.75	0.7837	0.4786
400	16.06	54.66	49.31	0.8919	0.4792
450	16.63	57.42	51.41	1.0057	0.4780
500	17.12	60.10	53.65	1.1249	0.4821
600	17.91	65.30	58.23	1.3783	0.4921
700	18.49	70.28	62.73	1.6507	0.4987
800	18.91	75.09	67.10	1.9416	0.5014
900	19.21	79.75	71.32	2.2508	0.5016
1000	19.42	84.28	75.43	2.5778	0.5002
1500	19.71	105.39	94.53	4.4729	0.4865
2000	19.46	124.70	112.05	6.7795	0.4741
2500	19.10	142.75	128.50	9.4726	0.4648
3000	18.75	159.88	144.17	12.5326	0.4576

Table 27. Properties of the binary mixture of argon and krypton with x_{Ar}=0.25 and x_{Kr}=0.75 as a function of temperature

T K or °C	B $10^{-3}m^3$/kmol	η μPa s	λ mW/m K	D(1.013 bar) $10^{-4}m^2$/s	α_T
50 K	-1734.05	4.84	2.12	0.0044	0.0662
100	-357.72	8.70	3.84	0.0165	0.0272
150	-168.34	12.75	5.62	0.0365	0.0178
200	-95.11	17.03	7.47	0.0642	0.0318
250	-61.01	21.25	9.29	0.0988	0.0525
300	-40.69	25.20	10.99	0.1397	0.0700
0°C	-50.48	23.11	10.09	0.1170	0.0610
20	-42.98	24.67	10.77	0.1337	0.0678
40	-36.60	26.19	11.42	0.1514	0.0741
60	-31.10	27.68	12.06	0.1700	0.0800
80	-26.31	29.12	12.69	0.1895	0.0855
100	-22.09	30.53	13.30	0.2098	0.0907
150	-13.47	33.92	14.76	0.2644	0.1023
200	-6.83	37.14	16.16	0.3239	0.1122
250	-1.59	40.21	17.49	0.3881	0.1207
300	2.64	43.14	18.77	0.4568	0.1281
350	6.11	45.97	20.00	0.5298	0.1346
400	8.98	48.69	21.18	0.6069	0.1402
450	11.38	51.32	22.33	0.6880	0.1452
500	13.40	53.87	23.44	0.7729	0.1496
600	16.55	58.75	25.57	0.9537	0.1568
700	18.84	63.39	27.60	1.1486	0.1624
800	20.52	67.83	29.54	1.3569	0.1668
900	21.77	72.09	31.41	1.5781	0.1701
1000	22.71	76.20	33.21	1.8118	0.1725
1500	25.23	95.03	41.53	3.1583	0.1755
2000	26.73	111.95	48.95	4.7926	0.1669
2500	27.67	127.71	55.84	6.7112	0.1611
3000	28.12	142.68	62.39	8.8982	0.1581

Table 28. Properties of the binary mixture of argon and krypton with x_{Ar}=0.50 and x_{Kr}=0.50 as a function of temperature

T K or °C	B $10^{-3}m^3$/kmol	η μPa s	λ mW/m K	D(1.013 bar) $10^{-4}m^2$/s	α_T
50 K	-1322.86	4.69	2.45	0.0044	0.0705
100	-295.62	8.52	4.49	0.0165	0.0289
150	-137.24	12.58	6.62	0.0365	0.0190
200	-77.74	16.81	8.79	0.0642	0.0341
250	-49.07	20.87	10.87	0.0988	0.0563
300	-31.70	24.65	12.80	0.1396	0.0749
0°C	-40.09	22.65	11.78	0.1169	0.0653
20	-33.67	24.14	12.54	0.1336	0.0725
40	-28.19	25.60	13.28	0.1513	0.0793
60	-23.45	27.01	14.01	0.1698	0.0856
80	-19.31	28.39	14.71	0.1893	0.0915
100	-15.66	29.73	15.40	0.2096	0.0970
150	-8.19	32.96	17.06	0.2639	0.1093
200	-2.45	36.02	18.63	0.3233	0.1198
250	2.07	38.94	20.13	0.3872	0.1289
300	5.71	41.73	21.57	0.4556	0.1368
350	8.68	44.41	22.95	0.5283	0.1436
400	11.12	47.00	24.29	0.6050	0.1496
450	13.14	49.50	25.58	0.6856	0.1549
500	14.83	51.93	26.83	0.7701	0.1595
600	17.44	56.57	29.24	0.9499	0.1672
700	19.30	60.99	31.53	1.1436	0.1731
800	20.64	65.22	33.72	1.3506	0.1777
900	21.63	69.28	35.84	1.5705	0.1811
1000	22.37	73.20	37.88	1.8029	0.1836
1500	24.57	91.20	47.35	3.1424	0.1863
2000	25.93	107.45	55.84	4.7707	0.1769
2500	26.67	122.63	63.73	6.6822	0.1708
3000	26.96	137.07	71.24	8.8607	0.1676

Table 29. Properties of the binary mixture of argon and krypton with x_{Ar}=0.75 and x_{Kr}=0.25 as a function of temperature

T K or °C	B $10^{-3}m^3$/kmol	η μPa s	λ mW/m K	D(1.013 bar) $10^{-4}m^2$/s	α_T
50 K	-982.66	4.52	2.86	0.0044	0.0756
100	-239.98	8.28	5.27	0.0165	0.0309
150	-109.71	12.32	7.84	0.0365	0.0205
200	-62.20	16.45	10.41	0.0642	0.0369
250	-38.32	20.31	12.81	0.0987	0.0608
300	-23.60	23.88	15.03	0.1395	0.0809
0°C	-30.74	22.00	13.86	0.1168	0.0705
20	-25.28	23.41	14.74	0.1335	0.0783
40	-20.61	24.78	15.59	0.1511	0.0856
60	-16.56	26.11	16.42	0.1697	0.0924
80	-13.02	27.41	17.23	0.1890	0.0987
100	-9.89	28.68	18.02	0.2093	0.1046
150	-3.49	31.72	19.92	0.2635	0.1178
200	1.43	34.60	21.72	0.3226	0.1291
250	5.29	37.34	23.44	0.3862	0.1389
300	8.38	39.97	25.08	0.4543	0.1473
350	10.87	42.50	26.66	0.5266	0.1546
400	12.91	44.93	28.19	0.6029	0.1611
450	14.59	47.29	29.66	0.6831	0.1667
500	15.97	49.57	31.09	0.7670	0.1716
600	18.08	53.95	33.84	0.9457	0.1798
700	19.55	58.11	36.46	1.1382	0.1861
800	20.59	62.10	38.97	1.3439	0.1909
900	21.35	65.94	41.38	1.5624	0.1945
1000	21.93	69.64	43.72	1.7933	0.1970
1500	23.88	86.69	54.55	3.1253	0.1992
2000	25.07	102.14	64.33	4.7472	0.1889
2500	25.61	116.62	73.45	6.6511	0.1824
3000	25.77	130.39	82.13	8.8208	0.1790

Table 30. Properties of the binary mixture of argon and xenon with x_{Ar}=0.25 and x_{Xe}=0.75 as a function of temperature

T K or °C	B $10^{-3}m^3$/kmol	η μPa s	λ mW/m K	D(1.013 bar) $10^{-4}m^2$/s	α_T
50 K	-6719.52	4.75	1.48	0.0037	0.1198
100	-753.26	8.38	2.65	0.0134	0.0687
150	-343.23	12.00	3.82	0.0295	0.0374
200	-200.97	15.78	4.98	0.0518	0.0359
250	-128.98	19.66	6.15	0.0799	0.0603
300	-89.03	23.55	7.32	0.1133	0.0841
0°C	-107.64	21.47	6.69	0.0947	0.0718
20	-93.29	23.02	7.16	0.1084	0.0810
40	-81.56	24.56	7.62	0.1229	0.0897
60	-71.62	26.08	8.07	0.1382	0.0979
80	-63.08	27.56	8.51	0.1542	0.1056
100	-55.66	29.01	8.94	0.1709	0.1128
150	-40.71	32.52	9.99	0.2159	0.1291
200	-29.38	35.85	10.98	0.2650	0.1431
250	-20.49	39.05	11.94	0.3182	0.1553
300	-13.32	42.11	12.85	0.3752	0.1660
350	-7.43	45.06	13.74	0.4359	0.1754
400	-2.51	47.90	14.59	0.5000	0.1837
450	1.65	50.65	15.42	0.5676	0.1911
500	5.19	53.31	16.22	0.6384	0.1976
600	10.88	58.42	17.76	0.7893	0.2087
700	15.19	63.26	19.22	0.9522	0.2175
800	18.50	67.89	20.63	1.1264	0.2245
900	21.08	72.32	21.98	1.3115	0.2301
1000	23.12	76.59	23.28	1.5070	0.2345
1500	28.74	96.08	29.27	2.6321	0.2440
2000	31.16	113.42	34.67	3.9885	0.2392
2500	32.52	129.39	39.57	5.5731	0.2318
3000	33.53	144.40	44.19	7.3769	0.2270

Table 31. Properties of the binary mixture of argon and xenon with x_{Ar}=0.50 and x_{Xe}=0.50 as a function of temperature

T K or °C	B $10^{-3}m^3$/kmol	η μPa s	λ mW/m K	D(1.013 bar) $10^{-4}m^2$/s	α_T
50 K	-3759.68	4.70	1.92	0.0037	0.1338
100	-509.46	8.37	3.51	0.0134	0.0768
150	-233.79	12.14	5.13	0.0295	0.0420
200	-135.22	16.06	6.72	0.0517	0.0406
250	-86.32	19.98	8.24	0.0799	0.0683
300	-58.28	23.78	9.73	0.1132	0.0952
0°C	-71.52	21.76	8.94	0.0947	0.0813
20	-61.34	23.27	9.53	0.1083	0.0918
40	-52.88	24.76	10.11	0.1228	0.1016
60	-45.66	26.21	10.67	0.1380	0.1108
80	-39.41	27.63	11.23	0.1540	0.1194
100	-33.95	29.02	11.77	0.1707	0.1275
150	-22.89	32.36	13.06	0.2155	0.1458
200	-14.45	35.54	14.30	0.2644	0.1615
250	-7.82	38.58	15.48	0.3174	0.1752
300	-2.48	41.49	16.62	0.3740	0.1872
350	1.90	44.28	17.71	0.4343	0.1977
400	5.53	46.98	18.76	0.4981	0.2070
450	8.57	49.59	19.79	0.5652	0.2152
500	11.15	52.12	20.78	0.6355	0.2225
600	15.22	56.96	22.68	0.7853	0.2347
700	18.24	61.56	24.50	0.9469	0.2445
800	20.51	65.95	26.24	1.1197	0.2523
900	22.24	70.17	27.92	1.3033	0.2584
1000	23.59	74.24	29.55	1.4972	0.2632
1500	27.37	92.84	37.06	2.6137	0.2732
2000	29.26	109.51	43.91	3.9622	0.2670
2500	30.31	124.96	50.15	5.5383	0.2587
3000	30.95	139.56	56.05	7.3323	0.2534

Table 32. Properties of the binary mixture of argon and xenon with x_{Ar}=0.75 and x_{Xe}=0.25 as a function of temperature

T K or °C	B $10^{-3}m^3$/kmol	η μPa s	λ mW/m K	D(1.013 bar) $10^{-4}m^2$/s	α_T
50 K	-1757.66	4.57	2.53	0.0036	0.1522
100	-321.97	8.27	4.65	0.0134	0.0873
150	-147.97	12.17	6.88	0.0295	0.0481
200	-84.39	16.18	9.07	0.0517	0.0469
250	-52.91	20.04	11.11	0.0798	0.0791
300	-34.07	23.66	13.05	0.1131	0.1101
0°C	-43.11	21.74	12.02	0.0946	0.0941
20	-36.18	23.18	12.79	0.1083	0.1062
40	-30.32	24.58	13.54	0.1227	0.1175
60	-25.27	25.95	14.26	0.1379	0.1281
80	-20.87	27.28	14.97	0.1538	0.1380
100	-17.00	28.58	15.67	0.1704	0.1474
150	-9.10	31.71	17.33	0.2150	0.1683
200	-3.06	34.67	18.91	0.2638	0.1864
250	1.69	37.50	20.42	0.3164	0.2020
300	5.51	40.20	21.86	0.3727	0.2157
350	8.60	42.81	23.25	0.4326	0.2277
400	11.15	45.32	24.60	0.4959	0.2383
450	13.26	47.74	25.90	0.5625	0.2477
500	15.03	50.09	27.16	0.6323	0.2560
600	17.75	54.60	29.50	0.7809	0.2699
700	19.70	58.89	31.89	0.9411	0.2809
800	21.13	62.98	34.10	1.1123	0.2897
900	22.19	66.92	36.23	1.2942	0.2965
1000	23.00	70.73	38.30	1.4864	0.3018
1500	25.51	88.19	47.87	2.5936	0.3121
2000	26.92	103.95	56.64	3.9334	0.3039
2500	27.64	118.66	64.69	5.5003	0.2943
3000	27.95	132.61	72.34	7.2837	0.2883

Table 33. Properties of the binary mixture of krypton and xenon with x_{Kr}=0.25 and x_{Xe}=0.75 as a function of temperature

T K or °C	B $10^{-3}m^3$/kmol	η μPa s	λ mW/m K	D(1.013 bar) $10^{-4}m^2$/s	α_T
50 K	-7662.88	4.82	1.28	0.0025	0.0634
100	-856.20	8.46	2.25	0.0091	0.0416
150	-393.72	12.05	3.20	0.0197	0.0249
200	-230.23	15.82	4.21	0.0346	0.0164
250	-148.03	19.77	5.25	0.0535	0.0180
300	-103.30	23.76	6.30	0.0763	0.0280
0°C	-124.16	21.62	5.74	0.0636	0.0221
20	-108.08	23.22	6.16	0.0730	0.0265
40	-94.93	24.80	6.57	0.0829	0.0307
60	-83.81	26.35	6.98	0.0934	0.0347
80	-74.26	27.87	7.38	0.1044	0.0385
100	-65.97	29.36	7.77	0.1159	0.0421
150	-49.29	32.95	8.72	0.1469	0.0504
200	-36.66	36.37	9.62	0.1809	0.0577
250	-26.74	39.65	10.48	0.2179	0.0641
300	-18.73	42.79	11.31	0.2575	0.0698
350	-12.13	45.81	12.11	0.2998	0.0749
400	-6.60	48.73	12.88	0.3447	0.0794
450	-1.91	51.55	13.63	0.3919	0.0835
500	2.10	54.29	14.35	0.4415	0.0872
600	8.57	59.52	15.74	0.5474	0.0935
700	13.50	64.49	17.06	0.6619	0.0987
800	17.33	69.23	18.31	0.7845	0.1030
900	20.33	73.77	19.52	0.9148	0.1066
1000	22.71	78.15	20.68	1.0526	0.1095
1500	29.13	98.08	25.98	1.8458	0.1179
2000	31.64	115.77	30.69	2.8000	0.1196
2500	33.22	132.02	35.03	3.9075	0.1142
3000	34.45	147.28	39.07	5.1740	0.1082

Table 34. Properties of the binary mixture of krypton and xenon with x_{Kr}=0.50 and x_{Xe}=0.50 as a function of temperature

T K or °C	B $10^{-3}m^3$/kmol	η μPa s	λ mW/m K	D(1.013 bar) $10^{-4}m^2$/s	α_T
50 K	-5267.95	4.88	1.44	0.0025	0.0669
100	-685.95	8.59	2.55	0.0091	0.0440
150	-320.66	12.30	3.66	0.0197	0.0264
200	-185.21	16.23	4.83	0.0346	0.0175
250	-119.28	20.33	6.03	0.0535	0.0191
300	-83.00	24.37	7.21	0.0763	0.0298
0°C	-100.12	22.22	6.58	0.0636	0.0236
20	-86.96	23.83	7.06	0.0730	0.0283
40	-76.04	25.41	7.52	0.0829	0.0327
60	-66.76	26.96	7.97	0.0933	0.0370
80	-58.75	28.47	8.42	0.1043	0.0410
100	-51.77	29.95	8.85	0.1158	0.0449
150	-37.66	33.52	9.90	0.1468	0.0536
200	-26.91	36.91	10.89	0.1808	0.0613
250	-18.44	40.16	11.85	0.2177	0.0681
300	-11.60	43.26	12.76	0.2572	0.0742
350	-5.95	46.25	13.64	0.2994	0.0795
400	-1.24	49.14	14.49	0.3441	0.0843
450	2.76	51.92	15.31	0.3912	0.0887
500	6.16	54.62	16.11	0.4407	0.0926
600	11.63	59.79	17.63	0.5462	0.0992
700	15.76	64.70	19.08	0.6602	0.1047
800	18.93	69.38	20.46	0.7823	0.1093
900	21.38	73.88	21.79	0.9121	0.1130
1000	23.29	78.20	23.07	1.0492	0.1162
1500	28.34	97.94	28.92	1.8388	0.1249
2000	30.46	115.51	34.14	2.7892	0.1266
2500	31.93	131.69	38.97	3.8939	0.1206
3000	32.95	146.96	43.48	5.1576	0.1143

Table 35. Properties of the binary mixture of krypton and xenon with $x_{Kr}=0.75$ and $x_{Xe}=0.25$ as a function of temperature

T K or °C	B $10^{-3}m^3/kmol$	η μPa s	λ mW/m K	D(1.013 bar) $10^{-4}m^2/s$	α_T
50 K	-3452.41	4.93	1.63	0.0025	0.0710
100	-542.64	8.71	2.89	0.0091	0.0467
150	-257.09	12.57	4.18	0.0197	0.0281
200	-146.57	16.68	5.55	0.0346	0.0187
250	-94.65	20.91	6.94	0.0535	0.0205
300	-65.43	24.99	8.28	0.0763	0.0319
0°C	-79.37	22.83	7.57	0.0636	0.0253
20	-68.67	24.44	8.10	0.0730	0.0303
40	-59.68	26.02	8.62	0.0829	0.0351
60	-52.00	27.57	9.13	0.0933	0.0396
80	-45.34	29.07	9.62	0.1043	0.0439
100	-39.51	30.55	10.11	0.1158	0.0480
150	-27.67	34.09	11.28	0.1467	0.0574
200	-18.60	37.46	12.39	0.1806	0.0656
250	-11.43	40.68	13.45	0.2174	0.0728
300	-5.63	43.76	14.46	0.2569	0.0793
350	-0.86	46.72	15.44	0.2990	0.0850
400	3.13	49.58	16.39	0.3435	0.0901
450	6.49	52.34	17.30	0.3905	0.0947
500	9.35	55.02	18.18	0.4397	0.0988
600	13.91	60.14	19.87	0.5448	0.1059
700	17.31	65.00	21.48	0.6584	0.1118
800	19.89	69.64	23.02	0.7799	0.1166
900	21.86	74.09	24.49	0.9091	0.1206
1000	23.37	78.39	25.91	1.0456	0.1239
1500	27.25	97.99	32.42	1.8314	0.1331
2000	29.07	115.48	38.23	2.7777	0.1347
2500	30.40	131.66	43.63	3.8793	0.1280
3000	31.22	146.98	48.70	5.1401	0.1214

Table 36. Properties of the equimolar ternary mixture of helium, neon and argon as a function of temperature

T K or °C	B $10^{-3}m^3/kmol$	η μPa s	λ mW/m K
50 K	-115.03	6.01	13.09
100	-24.28	11.11	22.94
150	-4.36	15.58	31.23
200	3.35	19.56	38.58
250	7.44	23.15	45.22
300	9.93	26.43	51.54
0°C	8.73	24.70	48.19
20	9.64	26.00	50.69
40	10.42	27.26	53.00
60	11.10	28.49	55.26
80	11.67	29.69	57.52
100	12.17	30.86	59.75
150	13.16	33.68	65.20
200	13.87	36.38	70.44
250	14.39	38.97	75.49
300	14.79	41.47	80.38
350	15.09	43.89	85.13
400	15.33	46.24	89.72
450	15.52	48.53	94.20
500	15.67	50.76	98.60
600	15.87	55.09	107.17
700	15.96	59.26	115.46
800	15.99	63.30	123.50
900	15.97	67.21	131.33
1000	15.93	71.03	138.98
1500	15.61	88.91	175.04
2000	15.20	105.39	208.48
2500	14.78	120.91	240.10
3000	14.38	135.70	270.35

Table 37. Properties of the equimolar ternary mixture of helium, neon and krypton as a function of temperature

T K or °C	B $10^{-3}m^3/kmol$	η μPa s	λ mW/m K
50 K	-291.04	6.44	11.22
100	-52.49	11.81	19.48
150	-17.86	16.57	26.41
200	-3.73	21.01	32.61
250	3.01	25.17	38.27
300	6.96	29.01	43.68
0°C	5.06	26.98	40.81
20	6.52	28.50	42.95
40	7.75	29.97	45.07
60	8.80	31.41	47.20
80	9.71	32.81	49.22
100	10.50	34.17	51.16
150	12.08	37.47	55.80
200	13.24	40.61	60.24
250	14.12	43.63	64.54
300	14.79	46.53	68.73
350	15.33	49.34	72.82
400	15.76	52.06	76.82
450	16.12	54.71	80.68
500	16.42	57.30	84.48
600	16.87	62.29	91.90
700	17.16	67.08	99.08
800	17.34	71.70	106.06
900	17.43	76.19	112.86
1000	17.47	80.54	119.50
1500	17.25	100.87	150.76
2000	16.87	119.46	179.72
2500	16.50	136.89	207.08
3000	16.12	153.49	233.23

Table 38. Properties of the equimolar ternary mixture of helium, neon and xenon as a function of temperature

T K or °C	B $10^{-3}m^3/kmol$	η μPa s	λ mW/m K
50 K	-1235.59	6.31	9.90
100	-123.55	11.48	17.07
150	-47.81	16.00	23.09
200	-21.15	20.21	28.46
250	-7.28	24.26	33.39
300	0.38	28.17	38.14
0°C	-3.18	26.09	35.62
20	-0.44	27.64	37.51
40	1.81	29.18	39.29
60	3.70	30.67	41.02
80	5.32	32.14	42.73
100	6.71	33.57	44.41
150	9.46	37.01	48.49
200	11.48	40.30	52.43
250	13.01	43.46	56.24
300	14.20	46.49	59.94
350	15.16	49.42	63.54
400	15.96	52.26	67.06
450	16.63	55.02	70.29
500	17.20	57.71	73.55
600	18.09	62.89	80.02
700	18.74	67.86	86.31
800	19.20	72.63	92.42
900	19.53	77.25	98.36
1000	19.75	81.73	104.15
1500	20.05	102.53	131.34
2000	19.77	121.43	156.48
2500	19.40	139.03	180.19
3000	19.06	155.68	202.85

Table 39. Properties of the equimolar ternary mixture of helium, argon and krypton as a function of temperature

T K or °C	B $10^{-3}m^3$/kmol	η μPa s	λ mW/m K
50 K	-598.24	5.25	8.18
100	-128.04	9.45	14.21
150	-53.70	13.62	19.49
200	-25.77	17.79	24.36
250	-12.43	21.74	28.94
300	-4.39	25.40	33.28
0°C	-8.28	23.47	30.97
20	-5.31	24.91	32.69
40	-2.75	26.32	34.32
60	-0.53	27.69	35.94
80	1.42	29.03	37.51
100	3.13	30.33	39.04
150	6.65	33.47	42.73
200	9.32	36.45	46.26
250	11.41	39.30	49.66
300	13.07	42.04	52.95
350	14.39	44.69	56.16
400	15.47	47.24	59.28
450	16.34	49.71	62.33
500	17.06	52.12	65.31
600	18.12	56.75	71.10
700	18.84	61.17	76.68
800	19.32	65.41	82.09
900	19.65	69.50	87.35
1000	19.86	73.46	92.48
1500	20.28	91.78	116.60
2000	20.43	108.42	138.83
2500	20.37	124.01	159.78
3000	20.17	138.85	179.82

Table 40. Properties of the equimolar ternary mixture of helium, argon and xenon as a function of temperature

T K or °C	B $10^{-3}m^3$/kmol	η μPa s	λ mW/m K
50 K	-1682.32	5.25	7.29
100	-222.50	9.31	12.61
150	-95.60	13.25	17.22
200	-50.17	17.21	21.44
250	-27.79	21.09	25.41
300	-14.96	24.81	29.23
0°C	-21.03	22.83	27.20
20	-16.37	24.31	28.72
40	-12.47	25.77	30.09
60	-9.12	27.19	31.42
80	-6.22	28.57	32.76
100	-3.68	29.93	34.09
150	1.45	33.20	37.35
200	5.34	36.31	40.49
250	8.37	39.29	43.51
300	10.79	42.15	46.42
350	12.75	44.91	49.25
400	14.35	47.57	52.01
450	15.67	50.15	54.69
500	16.78	52.66	57.32
600	18.49	57.48	62.41
700	19.71	62.07	67.32
800	20.59	66.48	72.07
900	21.23	70.72	76.70
1000	21.70	74.82	81.20
1500	22.77	93.71	102.41
2000	23.10	110.75	122.02
2500	23.13	126.61	140.42
3000	23.05	141.63	157.99

Table 41. Properties of the equimolar ternary mixture of helium, krypton and xenon as a function of temperature

T K or °C	B $10^{-3}m^3$/kmol	η μPa s	λ mW/m K
50 K	-2354.30	5.41	6.49
100	-301.03	9.52	11.16
150	-133.84	13.45	15.14
200	-71.83	17.47	18.84
250	-41.79	21.56	22.38
300	-25.27	25.55	25.80
0°C	-33.08	23.43	23.98
20	-27.08	25.01	25.34
40	-22.08	26.57	26.64
60	-17.80	28.09	27.94
80	-14.11	29.57	29.19
100	-10.88	31.03	30.40
150	-4.37	34.53	33.29
200	0.56	37.87	36.07
250	4.42	41.07	38.76
300	7.52	44.13	41.36
350	10.04	47.09	43.90
400	12.13	49.95	46.37
450	13.87	52.71	48.79
500	15.35	55.40	51.16
600	17.67	60.56	55.75
700	19.37	65.47	60.18
800	20.64	70.17	64.47
900	21.59	74.69	68.64
1000	22.31	79.06	72.70
1500	23.90	99.12	91.76
2000	24.29	117.11	109.30
2500	24.48	133.76	125.82
3000	24.55	149.51	141.55

Table 42. Properties of the equimolar ternary mixture of neon, argon and krypton as a function of temperature

T K or °C	B $10^{-3}m^3$/kmol	η μPa s	λ mW/m K
50 K	-655.07	5.36	4.25
100	-147.71	10.09	7.95
150	-65.16	14.64	11.37
200	-33.11	19.03	14.54
250	-17.24	23.13	17.46
300	-7.64	26.91	20.15
0 °C	-12.27	24.92	18.73
20	-8.73	26.41	19.80
40	-5.72	27.86	20.83
60	-3.13	29.26	21.84
80	-0.89	30.64	22.82
100	1.07	31.97	23.78
150	5.02	35.18	26.09
200	8.01	38.23	28.29
250	10.32	41.14	30.41
300	12.17	43.93	32.45
350	13.67	46.62	34.43
400	14.93	49.21	36.33
450	16.00	51.73	38.14
500	16.90	54.18	39.92
600	18.31	58.89	43.38
700	19.31	63.40	46.71
800	20.03	67.73	49.91
900	20.54	71.91	53.02
1000	20.91	75.96	56.03
1500	21.83	94.75	70.10
2000	22.21	111.86	82.94
2500	22.27	127.89	94.95
3000	22.13	143.14	106.40

Table 43. Properties of the equimolar ternary mixture of neon, argon and xenon as a function of temperature

T K or °C	B $10^{-3}m^3$/kmol	η μPa s	λ mW/m K
50 K	-1745.94	5.36	3.68
100	-244.71	9.93	6.80
150	-108.67	14.27	9.68
200	-58.63	18.48	12.30
250	-33.42	22.52	14.72
300	-18.86	26.36	17.00
0 °C	-25.75	24.32	15.79
20	-20.46	25.84	16.70
40	-16.06	27.33	17.57
60	-12.32	28.78	18.43
80	-9.09	30.20	19.27
100	-6.29	31.58	20.09
150	-0.66	34.91	22.07
200	3.57	38.06	23.95
250	6.86	41.08	25.77
300	9.48	43.97	27.53
350	11.63	46.76	29.23
400	13.44	49.45	30.87
450	14.98	52.06	32.31
500	16.29	54.60	33.80
600	18.38	59.47	36.76
700	19.92	64.12	39.64
800	21.07	68.59	42.41
900	21.93	72.89	45.09
1000	22.58	77.06	47.69
1500	24.22	96.30	59.76
2000	24.83	113.72	70.80
2500	25.01	129.96	81.05
3000	25.01	145.34	90.80

Table 44. Properties of the equimolar ternary mixture of neon, krypton and xenon as a function of temperature

T K or °C	B $10^{-3}m^3$/kmol	η μPa s	λ mW/m K
50 K	-2423.68	5.51	3.12
100	-325.11	10.10	5.66
150	-148.12	14.42	7.99
200	-81.18	18.69	10.15
250	-48.11	22.91	12.20
300	-29.70	26.99	14.13
0 °C	-38.40	24.83	13.10
20	-31.72	26.44	13.87
40	-26.16	28.02	14.62
60	-21.45	29.56	15.35
80	-17.40	31.07	16.06
100	-13.89	32.54	16.76
150	-6.83	36.07	18.44
200	-1.52	39.43	20.06
250	2.62	42.64	21.61
300	5.94	45.72	23.11
350	8.66	48.68	24.57
400	10.96	51.54	25.99
450	12.93	54.31	27.22
500	14.62	57.00	28.48
600	17.35	62.17	31.01
700	19.41	67.10	33.46
800	20.97	71.82	35.82
900	22.16	76.37	38.10
1000	23.08	80.77	40.30
1500	25.30	101.04	50.51
2000	26.00	119.30	59.79
2500	26.36	136.25	68.48
3000	26.52	152.28	76.69

Table 45. Properties of the equimolar ternary mixture of argon, krypton and xenon as a function of temperature

T K or °C	B $10^{-3}m^3$/kmol	η μPa s	λ mW/m K
50 K	-3092.79	4.78	1.89
100	-477.07	8.52	3.42
150	-222.41	12.37	4.99
200	-127.58	16.42	6.57
250	-81.65	20.48	8.12
300	-55.40	24.38	9.61
0 °C	-67.91	22.31	8.82
20	-58.31	23.86	9.41
40	-50.26	25.37	9.98
60	-43.37	26.85	10.55
80	-37.39	28.30	11.10
100	-32.16	29.71	11.63
150	-21.52	33.10	12.93
200	-13.39	36.33	14.16
250	-6.98	39.40	15.33
300	-1.80	42.35	16.46
350	2.44	45.18	17.55
400	5.97	47.91	18.60
450	8.93	50.55	19.61
500	11.44	53.11	20.60
600	15.39	58.01	22.49
700	18.32	62.67	24.29
800	20.51	67.11	26.01
900	22.18	71.38	27.67
1000	23.46	75.49	29.28
1500	26.95	94.33	36.69
2000	28.71	111.20	43.39
2500	29.80	126.85	49.54
3000	30.44	141.67	55.35

Table 46. Properties of the equimolar quaternary mixture of helium, neon, argon and krypton as a function of temperature

T K or °C	B $10^{-3}m^3$/kmol	η μPa s	λ mW/m K
50 K	-374.31	5.74	8.67
100	-80.06	10.60	15.31
150	-31.15	15.13	21.03
200	-12.21	19.43	26.21
250	-2.88	23.41	30.96
300	2.74	27.08	35.45
0 °C	0.03	25.14	33.07
20	2.10	26.59	34.85
40	3.87	28.00	36.55
60	5.40	29.37	38.24
80	6.73	30.70	39.87
100	7.89	32.01	41.47
150	10.23	35.14	45.32
200	11.98	38.13	49.00
250	13.32	40.98	52.55
300	14.37	43.73	56.00
350	15.21	46.38	59.35
400	15.90	48.94	62.61
450	16.47	51.44	65.76
500	16.94	53.86	68.85
600	17.66	58.54	74.87
700	18.14	63.03	80.70
800	18.45	67.35	86.34
900	18.65	71.54	91.83
1000	18.77	75.59	97.18
1500	18.89	94.49	122.36
2000	18.76	111.75	145.60
2500	18.52	127.95	167.51
3000	18.21	143.37	188.45

Table 47. Properties of the equimolar quaternary mixture of helium, neon, argon and xenon as a function of temperature

T K or °C	B $10^{-3}m^3$/kmol	η μPa s	λ mW/m K
50 K	-988.52	5.73	7.89
100	-134.30	10.47	13.84
150	-55.06	14.84	18.97
200	-25.92	19.01	23.57
250	-11.31	22.98	27.81
300	-2.87	26.73	31.86
0 °C	-6.87	24.74	29.71
20	-3.80	26.23	31.32
40	-1.23	27.68	32.81
60	0.96	29.10	34.27
80	2.85	30.48	35.71
100	4.49	31.84	37.14
150	7.78	35.09	40.62
200	10.24	38.19	43.96
250	12.13	41.15	47.19
300	13.62	44.00	50.31
350	14.83	46.75	53.34
400	15.82	49.41	56.29
450	16.66	51.99	59.05
500	17.37	54.50	61.81
600	18.46	59.34	67.23
700	19.23	63.97	72.49
800	19.78	68.43	77.59
900	20.17	72.73	82.54
1000	20.44	76.90	87.36
1500	20.93	96.24	110.02
2000	20.91	113.82	130.95
2500	20.71	130.24	150.63
3000	20.45	145.82	169.41

Table 48. Properties of the equimolar quaternary mixture of helium, neon, krypton and xenon as a function of temperature

T K or °C	B $10^{-3}m^3$/kmol	η μPa s	λ mW/m K
50 K	-1370.67	5.87	7.14
100	-179.57	10.66	12.44
150	-77.04	15.05	16.98
200	-38.29	19.31	21.09
250	-19.21	23.48	24.92
300	-8.59	27.47	28.58
0 °C	-13.61	25.35	26.63
20	-9.75	26.94	28.09
40	-6.53	28.48	29.49
60	-3.79	29.99	30.88
80	-1.43	31.47	32.22
100	0.62	32.91	33.53
150	4.73	36.38	36.67
200	7.80	39.68	39.68
250	10.18	42.83	42.59
300	12.06	45.87	45.41
350	13.60	48.79	48.17
400	14.87	51.63	50.86
450	15.95	54.37	53.37
500	16.87	57.04	55.88
600	18.32	62.18	60.82
700	19.38	67.09	65.61
800	20.15	71.81	70.25
900	20.72	76.36	74.76
1000	21.14	80.76	79.15
1500	21.93	101.15	99.75
2000	21.94	119.59	118.73
2500	21.82	136.76	136.62
3000	21.64	153.02	153.66

Table 49. Properties of the equimolar quaternary mixture of helium, argon, krypton and xenon as a function of temperature

T K or °C	B $10^{-3}m^3$/kmol	η μPa s	λ mW/m K
50 K	-1749.74	5.17	5.62
100	-265.58	9.19	9.78
150	-118.65	13.17	13.45
200	-63.93	17.24	16.87
250	-37.53	21.27	20.12
300	-22.46	25.12	23.24
0 °C	-29.65	23.08	21.58
20	-24.13	24.61	22.82
40	-19.49	26.10	23.98
60	-15.50	27.56	25.13
80	-12.03	28.98	26.26
100	-8.99	30.37	27.36
150	-2.82	33.71	30.01
200	1.88	36.89	32.55
250	5.57	39.93	35.00
300	8.52	42.85	37.37
350	10.92	45.66	39.67
400	12.90	48.37	41.91
450	14.55	51.00	44.09
500	15.93	53.55	46.22
600	18.08	58.44	50.35
700	19.64	63.10	54.33
800	20.77	67.56	58.17
900	21.60	71.85	61.91
1000	22.22	76.00	65.54
1500	23.70	95.07	82.60
2000	24.28	112.24	98.30
2500	24.55	128.22	113.02
3000	24.61	143.36	127.04

Table 50. Properties of the equimolar quaternary mixture of neon, argon, krypton and xenon as a function of temperature

T K or °C	B $10^{-3}m^3$/kmol	η μPa s	λ mW/m K
50 K	-1801.69	5.24	3.13
100	-283.62	9.64	5.75
150	-129.32	13.90	8.22
200	-70.88	18.14	10.53
250	-42.19	22.28	12.70
300	-25.70	26.19	14.74
0 °C	-33.56	24.12	13.66
20	-27.53	25.67	14.47
40	-22.47	27.19	15.25
60	-18.15	28.66	16.02
80	-14.42	30.10	16.77
100	-11.16	31.50	17.50
150	-4.59	34.88	19.27
200	0.38	38.09	20.96
250	4.26	41.15	22.58
300	7.38	44.08	24.14
350	9.93	46.90	25.66
400	12.07	49.63	27.12
450	13.89	52.27	28.45
500	15.43	54.83	29.79
600	17.89	59.75	32.42
700	19.71	64.44	34.96
800	21.06	68.94	37.41
900	22.07	73.27	39.77
1000	22.84	77.45	42.06
1500	24.79	96.75	52.70
2000	25.58	114.18	62.39
2500	25.98	130.41	71.40
3000	26.11	145.80	79.95

Table 51. Properties of the equimolar quintuple mixture of helium, neon, argon, krypton and xenon as a function of temperature

T	B	η	λ
K or °C	10^{-3} m^3/kmol	μPa s	mW/m K
50 K	-1159.54	5.54	6.27
100	-179.01	10.10	11.05
150	-77.74	14.41	15.22
200	-39.41	18.64	19.04
250	-20.64	22.72	22.59
300	-9.86	26.58	25.97
0 °C	-15.00	24.54	24.17
20	-11.06	26.06	25.52
40	-7.74	27.55	26.79
60	-4.90	29.00	28.05
80	-2.44	30.42	29.27
100	-0.29	31.80	30.47
150	4.04	35.13	33.36
200	7.30	38.29	36.14
250	9.83	41.32	38.81
300	11.85	44.22	41.40
350	13.49	47.02	43.92
400	14.84	49.73	46.37
450	15.99	52.35	48.68
500	16.95	54.90	50.98
600	18.46	59.80	55.47
700	19.54	64.49	59.82
800	20.33	68.98	64.04
900	20.90	73.32	68.12
1000	21.31	77.52	72.10
1500	22.18	96.94	90.76
2000	22.38	114.54	107.95
2500	22.38	130.96	124.09
3000	22.24	146.54	139.47

TABLE 52. Quantum-mechanically calculated low-temperature properties of helium-3 as a function of temperature

T	B	η	λ	D(1.013 bar)
K	10^{-3} m^3/kmol	μPa s	mW/m K	10^{-4} m^2/s
0.10		0.0713	0.7390	0.2037×10^{-5}
0.20		0.1582	1.6358	0.1026×10^{-4}
0.30		0.2234	2.3148	0.2367×10^{-4}
0.40		0.2738	2.8399	0.3989×10^{-4}
0.50		0.3198	3.3148	0.5818×10^{-4}
0.60		0.3664	3.7931	0.7898×10^{-4}
0.70		0.4149	4.2922	0.1029×10^{-3}
0.80		0.4657	4.8163	0.1304×10^{-3}
0.90		0.5179	5.3553	0.1616×10^{-3}
1.00		0.5711	5.9049	0.1966×10^{-3}
1.20		0.6763	6.9933	0.2777×10^{-3}
1.40		0.7745	8.0149	0.3713×10^{-3}
1.50	− 167.704			
1.60		0.8619	8.9336	0.4752×10^{-3}
2.00	− 128.757	0.9982	10.4055	0.7026×10^{-3}
2.40		1.0889	11.4168	0.9457×10^{-3}
2.80		1.1481	12.0766	0.1197×10^{-2}
3.00	− 85.002			
3.20		1.1901	12.5280	0.1454×10^{-2}
3.60		1.2249	12.8841	0.1718×10^{-2}
4.00	− 61.352	1.2591	13.2237	0.1992×10^{-2}
4.50		1.3035	13.6607	0.2350×10^{-2}
5.00	− 46.663	1.3518	14.1389	0.2727×10^{-2}
5.50		1.4038	14.6584	0.3124×10^{-2}
6.00	− 36.592	1.4589	15.2143	0.3543×10^{-2}
7.00		1.5743	16.3892	0.4442×10^{-2}
8.00	− 23.766	1.6932	17.6100	0.5425×10^{-2}
9.00		1.8124	18.8388	0.6486×10^{-2}
10.00	− 15.862	1.9302	20.0558	0.7623×10^{-2}
12.00		2.1582	22.4181	0.1011×10^{-1}
14.00		2.3752	24.6697	0.1287×10^{-1}
15.00	− 5.144			
16.00		2.5827	26.8235	0.1590×10^{-1}
20.00	0.261	2.9717	30.8627	0.2269×10^{-1}
25.00	3.485	3.4198	35.5147	0.3245×10^{-1}
30.00	5.614	3.8370	39.8444	0.4352×10^{-1}
35.00		4.2310	43.9344	0.5586×10^{-1}
40.00	8.188	4.6052	47.8183	0.6939×10^{-1}
45.00		4.9637	51.8386	0.8408×10^{-1}
50.00	9.647	5.3096	55.1282	0.9985×10^{-1}
60.00	10.551	5.9680	61.9601	0.1345
70.00	11.150	6.5910	68.4234	0.1703
80.00	11.560	7.1842	74.5754	0.2160
90.00		7.7529	80.4728	0.2625
100.00	12.046	8.3044	86.1918	0.3127

TABLE 53. Quantum-mechanically calculated low-temperature properties of helium-4 as a function of temperature

T K	B 10^{-3} m^3/kmol	η μPa s	λ mW/m K	D(1.013 bar) 10^{-4} m^2/s
0.10		0.0074	0.0589	0.1135×10^{-6}
0.20		0.0302	0.2454	0.1012×10^{-5}
0.30		0.0779	0.6416	0.3976×10^{-5}
0.40		0.1492	1.2128	0.1028×10^{-4}
0.50		0.2162	1.7043	0.1851×10^{-4}
0.60		0.2655	2.0688	0.2740×10^{-4}
0.70		0.3001	2.3615	0.3783×10^{-4}
0.80		0.3186	2.5337	0.4873×10^{-4}
0.90		0.3270	2.6096	0.6008×10^{-4}
1.00		0.3309	2.6374	0.7176×10^{-4}
1.20		0.3399	2.6882	0.9681×10^{-4}
1.40		0.3576	2.8071	0.1252×10^{-3}
1.50	− 271.331			
1.60		0.3846	3.0052	0.1579×10^{-3}
2.00	− 190.637	0.4606	3.5878	0.2377×10^{-3}
2.40		0.5564	4.3354	0.3383×10^{-3}
2.80		0.6628	5.1666	0.4594×10^{-3}
3.00	− 118.211			
3.20		0.7728	6.0241	0.6013×10^{-3}
3.60		0.8816	6.8692	0.7621×10^{-3}
4.00	− 83.709	0.9868	7.6873	0.9407×10^{-3}
4.50		1.1111	8.6548	0.1187×10^{-2}
5.00	− 63.304	1.2276	9.5654	0.1457×10^{-2}
5.50		1.3362	10.4160	0.1781×10^{-2}
6.00	− 49.791	1.4377	11.2122	0.2060×10^{-2}
7.00		1.6243	12.6773	0.2744×10^{-2}
8.00	− 32.866	1.7947	14.0151	0.3504×10^{-2}
9.00		1.9546	15.2693	0.4336×10^{-2}
10.00	− 22.706	2.1050	16.4483	0.5235×10^{-2}
12.00		2.3874	18.6618	0.7234×10^{-2}
14.00		2.6506	20.7233	0.9479×10^{-2}
15.00	− 9.310			
16.00		2.8966	22.6495	0.1194×10^{-1}
20.00	− 2.649	3.3557	26.2440	0.1750×10^{-1}
25.00	1.341	3.8839	30.3793	0.2558×10^{-1}
30.00	3.934	4.3724	34.2018	0.3485×10^{-1}
35.00		4.8307	37.7869	0.4524×10^{-1}
40.00	7.085	5.2648	41.1821	0.5674×10^{-1}
45.00		5.6796	44.4259	0.6928×10^{-1}
50.00	8.833	6.0798	47.5557	0.8276×10^{-1}
60.00	9.893	6.8466	53.5548	0.1123
70.00	10.584	7.5718	59.2265	0.1451
80.00	11.066	8.2567	64.5781	0.1815
90.00		8.9118	69.6966	0.2213
100.00	11.662	9.5487	74.6732	0.2644

TABLE 54. Quantum-mechanically calculated low-temperature properties of the equimolar binary mixture of helium-3 and helium-4 as a function of temperature

T	B	η	λ	D(1.013 bar)	α_T	
K	10^{-3} m^3/kmol	μPa s	mW/m K	10^{-4} m^2/s	$x(^4\text{He}) = 1$	$x(^4\text{He}) = 0$
0.10		0.0184	0.1768	0.4421×10^{-6}	−0.3079	−1.4672
0.20		0.0603	0.5791	0.3025×10^{-5}	−0.3376	−1.1310
0.30		0.1197	1.1227	0.9086×10^{-5}	−0.2310	−0.5768
0.40		0.1855	1.6960	0.1849×10^{-4}	−0.1194	−0.2493
0.50		0.2447	2.1996	0.3045×10^{-4}	−0.0490	−0.0926
0.60		0.2944	2.6346	0.4446×10^{-4}	−0.0089	−0.0157
0.70		0.3362	3.0218	0.6039×10^{-4}	0.0163	0.0272
0.80		0.3705	3.3485	0.7800×10^{-4}	0.0322	0.0522
0.90		0.3991	3.6230	0.9736×10^{-4}	0.0425	0.0684
1.00		0.4242	3.8618	0.1184×10^{-3}	0.0495	0.0802
1.20		0.4705	4.2951	0.1653×10^{-3}	0.0577	0.0969
1.40		0.5163	4.7167	0.2187×10^{-3}	0.0625	0.1085
1.50	−203.721					
1.60		0.5632	5.1458	0.2780×10^{-3}	0.0658	0.1165
2.00	−158.802	0.6591	6.0246	0.4138×10^{-3}	0.0701	0.1234
2.40		0.7543	6.8938	0.5704×10^{-3}	0.0723	0.1218
2.80		0.8460	7.7220	0.7467×10^{-3}	0.0735	0.1166
3.00	−101.178					
3.20		0.9330	8.4964	0.9411×10^{-3}	0.0741	0.1107
3.60		1.0151	9.2201	0.1153×10^{-2}	0.0744	0.1051
4.00	−72.272	1.0932	9.9042	0.1381×10^{-2}	0.0746	0.1006
4.50		1.1858	10.7123	0.1688×10^{-2}	0.0746	0.0958
5.00	−54.791	1.2742	11.4847	0.2018×10^{-2}	0.0748	0.0923
5.50		1.3587	12.2254	0.2370×10^{-2}	0.0750	0.0898
6.00	−43.066	1.4402	12.9415	0.2744×10^{-2}	0.0753	0.0881
7.00		1.5954	14.3120	0.3552×10^{-2}	0.0758	0.0858
8.00	−28.234	1.7424	15.6147	0.4437×10^{-2}	0.0763	0.0846
9.00		1.8831	16.8649	0.5396×10^{-2}	0.0766	0.0839
10.00	−19.222	2.0178	18.0643	0.6425×10^{-2}	0.0768	0.0836
12.00		2.2732	20.3413	0.8687×10^{-2}	0.0774	0.0835
14.00		2.5130	22.4828	0.1121×10^{-1}	0.0780	0.0837
15.00	−7.187					
16.00		2.7397	24.5100	0.1399×10^{-1}	0.0785	0.0840
20.00	−1.174	3.1627	28.2893	0.2021×10^{-1}	0.0784	0.0837
25.00	2.415	3.6496	32.6374	0.2917×10^{-1}	0.0778	0.0828
30.00	4.766	4.1018	36.6769	0.3939×10^{-1}	0.0773	0.0821
35.00		4.5274	40.4792	0.5080×10^{-1}	0.0768	0.0815
40.00	7.622	4.9315	44.0896	0.6333×10^{-1}	0.0763	0.0809
45.00		5.3182	47.5437	0.7693×10^{-1}	0.0759	0.0803
50.00	9.230	5.6908	50.8725	0.9158×10^{-1}	0.0754	0.0798
60.00	10.221	6.4017	57.2220	0.1239	0.0745	0.0788
70.00	10.871	7.0740	63.2249	0.1600	0.737	0.0780
80.00	11.320	7.7140	68.9408	0.1997	0.0731	0.0772
90.00		8.3274	74.4184	0.2430	0.0725	0.0765
100.00	11.858	8.9219	79.7258	0.2896	0.0720	0.0759

Note: Thermal diffusion factors are given at $x(^4\text{He}) = 1$ and $x(^4\text{He}) = 0$.

10. Acknowledgments

The critical evaluation of experimental data, the validation of all computational algorithms and the calculation of the numerical data for the tables were performed under Grant No. NB 81 NADA 2013 awarded to Brown University by the Office of Standard Reference Data of the National Bureau of Standards and utilizing funds provided by the National Science Foundation. The authors express their thanks to the Office Chief, Dr. D. R. Lide, and to the Program Manager, Dr. H. J. White, for their continuing interest in the progress of this work.

The authors also thank Dr. C. Y. Ho, Director of the Center for Information and Numerical Data Analysis of Purdue University, for the extensive bibliography which he retrieved from the Center's computer and put at their disposal. They repeat here their appreciation to Dr. W. L. Taylor and Dr. G. T. McConville for the numerical results of their quantum-mechanical calculations.

11. References to Introductory Text

[1]J. Kestin, S. T. Ro, and W. A. Wakeham, Physica **58**, 165 (1972).
[2]B. Najafi, E. A. Mason, and J. Kestin, Physica **119A**, 387 (1983).
[3]S. Chapman and T. G. Cowling, *The Mathematical Theory of Non-Uniform Gases* (Cambridge University, Cambridge, 1970).
[4]J. O. Hirschfelder, C. F. Curtiss, and R. B. Bird, *The Molecular Theory of Gases and Liquids* (Wiley, New York, 1964), Chap. 8.
[5]J. H. Ferziger and H. G. Kaper, *Mathematical Theory of Transport Processes in Gases* (North-Holland, Amsterdam, 1972), Chaps. 6 and 7.
[6]G. C. Maitland, M. Rigby, E. B. Smith, and W. A. Wakeham, *Intermolecular Forces* (Clarendon, Oxford, 1981), Chap. 5.
[7]C. F. Curtiss and J. O. Hirschfelder, J. Chem. Phys. **17**, 550 (1949).
[8]C. Muckenfuss and C. F. Curtiss, J. Chem. Phys. **29**, 1273 (1958).
[9]J. Kestin, *A Course in Thermodynamics*, revised printing (Hemisphere, Washington, 1979), Vol. 1, Chap. 12.
[10]J. Kestin, S. T. Ro, and W. A. Wakeham, J. Chem. Phys. **56**, 4119 (1972).
[11]J. Kestin, S. T. Ro, and W. A. Wakeham, J. Chem. Phys. **56**, 5837 (1972).
[12]J. M. Hellemans, J. Kestin, and S. T. Ro, Physica **71**, 1 (1974).
[13]J. Kestin, H. E. Khalifa, and W. A. Wakeham, J. Chem. Phys. **67**, 4254 (1977).
[14]J. Kestin, H. E. Khalifa, and W. A. Wakeham, Physica **90A**, 215 (1978).
[15]A. A. Clifford, R. Fleeter, J. Kestin, and W. A. Wakeham, Physica **98A**, 467 (1979).
[16]K. T. Tang, J. M. Norbeck, and P. R. Certain, J. Chem. Phys. **64**, 3063 (1976).
[17]Lord Rayleigh, Proc. R. Soc. London **66**, 68 (1900).
[18]A. Dalgarno, M. R. C. McDowell, and A. Williams, Philos. Trans. R. Soc. London Ser. A **250**, 411 (1958).
[19]E. A. Mason and J. T. Vanderslice, Phys. Rev. **114**, 497 (1959).
[20]J. M. Farrar, T. P. Schafer, and Y. T. Lee, AIP Conf. Proc. **11**, 279 (1973).
[21]G. C. Maitland, E. A. Mason, L. A. Viehland, and W. A. Wakeham, Mol. Phys. **36**, 797 (1978).
[22]H. E. Cox, F. W. Crawford, E. B. Smith, and A. R. Tindell, Mol. Phys. **40**, 705 (1980).
[23]I. Amdur and J. E. Jordan, Adv. Chem. Phys. **10**, 29 (1966).
[24]J. E. Jordan, E. A. Mason, and I. Amdur, in *Physical Methods of Chemistry*, edited by D. A. Weissberger and B. W. Rossiter (Wiley, New York, 1972), Vol. I, Part III D, Chap. 6.
[25]I. Amdur, M. J. Engler, J. E. Jordan, and E. A. Mason, J. Chem. Phys. **63**, 597 (1975).
[26]R. G. Gordon and Y. S. Kim, J. Chem. Phys. **56**, 3122 (1972).
[27]N. A. Sondergaard and E. A. Mason, J. Chem. Phys. **62**, 1299 (1975).
[28]E. R. Cohen, At. Data Nucl. Data Tables **18**, 587 (1976).
[29]N. E. Holden, Pure Appl. Chem. **52**, 2349 (1980).
[30]R. A. Aziz and H. H. Chen, J. Chem. Phys. **67**, 5719 (1977).
[31]C. E. Moore, "Ionization Potentials and Ionization Limits Derived from the Analyses of Optical Spectra," Report No. NSRDS-NBS 34, September 1970.
[32]R. A. Aziz, V. P. S. Nain, J. S. Carley, W. L. Taylor, and G. T. McConville, J. Chem. Phys. **70**, 4330 (1979).

Appendix A. Material and Physical Constants Including Scaling Factors; Onset of Ionization

TABLE A1. Universal constants[a]

Planck constant	$h = 6.626\,176 \times 10^{-34}$ J s
Boltzmann constant	$k = 1.380\,662 \times 10^{-23}$ J K^{-1}
Avogadro constant	$N_A = 6.022\,045 \times 10^{23}$ mol^{-1}
Universal gas constant	$R = 8.314\,41$ J mol^{-1} K^{-1}

[a]Reference 28.

TABLE A2. Atomic weights[a] (average isotopic composition)

	He	Ne	Ar	Kr	Xe
He	4.0026	6.6802	7.2762	7.6403	7.7684
Ne		20.179	26.814	32.526	34.981
Ar			39.948	54.104	61.257
Kr				83.800	102.30
Xe					131.29

[a]Reference 29.
[3]He: 3.0160; [4]He: 4.0026; values rounded to five significant figures.

TABLE A3. Scaling parameters σ_{ij} and ϵ_{ij} for the correlation

σ(nm)

	He	Ne	Ar	Kr	Xe
He	0.2610	0.2691	0.3084	0.3267	0.3533
Ne		0.2755	0.3119	0.3264	0.3488
Ar			0.3350	0.3464	0.3660
Kr				0.3571	0.3753
Xe					0.3885

ϵ/k(K)

	He	Ne	Ar	Kr	Xe
He	10.40	19.44	30.01	31.05	29.77
Ne		42.00	64.17	67.32	67.25
Ar			141.5	165.8	182.6
Kr				197.8	225.4
Xe					274.0

TABLE A4. Quantum-mechanical de Boer parameters Λ^*

	^{3}He	^{4}He	Ne	Ar	Kr	Xe
^{3}He	3.00	2.81	1.61	1.10	1.00	0.94
^{4}He		2.60	1.43	0.96	0.87	0.80
Ne			0.54	0.34	0.29	0.26
Ar				0.17	0.13	0.11
Kr					0.09	0.08
Xe						0.06

TABLE A5. The low-temperature dimensionless scaling parameters, $C_6^* = C_6/\epsilon\sigma^6$

	He	Ne	Ar	Kr	Xe
He	3.09	2.940	2.681	2.498	2.346
Ne		2.594	2.429	2.424	2.204
Ar			2.210	2.426	2.053
Kr				2.164	2.051
Xe					2.162

TABLE A6. The high-temperature dimensionless scaling parameters, $\rho^* = \rho/\sigma$ and $V_o^* = V_o/\epsilon$

ρ^*

	He	Ne	Ar	Kr	Xe
He	0.0797	0.0788	0.0791	0.0772	0.0764
Ne		0.0784	0.0795	0.0786	0.0785
Ar			0.0836	0.0833	0.0835
Kr				0.0831	0.0837
Xe					0.0854

$V_o^* \times 10^{-5}$

	He	Ne	Ar	Kr	Xe
He	8.50	10.60	9.740	10.89	13.37
Ne		11.09	9.235	9.929	11.20
Ar			5.117	4.849	4.878
Kr				4.491	4.337
Xe					3.898

TABLE A7. First ionization limit. Temperature at which 1% of atoms are ionized

Gases	Temperature T, K; Pressure P, kPa	
	100	1
He	14500	12000
Ne	12500	10500
Ar	9500	7700
Kr	8500	7000
Xe	7500	6200

Appendix B. Correlation Equations for Functionals

Second Virial Coefficients

$$B^* = B_0^* + (\Lambda^*)^2 B_1^* + (\Lambda^*)^4 B_2^* + (\Lambda^*)^6 B_3^* + \cdots + (\Lambda^*)^3 B_{\text{perfect}}^*. \quad \text{(B1)}$$

B_0^*

$T^* \leqslant 1.1$

$$B_0^* = -(T^*)^{1/2} \exp(1/T^*)[1.186\,23 + 1.008\,24T^* + 4.255\,71(T^*)^2 - 18.6033(T^*)^3 + 20.4732(T^*)^4 - 8.719\,03(T^*)^5 + 1.148\,29(T^*)^6]. \quad \text{(B2a)}$$

$1.1 < T^* < 10$

$$B_0^* = -(T^*)^{1/2} \exp(1/T^*)[0.746\,85 - 1.0384(\ln T^*) + 0.316\,34(\ln T^*)^2 + 0.020\,96(\ln T^*)^3 - 0.014\,98(\ln T^*)^4]. \quad \text{(B2b)}$$

$T^* \geqslant 10$

$$B_0^* = \beta[1 + c_2(\ln T^*)^{-2} + c_4(\ln T^*)^{-4} + c_6(\ln T^*)^{-6}], \quad \text{(B2c)}$$

where

$$\beta = (\rho^*)^3[(\alpha + \gamma)^3 + (\pi^2/2)(\alpha + \gamma) + 2.404\,11],$$

$$\alpha = \ln V_o^* - \ln T^*,$$

$\gamma = 0.577\,215...$is Euler's constant,

and

$$c_2 = -15.9057 + (9.859\,58/\beta_{10}) + [(\rho^*)^3/\beta_{10}^2][25.6607(\alpha_{10} + \gamma)^2 - 9.737\,66(\alpha_{10} + \gamma) + 42.2102] + 3.245\,89[(\rho^*)^2/\beta_{10}]^3 \times [3(\alpha_{10} + \gamma)^2 + \pi^2/2]^2,$$

$$c_4 = 84.3304 - (61.9124/\beta_{10}) + [(\rho^*)^3/\beta_{10}^2][-227.258(\alpha_{10} + \gamma)^2 + 103.256(\alpha_{10} + \gamma) - 373.824] - 34.4187[(\rho^*)^2/\beta_{10}]^3 \times [3(\alpha_{10} + \gamma)^2 + \pi^2/2]^2,$$

$$c_6 = -149.037 + (119.937/\beta_{10}) + [(\rho^*)^3/\beta_{10}^2][483.571(\alpha_{10} + \gamma)^2 - 273.727(\alpha_{10} + \gamma) + 795.442] + 91.2423[(\rho^*)^2/\beta_{10}]^3 \times [3(\alpha_{10} + \gamma)^3 + \pi^2/2]^2,$$

in which β_{10} is the value of β and α_{10} is the value of α at the matching point of $T^* = 10$.

B_1^*

$T^* \leqslant 1.1$

$$B_1^* = (T^*)^{-3/2} \exp(1/T^*)[0.158\,192 - 0.037\,145\,1T^* - 0.010\,312\,5T^{*2} + 0.070\,185\,2T^{*3} - 0.032\,839\,9T^{*4}]. \quad \text{(B3a)}$$

$1.1 \leqslant T^* \leqslant 10$

$$B_1^* = (T^*)^{-3/2} \exp(1/T^*)[0.148 + 0.0241(\ln T^*) - 0.0123(\ln T^*)^2 + 0.0096(\ln T^*)^3 - 0.0014(\ln T^*)^4]. \quad \text{(B3b)}$$

$T^* \geqslant 10$

$$B_1^* = \beta_1[1 + (3.681\,60/T^*) - (3.361\,12/T^*)^{3/2} + (2.705\,97/T^*)^2], \quad \text{(B3c)}$$

where

$$\beta_1 = (5.047\,06 \times 10^{-4}/T^*)[(\ln T^*)^2 - 26.4604 \ln T^* + 175.683].$$

B_2^*

$T^* \leqslant 10$

$$B_2^* = -(T^*)^{-7/2} \exp(1/T^*)[0.0152 + 0.0126T^* + 0.0001T^{*2}]. \quad \text{(B4a)}$$

$T^* \geqslant 10$

$$B_2^* = \beta_2[1 + 15.0485/T^* - (10.0510/T^*)^{3/2} + (6.435\,40/T^*)^2], \quad \text{(B4b)}$$

where

$$\beta_2 = -33.5437 \times 10^{-6}(1/T^*)^2[(\ln T^*)^2 - 21.4604(\ln T^*) + 126.532].$$

B_3^*

$T^* \leqslant 1.1$

$$B_3^* = (T^*)^{-11/2} \exp(1/T^*)[0.001\,300 + 0.006\,766T^* - 0.0197T^{*3} + 0.032\,76T^{*4} - 0.0128T^{*5}]. \quad \text{(B5a)}$$

$1.1 \leqslant T^* \leqslant 10$

$$B_3^* = -(T^*)^{-11/2} \exp(1/T^*)[0.0051 - 0.0113T^* - 0.0021T^{*2}]. \quad \text{(B5b)}$$

$T^* \geqslant 10$

$$B_3^* = 8.877\,59 \times 10^{-5}(T^*)^{-8/3} \times [1.0 - (5.680\,52/T^*) + (32.1756/T^*)^{3/2} - (6.281\,59/T^*)^2]. \quad \text{(B5c)}$$

B^*_{perfect}

$$B^*_{\text{perfect}}(^3\text{He}) = 2.679\,58 \times 10^{-3}(T^*)^{-3/2}, \quad \text{(B6a)}$$

$$B^*_{\text{perfect}}(^4\text{He}) = -5.359\,16 \times 10^{-3}(T^*)^{-3/2}. \quad \text{(B6b)}$$

Collision Integrals

$\Omega^{(2,2)^*}$

$T^* \leqslant 1.2$

$$\Omega^{(2,2)^*} = 1.1943(C_6^*/T^*)^{1/3} \times [1 + a_1(T^*)^{1/3} + a_2(T^*)^{2/3} + a_3(T^*) + a_4(T^*)^{4/3} + a_5(T^*)^{5/3} + a_6(T^*)^2], \quad \text{(B7a)}$$

where

$$a_1 = 0.18,$$
$$a_2 = 0,$$
$$a_3 = -1.204\,07 - 0.195\,866(C_6^*)^{-1/3},$$
$$a_4 = -9.863\,74 + 20.2221(C_6^*)^{-1/3},$$
$$a_5 = 16.6295 - 31.3613(C_6^*)^{-1/3},$$
$$a_6 = -6.738\,05 + 12.6611(C_6^*)^{-1/3}.$$

$1.2 \leqslant T^* \leqslant 10$

$$\Omega^{(2,2)^*} = \exp[0.466\,41 - 0.569\,91 \ln T^* + 0.195\,91(\ln T^*)^2 - 0.038\,79(\ln T^*)^3 + 0.002\,59(\ln T^*)^4]. \quad \text{(B7b)}$$

$T^* \geqslant 10$

$$\Omega^{(2,2)^*} = (\rho^*)^2\alpha^2[1.04 + a_1(\ln T^*)^{-1} + a_2(\ln T^*)^{-2} + a_3(\ln T^*)^{-3} + a_4(\ln T^*)^{-4}], \quad \text{(B7c)}$$

where

$$a_1 = 0,$$
$$a_2 = -33.0838 + (\alpha_{10}\rho^*)^{-2}[20.0862 + (72.1059/\alpha_{10}) + (8.276\,48/\alpha_{10})^2],$$
$$a_3 = 101.571 - (\alpha_{10}\rho^*)^{-2}[56.4472 + (286.393/\alpha_{10}) + (17.7610/\alpha_{10})^2],$$
$$a_4 = -87.7036 + (\alpha_{10}\rho^*)^{-2}[46.3130 + (277.146/\alpha_{10}) + (19.0573/\alpha_{10})^2],$$

in which $\alpha_{10} = \ln(V_o^*/10)$ is the value of $\alpha = \ln(V_o^*) - \ln T^*$ at the matching point of $T^* = 10$.

$\Omega^{(1,1)^*}$

$T^* \leqslant 1.2$

$$\Omega^{(1,1)^*} = 1.1874(C_6^*/T^*)^{1/3} \times [1 + b_1(T^*)^{1/3} + b_2(T^*)^{2/3} + b_3(T^*) + b_4(T^*)^{4/3} + b_5(T^*)^{5/3} + b_6(T^*)^2], \quad \text{(B8a)}$$

where

$$b_1 = 0,$$
$$b_2 = 0,$$
$$b_3 = 10.0161 - 10.5395(C_6^*)^{-1/3},$$
$$b_4 = -40.0394 + 46.0048(C_6^*)^{-1/3},$$
$$b_5 = 44.3202 - 53.0817(C_6^*)^{-1/3},$$
$$b_6 = -15.2912 + 18.8125(C_6^*)^{-1/3}.$$

$1.2 \leqslant T^* \leqslant 10$

$$\Omega^{(1,1)^*} = \exp[0.357\,588 - 0.472\,513 \ln T^* + 0.070\,090\,2(\ln T^*)^2 + 0.016\,574\,1(\ln T^*)^3 - 0.005\,920\,22(\ln T^*)^4]. \quad \text{(B8b)}$$

$T^* \geqslant 10$

$$\Omega^{(1,1)^*} = (\rho^*)^2\alpha^2[0.89 + b_2(T^*)^{-2} + b_4(T^*)^{-4} + b_6(T^*)^{-6}], \quad \text{(B8c)}$$

where

$$b_2 = -267.00 + (\alpha_{10}\rho^*)^{-2}[201.570 + (174.672/\alpha_{10}) + (7.369\,16/\alpha_{10})^2],$$

$$b_4 = 26.700\times10^3 - (\alpha_{10}\rho^*)^{-2}[19.2265 + (27.6938/\alpha_{10}) + (3.295\,59/\alpha_{10})^2]\times10^3,$$

$$b_6 = -8.90\times10^5 + (\alpha_{10}\rho^*)^{-2}[6.310\,13 + (10.2266/\alpha_{10}) + (2.330\,33/\alpha_{10})^2]\times10^5$$

in which $\alpha_{10} = \ln(V_o^*/10)$ is the value of $\alpha = \ln(V_o^*) - \ln T^*$ at the matching point of $T^* = 10$.

F^*

$$F^* = 0.9543 + 0.001\,24T^*.$$

Appendix C. General Formulas

Recursion Relation and Other Quantities

$$\Omega^{(l,s+1)^*} = \frac{T^*}{s+2}\frac{d\Omega^{(l,s)^*}}{dT^*} + \Omega^{(l,s)^*} = \Omega^{(l,s)^*}\left[1 + \frac{T^*}{s+2}\frac{d\ln\Omega^{(l,s)^*}}{dT^*}\right], \quad (C1)$$

$$A^* = \Omega^{(2,2)^*}/\Omega^{(1,1)^*}, \quad (C2)$$

$$E^* = \Omega^{(2,3)^*}/\Omega^{(2,2)^*} = 1 + \frac{T^*}{4}\frac{d\ln\Omega^{(2,2)^*}}{dT^*}, \quad (C3)$$

$$C^* = \Omega^{(1,2)^*}/\Omega^{(1,1)^*} = 1 + \frac{T^*}{3}\frac{d\ln\Omega^{(1,1)^*}}{dT^*}, \quad (C4)$$

$$B^* = [5\Omega^{(1,2)^*} - 4\Omega^{(1,3)^*}]/\Omega^{(1,1)^*} = 1 + 3C^* - 3(C^*)^2 - \frac{(T^*)^2}{3}\frac{d^2\ln\Omega^{(1,1)^*}}{dT^{*2}} = 4C^* - 3(C^*)^2 - \frac{1}{3}\frac{d^2\ln\Omega^{(1,1)^*}}{d(\ln T^*)^2}, \quad (C5)$$

$$H^* = (3B^* + 6C^* - 35/4)(6C^* - 5)^{-1}, \quad (C6)$$

$$F^* = \Omega^{(3,3)^*}/\Omega^{(1,1)^*}, \quad (C7)$$

$$f_\eta = 1 + \frac{3}{196}(8E^* - 7)^2, \quad (C8)$$

$$f_D = 1 + \frac{1}{8}(6C^* - 5)^2(2A^* + 5)^{-1}, \quad (C9)$$

$$f_\lambda = 1 + \frac{1}{42}(8E^* - 7)^2. \quad (C10)$$

Pure Substance

Second virial coefficient B

$$B = \frac{2}{3}\pi N_A\sigma^3 B^*. \quad (C11)$$

Viscosity η

$$\eta = \frac{5}{16}(mkT/\pi)^{1/2}\frac{f_\eta}{\sigma^2\Omega^{(2,2)^*}}. \quad (C12)$$

Thermal conductivity λ

$$\lambda = \frac{75}{64}(k^3T/\pi m)^{1/2}\frac{f_\lambda}{\sigma^2\Omega^{(2,2)^*}} = \frac{15}{4}\frac{\eta R}{M}\frac{f_\lambda}{f_\eta}. \quad (C13)$$

Self-diffusion coefficient D

$$D = \frac{3}{8}(k^3T^3/\pi m)^{1/2}\frac{f_D}{P\sigma^2\Omega^{(1,1)^*}}, \quad (C14)$$

where m is twice the reduced mass, $m = 2m_1m_2/(m_1 + m_2)$.

Isotopic thermal diffusion factor α_o

$$\alpha_o = \frac{15}{2}\frac{(6C^* - 5)(2A^* + 5)}{A^*(16A^* - 12B^* + 55)}(1 + \kappa_o), \quad (C15)$$

$$\kappa_o = \frac{1}{9}(7 - 8E^*)\left[\frac{2A^*}{35/4 + 7A^* + 4F^*}\left\{H^* + \frac{[A^*(7 - 8E^*) - 7(6C^* - 5)][35/8 + 28A^* - 6F^*]}{42A^*(2A^* + 5)}\right\} - \frac{5}{7}\left\{H^* + \frac{7}{5}\frac{(6C^* - 5)}{(2A^* + 5)} - \frac{3}{10}(7 - 8E^*)\right\}\right]. \quad (C15a)$$

Note: A table of numerical values of κ_o can be found in Ref. 2.

Binary Mixture

Second virial coefficient B

$$B_{ij} = \frac{2}{3}\pi N_A\sigma_{ij}^3 B_{ij}^*, \quad (C16)$$

$$B = x_1^2B_{11} + 2x_1x_2B_{12} + x_2^2B_{22}. \quad (C17)$$

Viscosity η_{mix}

$$\eta_{12} = \frac{5}{16}\left\{\frac{2m_1m_2kT}{\pi(m_1 + m_2)}\right\}^{1/2}\frac{1}{\sigma_{12}^2\Omega_{12}^{(2,2)^*}(T_{12}^*)}, \quad (C18)$$

$$\eta_{mix} = \frac{1 + Z_\eta}{X_\eta + Y_\eta}, \quad (C19)$$

$$X_\eta = \frac{x_1^2}{\eta_1} + \frac{2x_1x_2}{\eta_{12}} + \frac{x_2^2}{\eta_2},$$

$$Y_\eta = \frac{3}{5}A_{12}^*\left\{\frac{x_1^2}{\eta_1}\left(\frac{m_1}{m_2}\right) + \frac{2x_1x_2}{\eta_{12}}\frac{(m_1 + m_2)^2}{4m_1m_2}\left(\frac{\eta_{12}^2}{\eta_1\eta_2}\right) + \frac{x_2^2}{\eta_2}\left(\frac{m_2}{m_1}\right)\right\},$$

$$Z_\eta = \frac{3}{5} A^*_{12}\left(x_1^2\left(\frac{m_1}{m_2}\right) + 2x_1x_2 \times\left\{\left[\frac{(m_1+m_2)^2}{4m_1m_2}\right]\left(\frac{\eta_{12}}{\eta_1}+\frac{\eta_{12}}{\eta_1}\right)-1\right\} + x_2^2\left(\frac{m_2}{m_1}\right)\right).$$

Thermal conductivity λ_{mix}

$$\lambda_{12} = \frac{75}{64}\left\{\frac{k^3T(m_1+m_2)}{2\pi m_1m_2}\right\}^{1/2}\frac{(1+\Delta)}{\sigma_{12}^2\Omega_{12}^{(2,2)*}(T^*_{12})}. \quad \text{(C20)}$$

Note that the term, $1+\Delta$, has been included. The expression for Δ is given in Eq. (C22a).

$$\lambda_{\text{mix}} = \frac{1+Z_\lambda}{X_\lambda + Y_\lambda}, \quad \text{(C21)}$$

$$X_\lambda = \frac{x_1^2}{\lambda_1}+\frac{2x_1x_2}{\lambda_{12}}+\frac{x_2^2}{\lambda_2},$$

$$Y_\lambda = \frac{x_1^2}{\lambda_1}U^{(1)}+\frac{2x_1x_2}{\lambda_{12}}U^{(Y)}+\frac{x_2^2}{\lambda_2}U^{(2)},$$

$$Z_\lambda = x_1^2U^{(1)}+2x_1x_2u^{(Z)}+x_2^2U^{(2)},$$

$$U^{(1)} = \frac{4}{15}A^*_{12}-\frac{1}{12}\left(\frac{12}{5}B^*_{12}+1\right)\times\frac{m_1}{m_2}+\frac{1}{2}\frac{(m_1-m_2)^2}{m_1m_2},$$

$$U^{(2)} = \frac{4}{15}A^*_{12}-\frac{1}{12}\left(\frac{12}{5}B^*_{12}+1\right)\times\frac{m_2}{m_1}+\frac{1}{2}\frac{(m_2-m_1)^2}{m_1m_2},$$

$$U^{(Y)} = \frac{4}{15}A^*_{12}\left[\frac{(m_1+m_2)^2}{4m_1m_2}\right]\times\left(\frac{\lambda_{12}^2}{\lambda_1\lambda_2}\right)-\frac{1}{12}\left(\frac{12}{5}B^*_{12}+1\right)-\frac{5}{32A^*_{12}}\left(\frac{12}{5}B^*_{12}-5\right)\frac{(m_1-m_2)^2}{m_1m_2},$$

$$U^{(Z)} = \frac{4}{15}A^*_{12}\left\{\left[\frac{(m_1+m_2)^2}{4m_1m_2}\right]\times\left(\frac{\lambda_{12}}{\lambda_1}+\frac{\lambda_{12}}{\lambda_2}\right)-1\right\}-\frac{1}{12}\left(\frac{12}{5}B^*_{12}+1\right).$$

Binary diffusion coefficient

$$D_{12} = \frac{3}{8}\left\{\frac{k^3T^3(m_1+m_2)}{2\pi m_1m_2}\right\}^{1/2}\frac{(1+\Delta)}{P\sigma_{12}^2\Omega_{12}^{(1,1)*}(T^*_{12})}, \quad \text{(C22)}$$

$$\Delta = \xi(6C^*_{12}-5)^2ax_1/(1+bx_1), \quad \text{(C22a)}$$

where

$$\xi = 1.3,$$

$$a = \frac{2^{1/2}}{8(1+1.8c)^2}\frac{\Omega_{12}^{(1,1)*}}{\Omega_{22}^{(2,2)*}},$$

$$b = 10a(1+1.8c+3c^2)-1,$$

$$c = m_2/m_1 < 1,$$

in which subscript 1 denotes the heavier component and subscript 2 denotes the lighter.

Thermal diffusion factor

$$\alpha_T = (6C^*_{12}-5)\left(\frac{x_1S_1-x_2S_2}{x_1^2Q_1+x_2^2Q_2+x_1x_2Q_{12}}\right)(1+\kappa_2), \quad \text{(C23)}$$

where κ_2 is a correction term arising from the higher approximations of the theory and is small in magnitude, in most cases being negligible in comparison with experimental uncertainty. The other quantities in Eq. (C23) are

$$S_1 = \frac{m_1}{m_2}\left(\frac{2m_2}{m_1+m_2}\right)^{1/2}\frac{\Omega_{11}^{(2,2)*}}{\Omega_{12}^{(1,1)*}}\left(\frac{\sigma_{11}}{\sigma_{12}}\right)^2 - \frac{4m_1m_2A^*_{12}}{(m_1+m_2)^2}+\frac{15m_2(m_1-m_2)}{2(m_1+m_2)^2},$$

$$Q_1 = \frac{2}{m_2(m_1+m_2)}\left(\frac{2m_2}{m_1+m_2}\right)^{1/2}\frac{\Omega_{11}^{(2,2)*}}{\Omega_{12}^{(1,1)*}}\left(\frac{\sigma_{11}}{\sigma_{12}}\right)^2\left[\left(\frac{5}{2}-\frac{6}{5}B^*_{12}\right)m_1^2+3m_2^2+\frac{8}{5}m_1m_2A^*_{12}\right].$$

$$Q_{12} = 15\left(\frac{m_1-m_2}{m_1+m_2}\right)^2\left(\frac{5}{2}-\frac{6}{5}B^*_{12}\right)+\frac{4m_1m_2A^*_{12}}{(m_1+m_2)^2}\left(11-\frac{12}{5}B^*_{12}\right)+\frac{8(m_1+m_2)}{5(m_1m_2)^{1/2}}\left\{\frac{\sigma_{11}^2\Omega_{11}^{(2,2)*}}{\sigma_{12}^2\Omega_{12}^{(1,1)*}}\right\}\left\{\frac{\sigma_{22}^2\Omega_{22}^{(2,2)*}}{\sigma_{12}^2\Omega_{12}^{(1,1)*}}\right\}.$$

The expressions for S_2 and Q_2 are obtained from those for S_1 and Q_1 by interchange of subscripts.

This formula has been used for ^{3}He–^{4}He and all binary mixtures. The reduced thermal diffusion factor is defined to eliminate the composition dependence as

$$\alpha_R = \alpha_T\left(\frac{x_1S_1-x_2S_2}{x_1^2Q_1+x_2^2Q_2+x_1x_2Q_{12}}\right)^{-1} = (6C^*_{12}-5)(1+\kappa_2), \quad \text{(C23a)}$$

and is plotted in the deviation diagram. The solid line in the diagram indicates the calculated value of $(6C^*_{12}-5)$ as a function of temperature.

Multicomponent Mixture

Second virial coefficient B

$$B = \sum_{j=1}^{\nu}\sum_{i=1}^{\nu}x_ix_jB_{ij}. \quad \text{(C24)}$$

Viscosity

$$\eta_{\text{mix}} = -\frac{\begin{vmatrix} H_{11} & H_{12} & \cdots & H_{1\nu} & x_1 \\ H_{21} & H_{22} & \cdots & H_{2\nu} & x_2 \\ \vdots & \vdots & & & \\ H_{\nu1} & H_{\nu2} & \cdots & H_{\nu\nu} & x_\nu \\ x_1 & x_2 & \cdots & x_\nu & 0 \end{vmatrix}}{\begin{vmatrix} H_{11} & H_{12} & \cdots & H_{1\nu} \\ H_{21} & H_{22} & \cdots & H_{2\nu} \\ \vdots & \vdots & & \vdots \\ H_{\nu1} & H_{\nu2} & & H_{\nu\nu} \end{vmatrix}} \quad \text{(C25)}$$

where

$$H_{ii}=\frac{x_i^2}{\eta_i}+\sum_{\substack{k=1\\k\neq i}}^{\nu}\frac{2x_ix_k}{\eta_{ik}}\frac{m_im_k}{(m_i+m_k)^2}\left(\frac{5}{3A^*_{ik}}+\frac{m_k}{m_i}\right),$$

$$H_{ij}=-\frac{2x_ix_j}{\eta_{ij}}\frac{m_im_j}{(m_i+m_j)^2}\left(\frac{5}{3A^*_{ij}}-1\right)\quad i\neq j.$$

Thermal conductivity

$$\lambda_{\text{mix}}=4\frac{\begin{vmatrix} L_{11} & L_{12} & \cdots & L_{1\nu} & x_1\\ L_{21} & L_{22} & \cdots & L_{2\nu} & x_2\\ \vdots & \vdots & & & \\ L_{\nu 1} & L_{\nu 2} & & L_{\nu\nu} & x_\nu\\ x_1 & x_2 & \cdots & x_\nu & 0 \end{vmatrix}}{\begin{vmatrix} L_{11} & L_{12} & \cdots & L_{1\nu}\\ L_{21} & L_{22} & \cdots & L_{2\nu}\\ \vdots & & & \\ L_{\nu 1} & L_{\nu 2} & & L_{\nu\nu} \end{vmatrix}},\qquad \text{(C26)}$$

where

$$L_{ii}=-\frac{4x_i^2}{\lambda_i}-\sum_{\substack{k=1\\k\neq i}}^{\nu}\frac{2x_ix_k\left[\left(\frac{15}{2}\right)m_i^2+\left(\frac{25}{4}\right)m_k^2-3m_k^2B^*_{ik}+4m_im_kA^*_{ik}\right]}{(m_i+m_k)^2A^*_{ik}\lambda_{ik}(1+\Delta_{ij})},$$

$$L_{ij}=\frac{2x_ix_jm_im_j}{(m_i+m_j)^2A^*_{ij}\lambda_{ij}(1+\Delta_{ij})}\left(\frac{55}{4}-3B^*_{ij}-4A^*_{ij}\right).$$

Note: For multicomponent mixtures, Δ_{ij} in Eq. (C26) is the same as Δ in Eq. (C22a). However, x_1 should here be interpreted as the ratio

$$x_1=\frac{x_i}{x_i+x_j},$$

where x_1 refers to the heavier component of the i–j pair.

Appendix D. Deviation Plots

Note: In the deviation plots, the ordinate refers to the difference between the measured and calculated quantity, i.e., $X_{\text{meas}}-X_{\text{calc}}$ or to the ratio $(X_{\text{meas}}-X_{\text{calc}})/X_{\text{calc}}$.

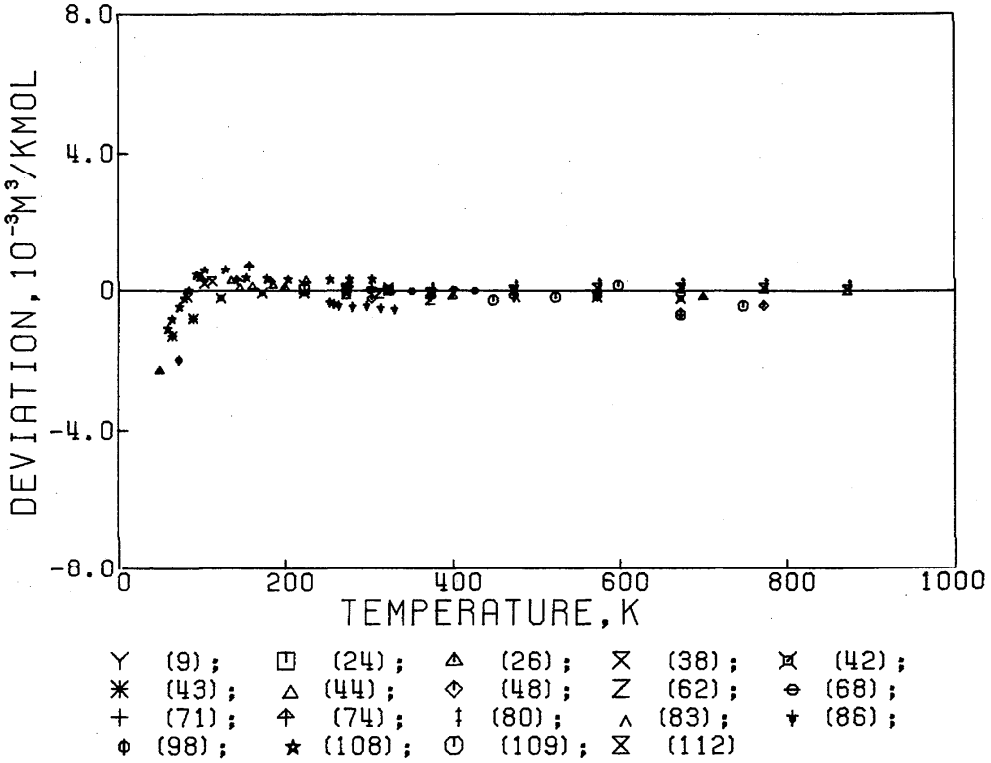

FIG. D1. Deviation plot for the second virial coefficient of He. [26]—primary data; others—secondary data.

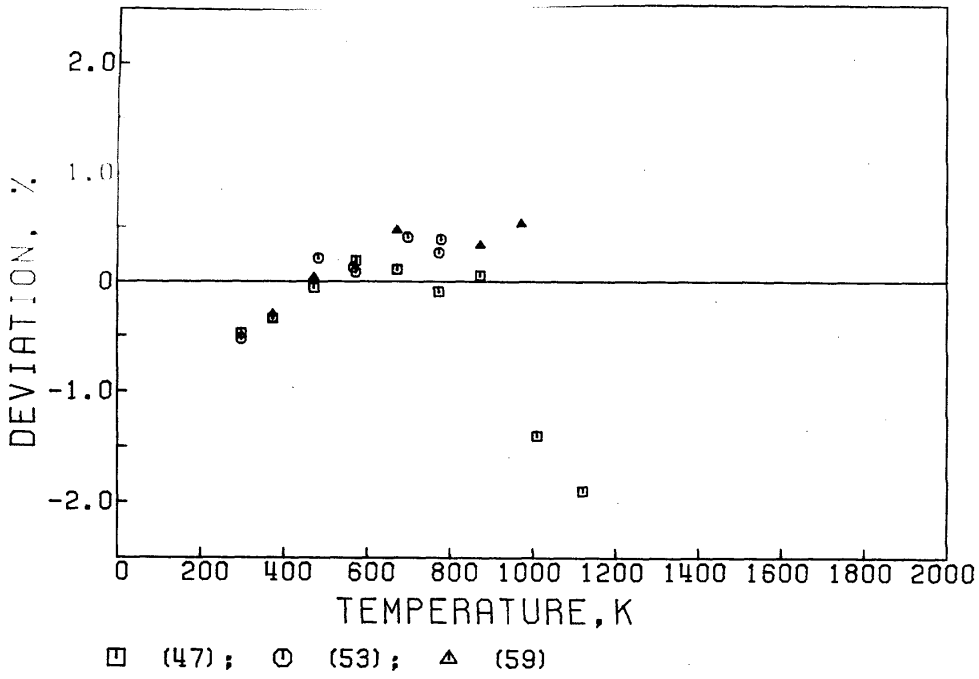

FIG. D2. Deviation plot for the viscosity of He. Primary data.

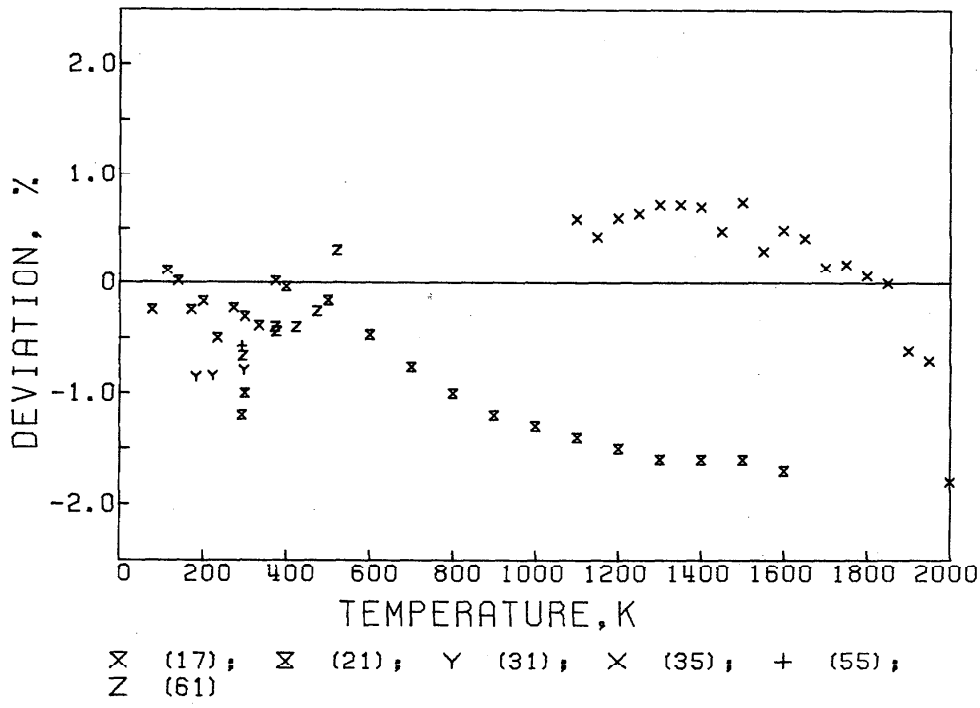

FIG. D3. Deviation plot for the viscosity of He. Secondary data.

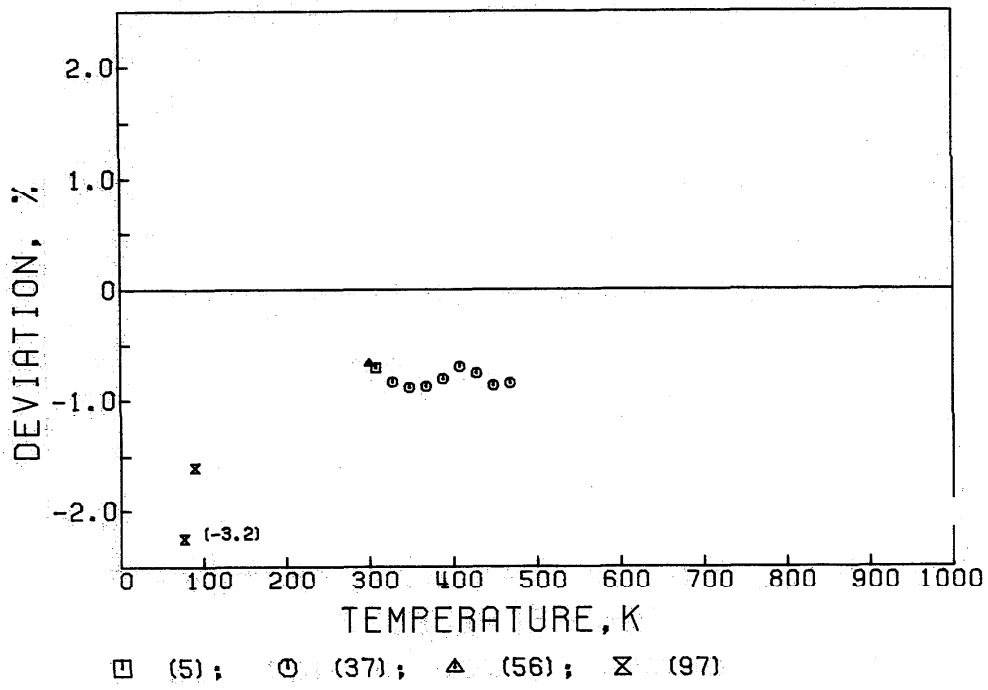

FIG. D4. Deviation plot for the thermal conductivity of He. Secondary data.

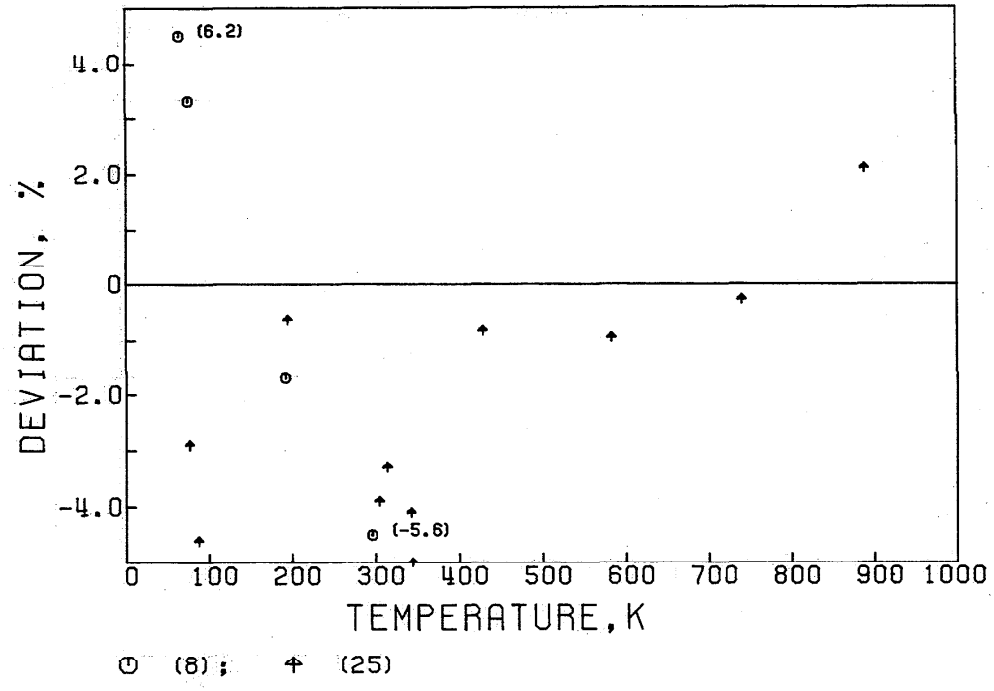

FIG. D5. Deviation plot for the binary diffusion coefficient of ^{3}He–^{4}He. Secondary data.

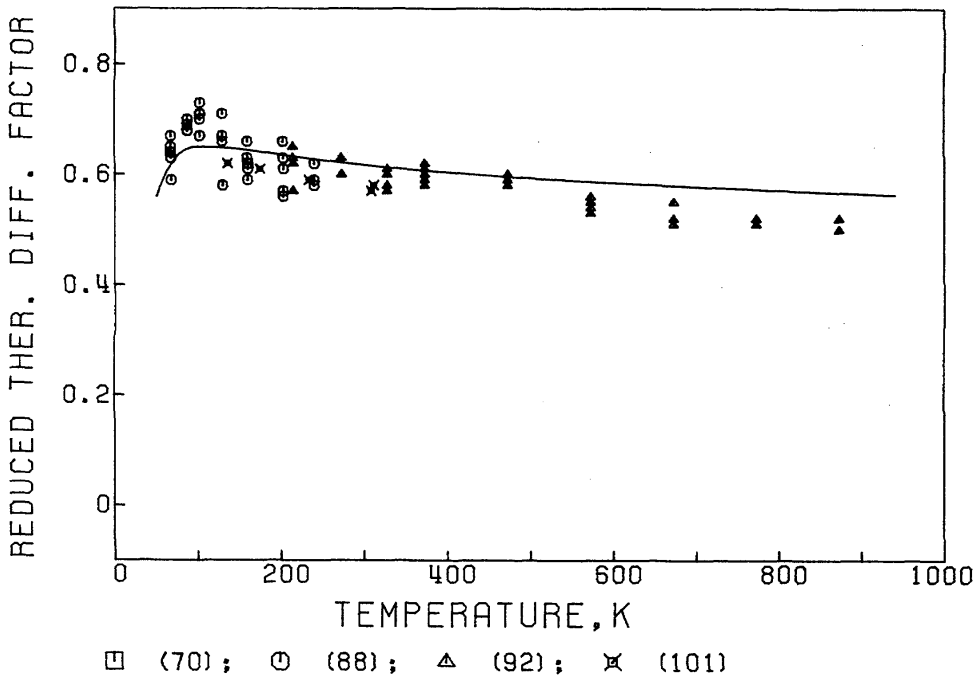

FIG. D6. Reduced thermal diffusion factor of ^{3}He–^{4}He. Secondary data.
This is defined as

$$\alpha_T\left[\frac{x_1S_1 - x_2S_2}{x_1^2Q_1 + x_2^2Q_2 + x_1x_2Q_{12}}\right]^{-1} = (6C_{12}^* - 5)(1 + \kappa_2).$$

The solid line represents the calculated function.

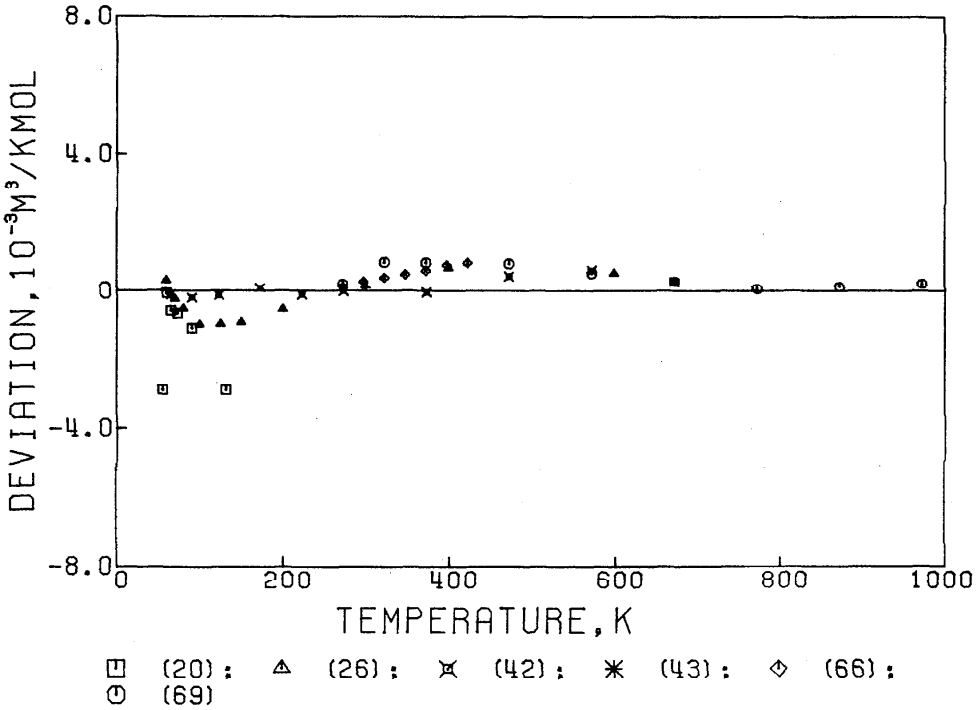

FIG. D7. Deviation plot for the second virial coefficient of Ne. [26]—primary data; others—secondary data.

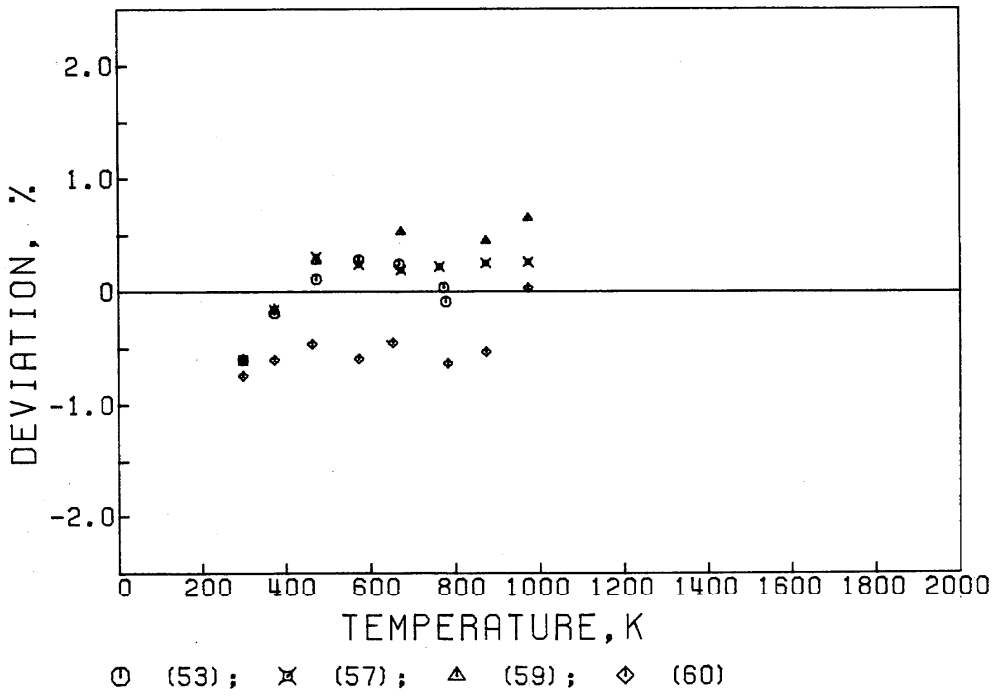

FIG. D8. Deviation plot for the viscosity of Ne. Primary data.

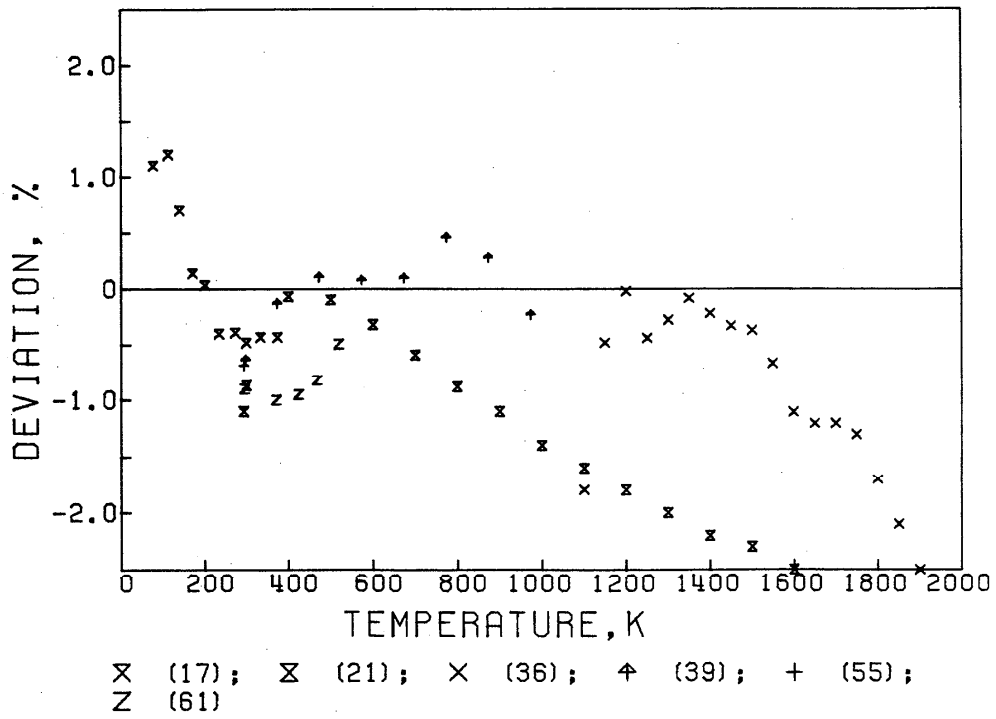

FIG. D9. Deviation plot for the viscosity of Ne. Secondary data.

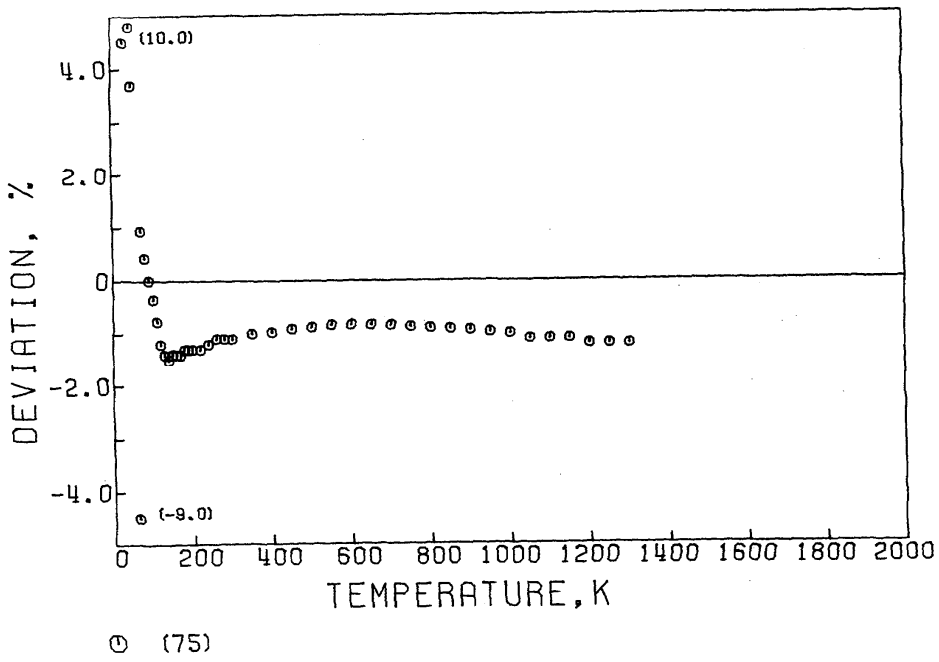

FIG. D10. Deviation plot for the viscosity of Ne. Data from [75] by Rabinovich.

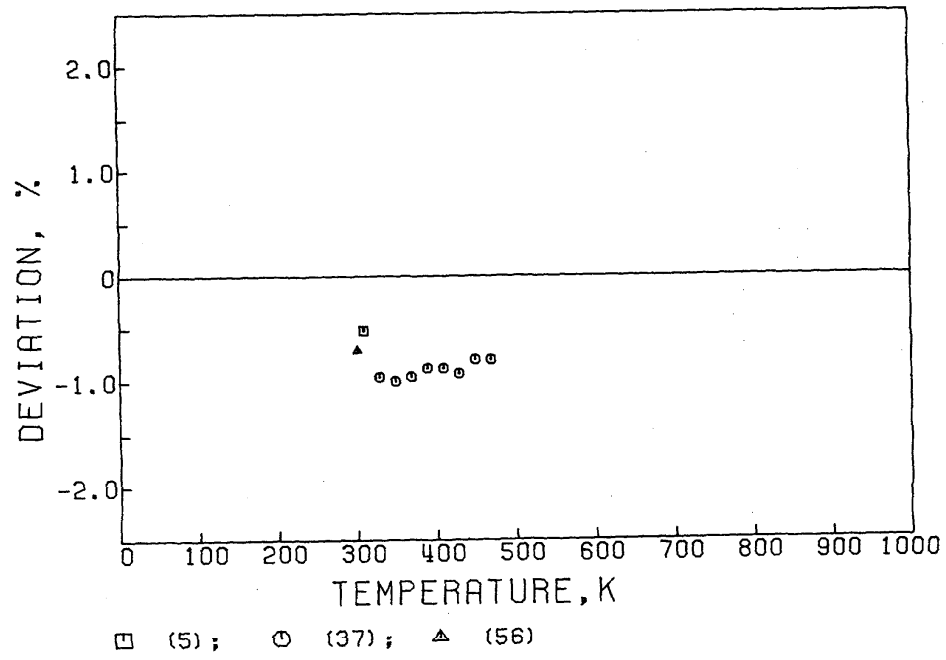

FIG. D11. Deviation plot for the thermal conductivity of Ne. Secondary data.

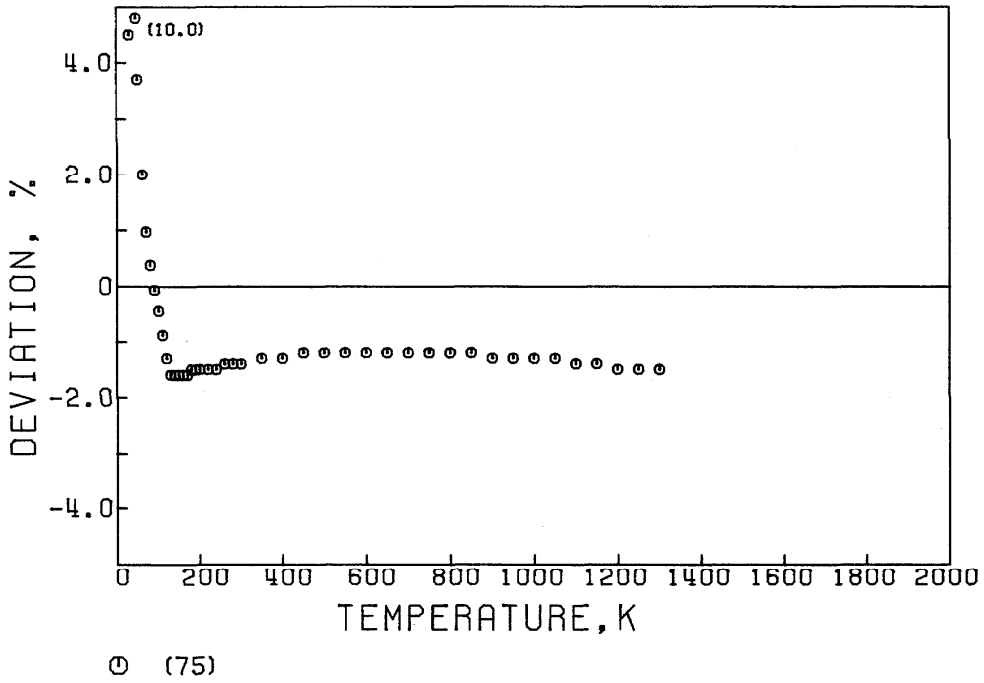

FIG. D12. Deviation plot for the thermal conductivity of Ne. Data from [75] by Rabinovich.

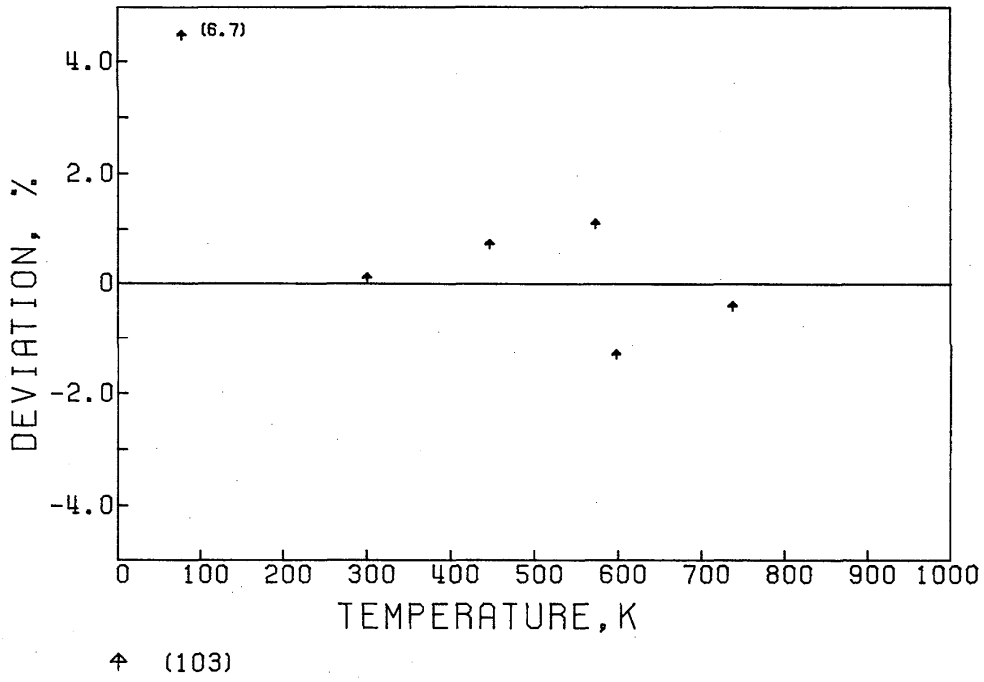

FIG. D13. Deviation plot for the self-diffusion coefficient of Ne. Secondary data.

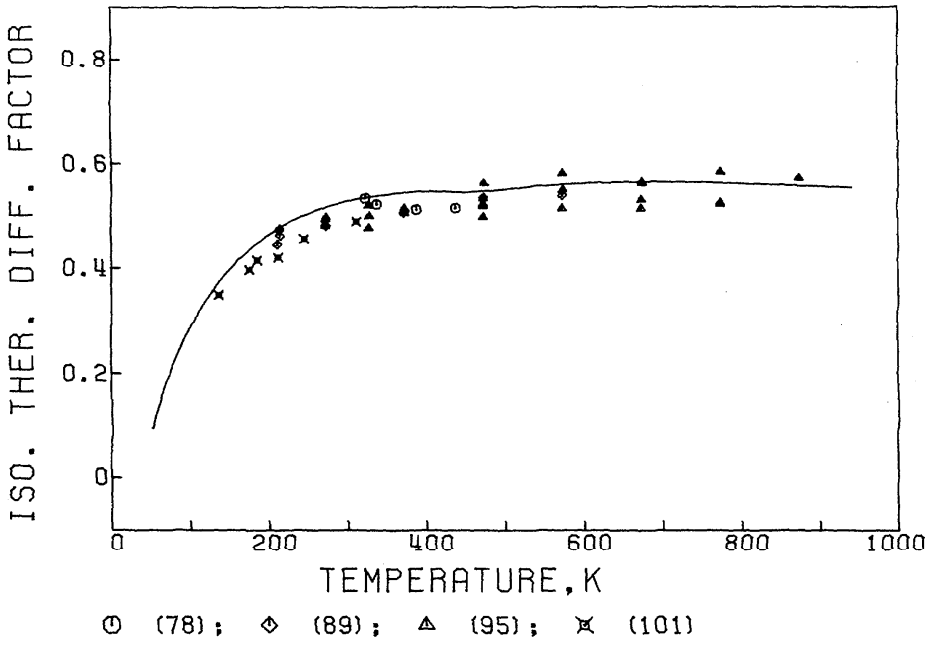

FIG. D14. Isotopic thermal diffusion factor of Ne. Secondary data.

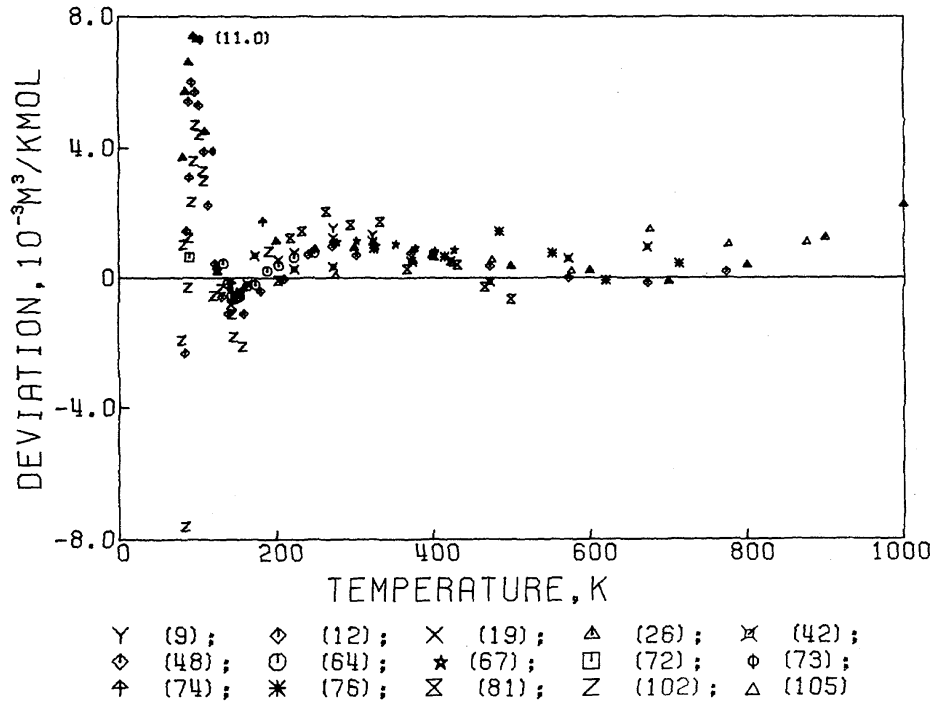

FIG. D15. Deviation plot for the second virial coefficient of Ar. [26]—primary data; others—secondary data.

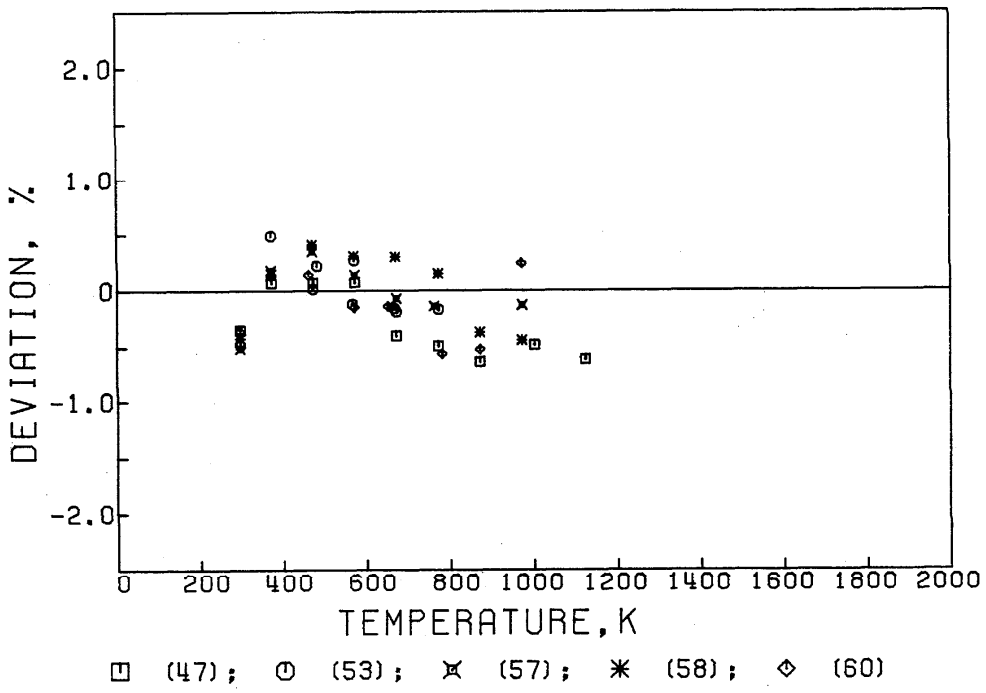

FIG. D16. Deviation plot for the viscosity of Ar. Primary data.

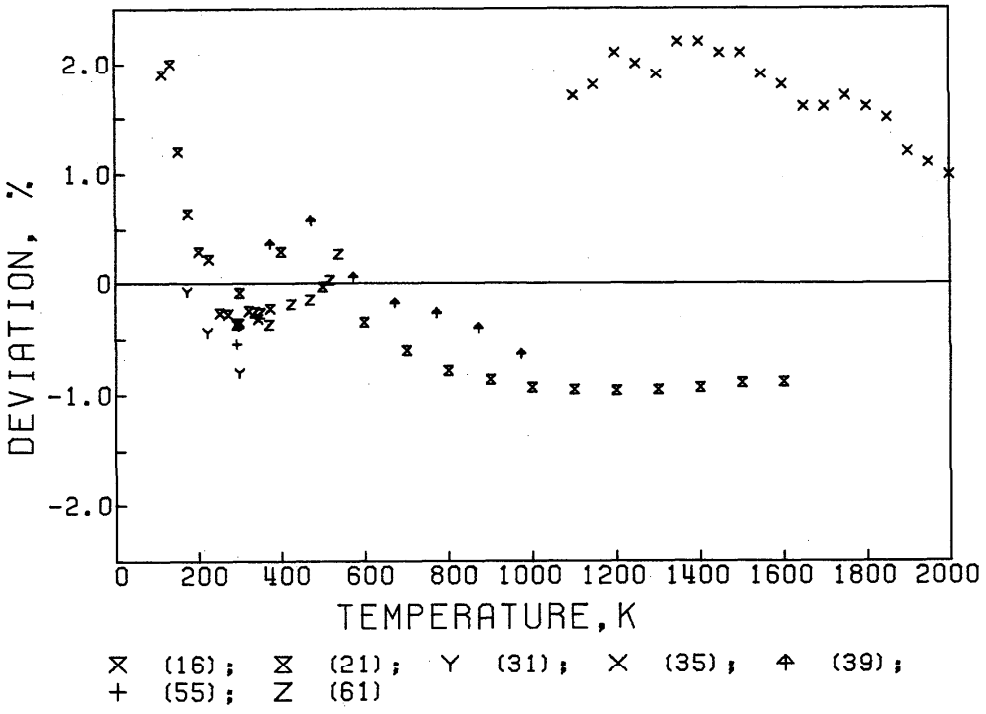

FIG. D17. Deviation plot for the viscosity of Ar. Secondary data.

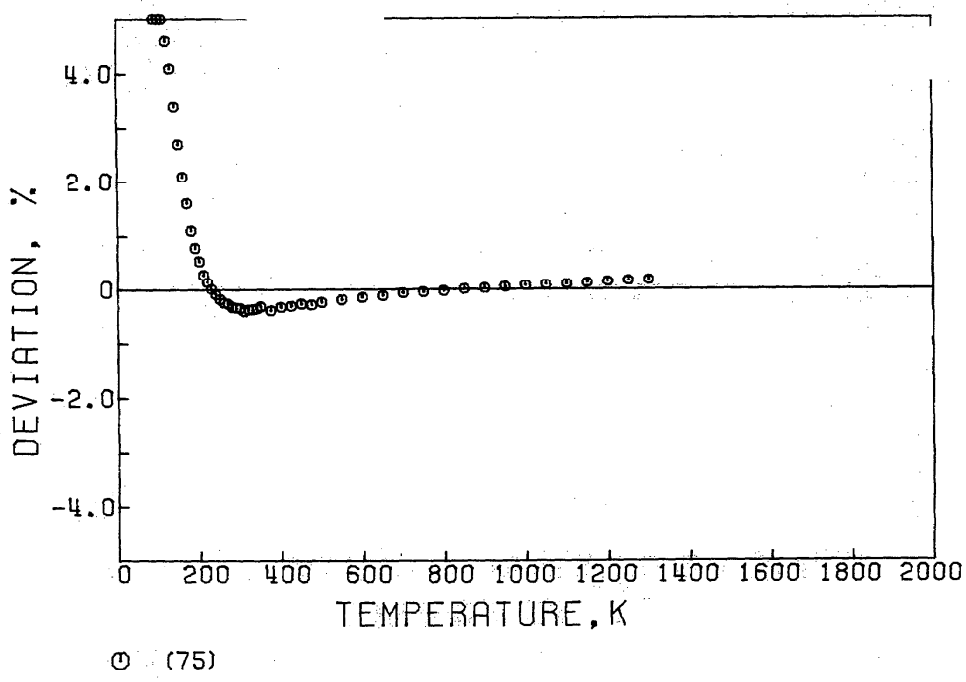

FIG. D18. Deviation plot for the viscosity of Ar. Data from [75] by Rabinovich.

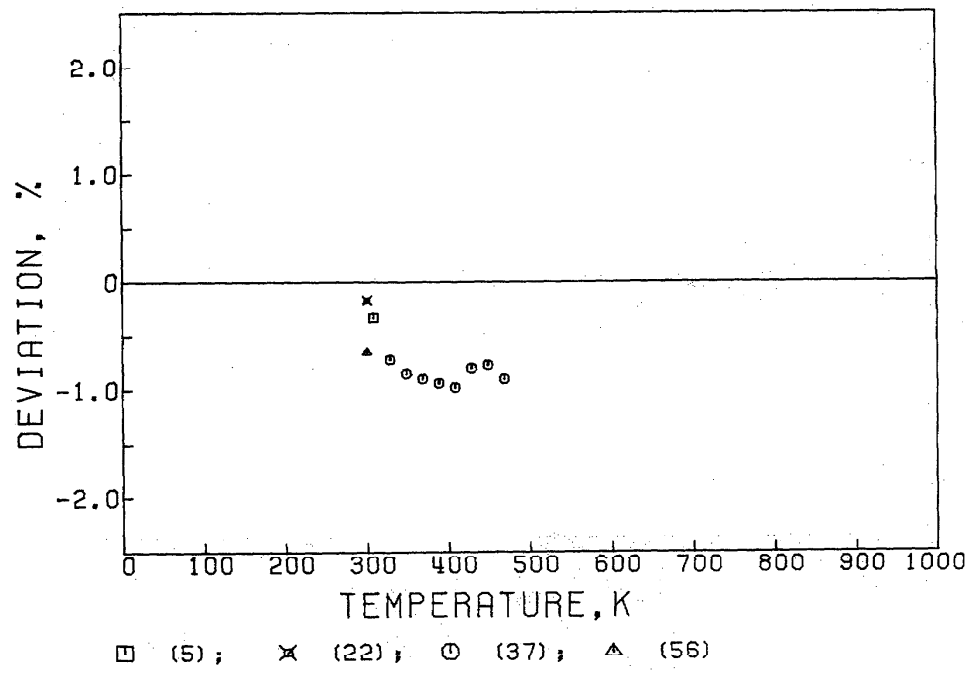

FIG. D19. Deviation plot for the thermal conductivity of Ar. Secondary data.

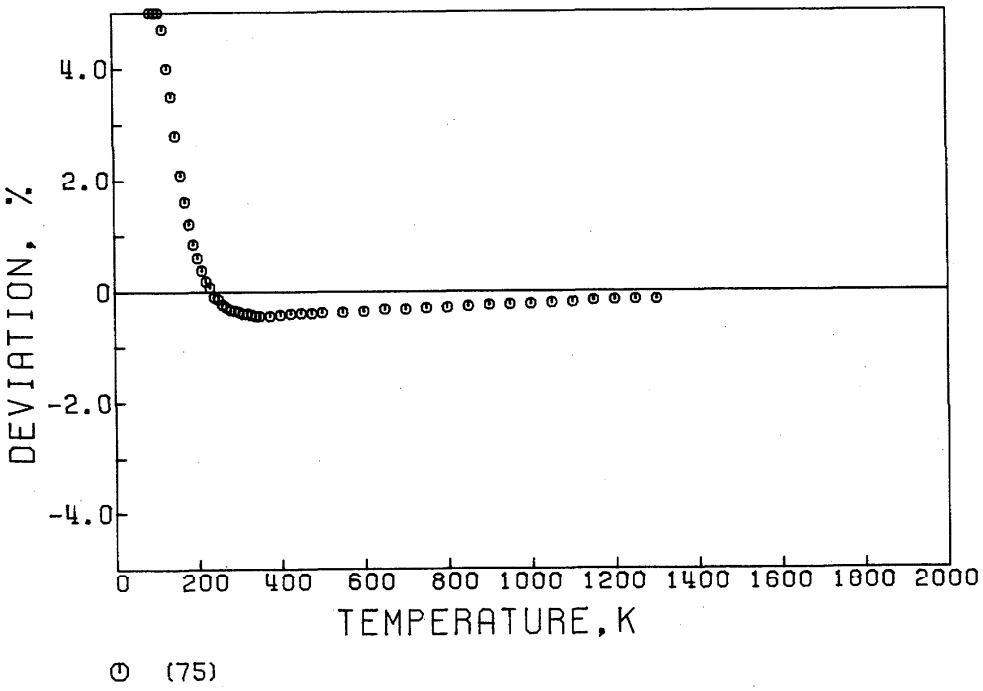

FIG. D20. Deviation plot for the thermal conductivity of Ar. Data from [75] by Rabinovich.

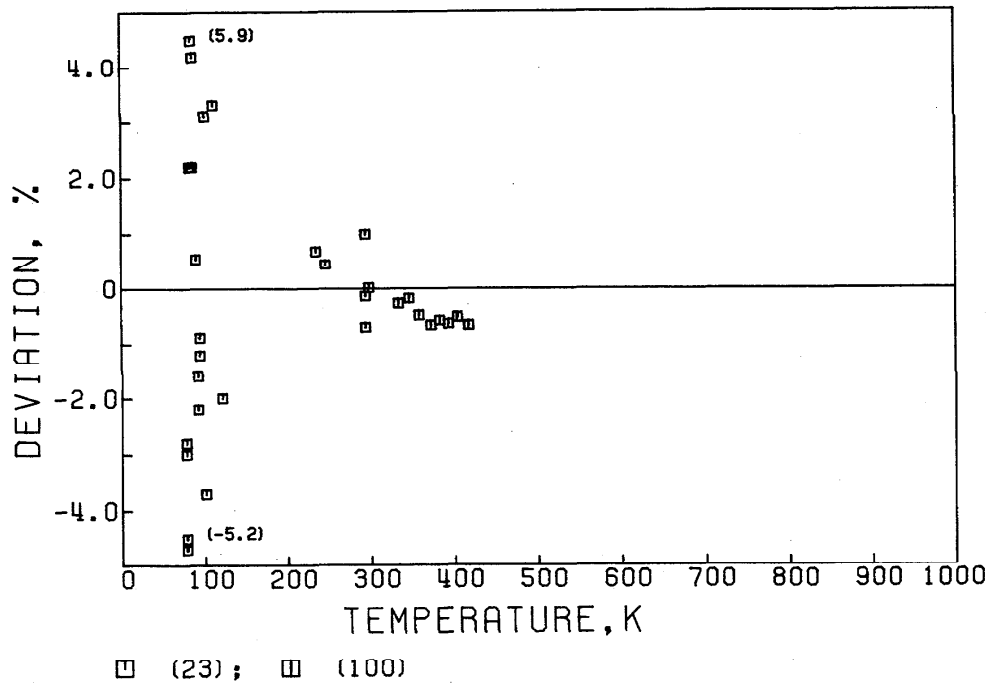

FIG. D21. Deviation plot for the self-diffusion coefficient of Ar. Secondary data.

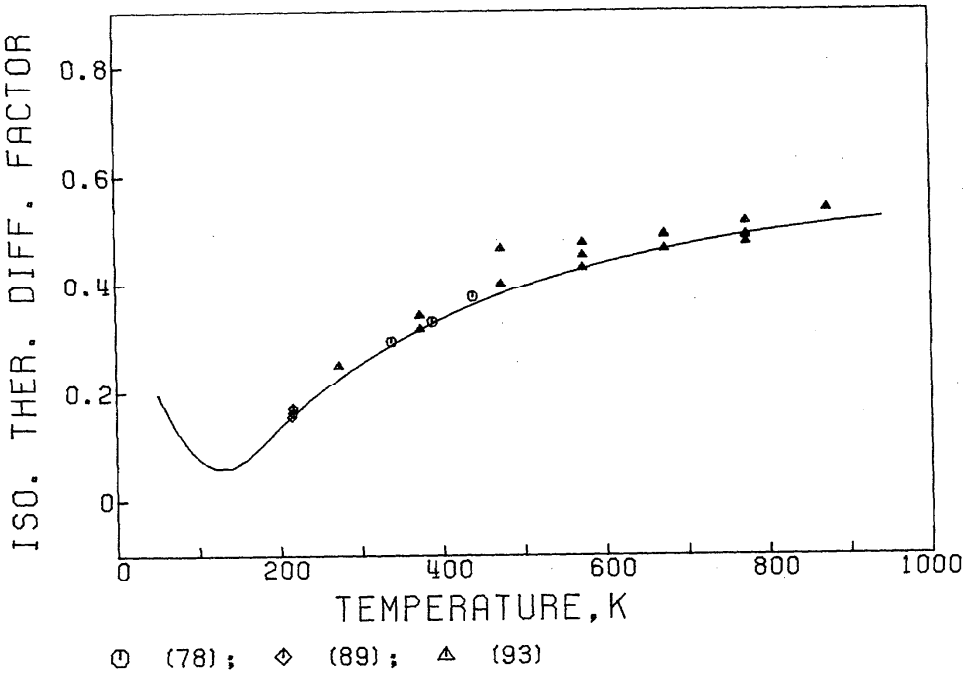

FIG. D22. Isotopic thermal diffusion factor of Ar. Secondary data.

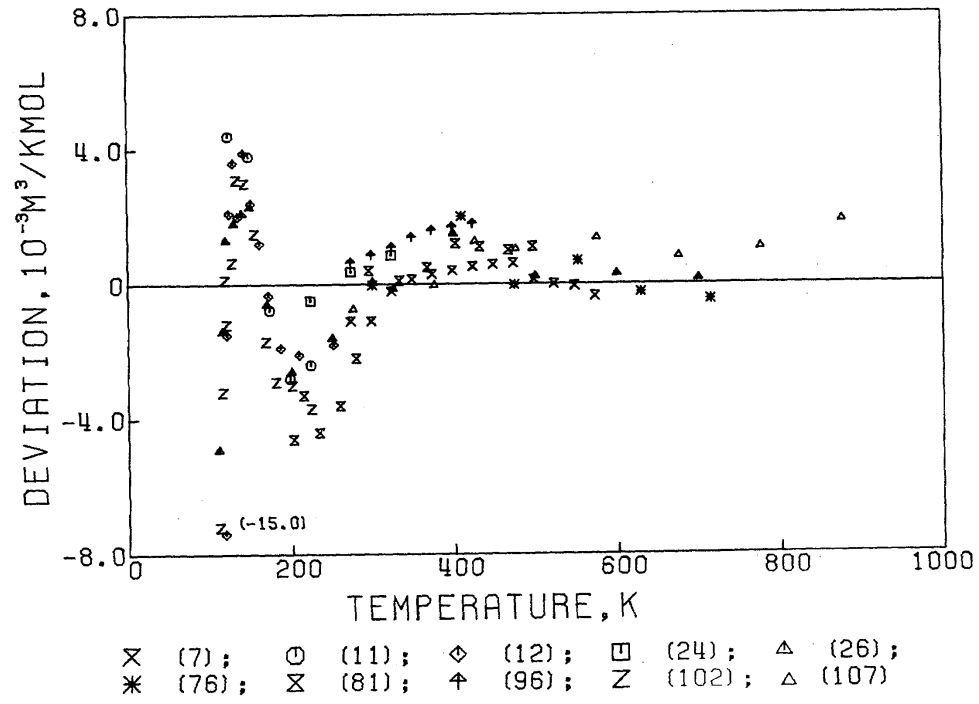

FIG. D23. Deviation plot for the second virial coefficient of Kr. [26]—primary data; others—secondary data.

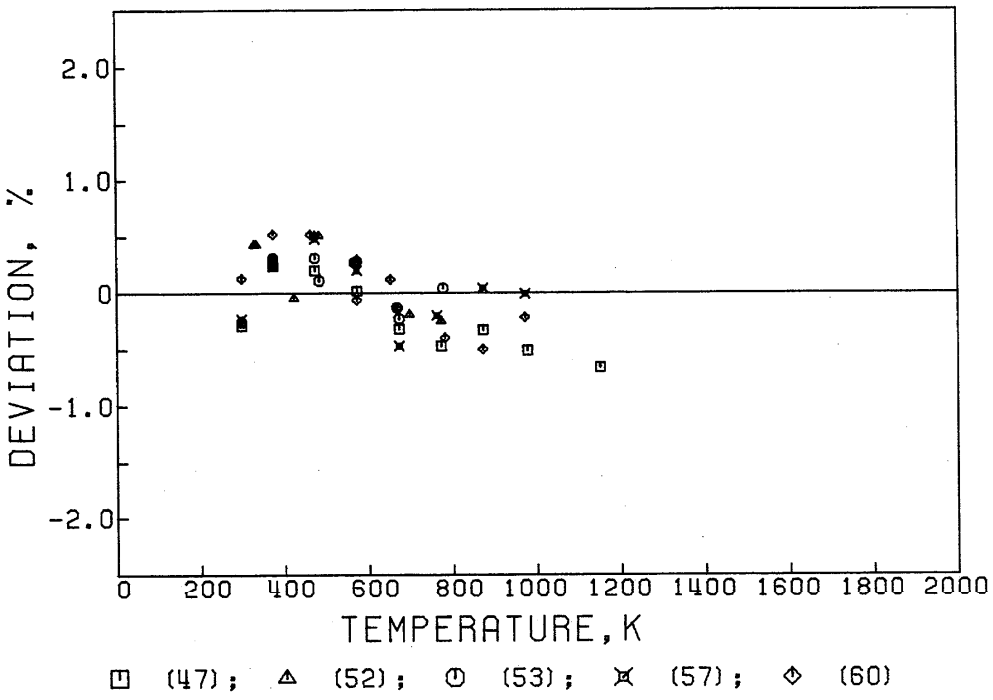

FIG. D24. Deviation plot for the viscosity of Kr. Primary data.

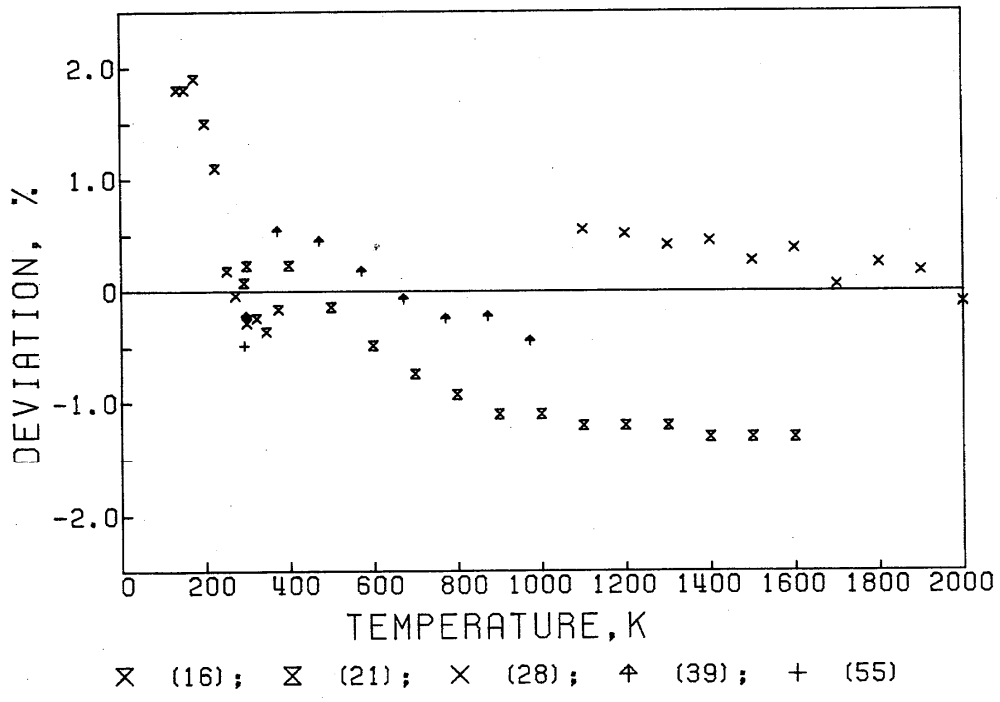

FIG. D25. Deviation plot for the viscosity of Kr. Secondary data.

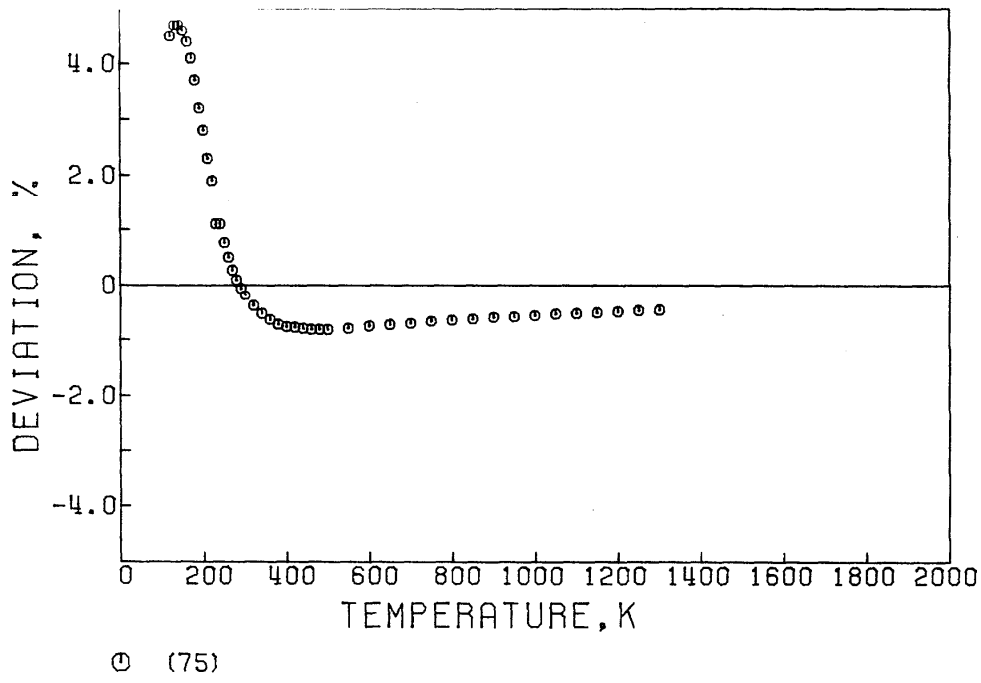

FIG. D26. Deviation plot for the viscosity of Kr. Data from [75] by Rabinovich.

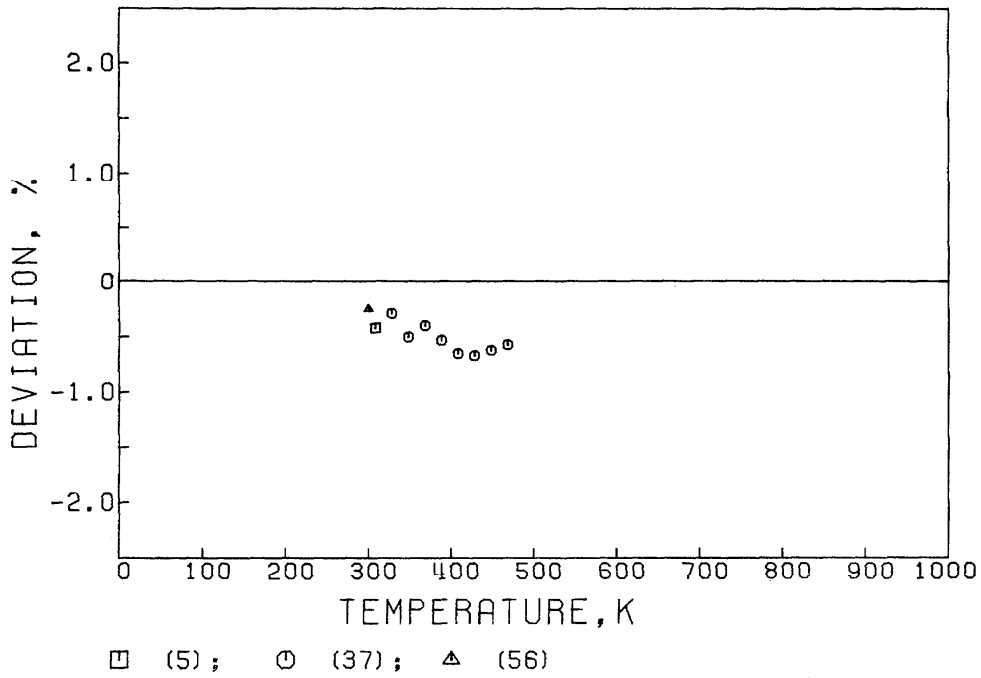

FIG. D27. Deviation plot for the thermal conductivity of Kr. Secondary data.

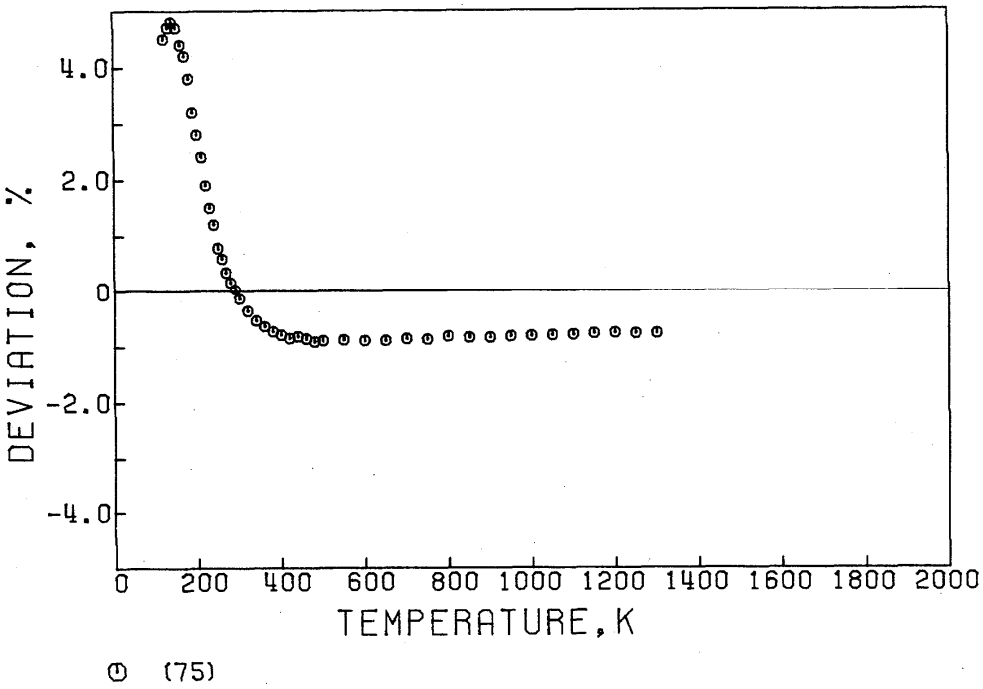

FIG. D28. Deviation plot for the thermal conductivity of Kr. Data from [75] by Rabinovich.

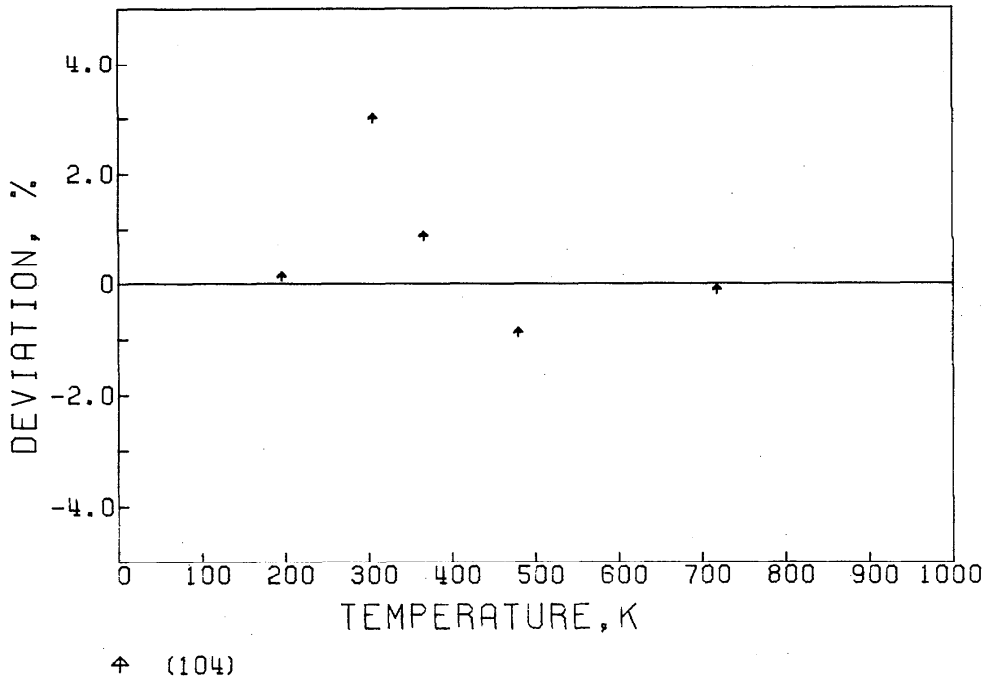

FIG. D29. Deviation for the the self-diffusion coefficient of Kr. Secondary data.

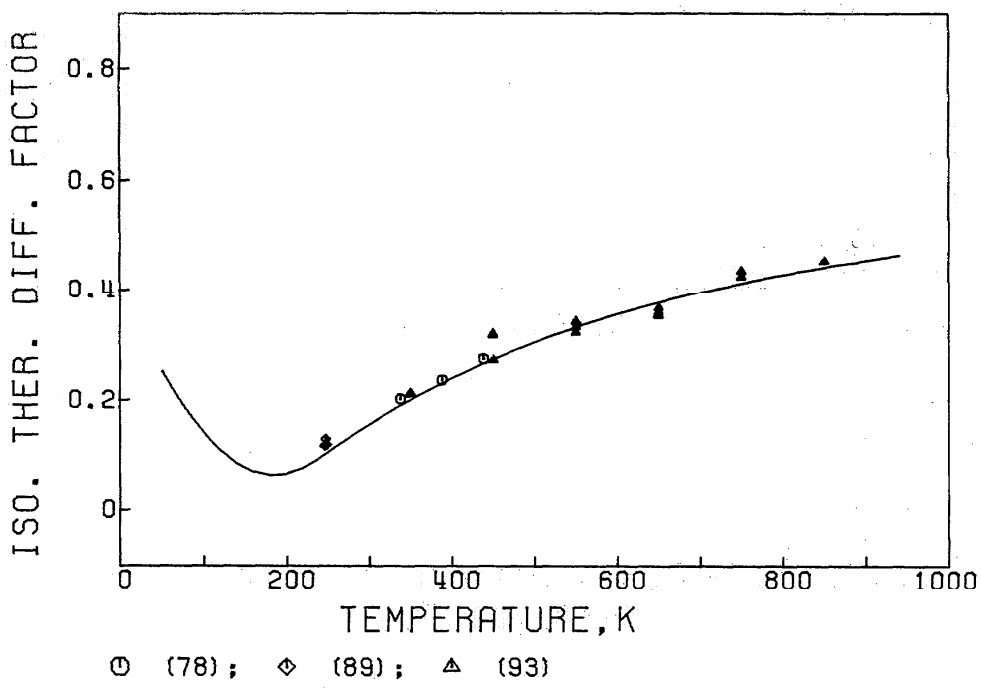

FIG. D30. Isotopic thermal diffusion factor of Kr. Secondary data.

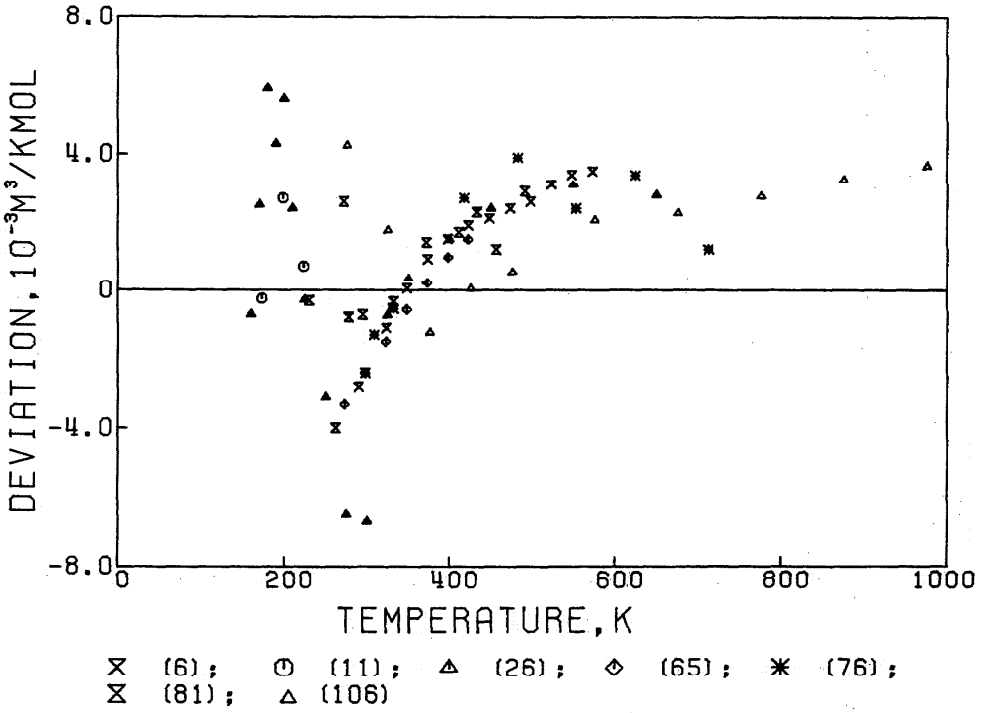

FIG. D31. Deviation plot for the second virial coefficient of Xe. [26]—primary data; others—secondary data.

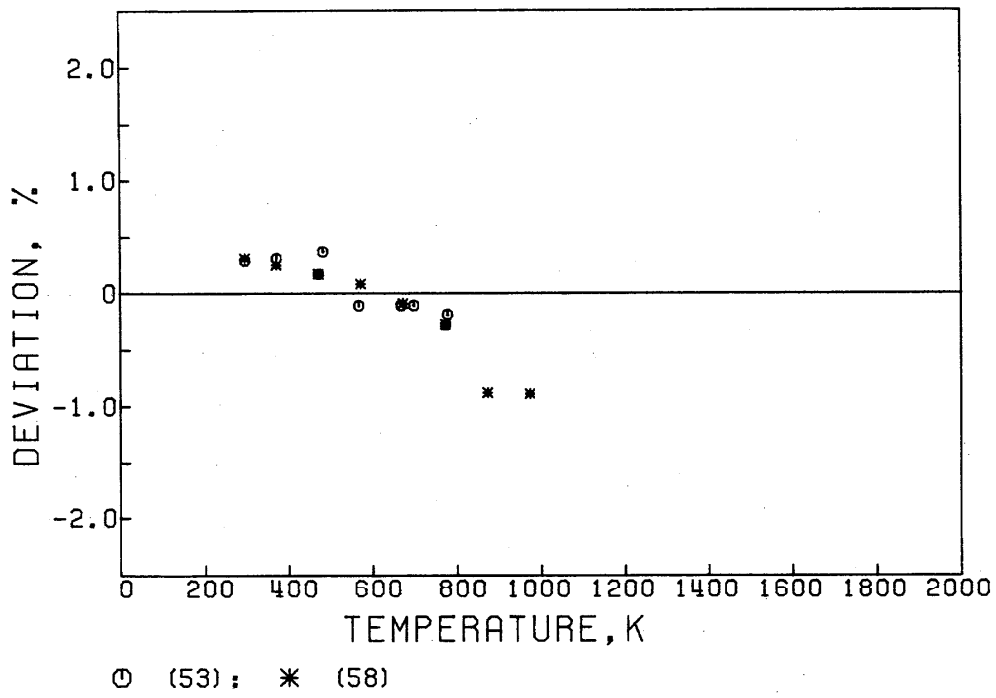

FIG. D32. Deviation plot for the viscosity of Xe. Primary data.

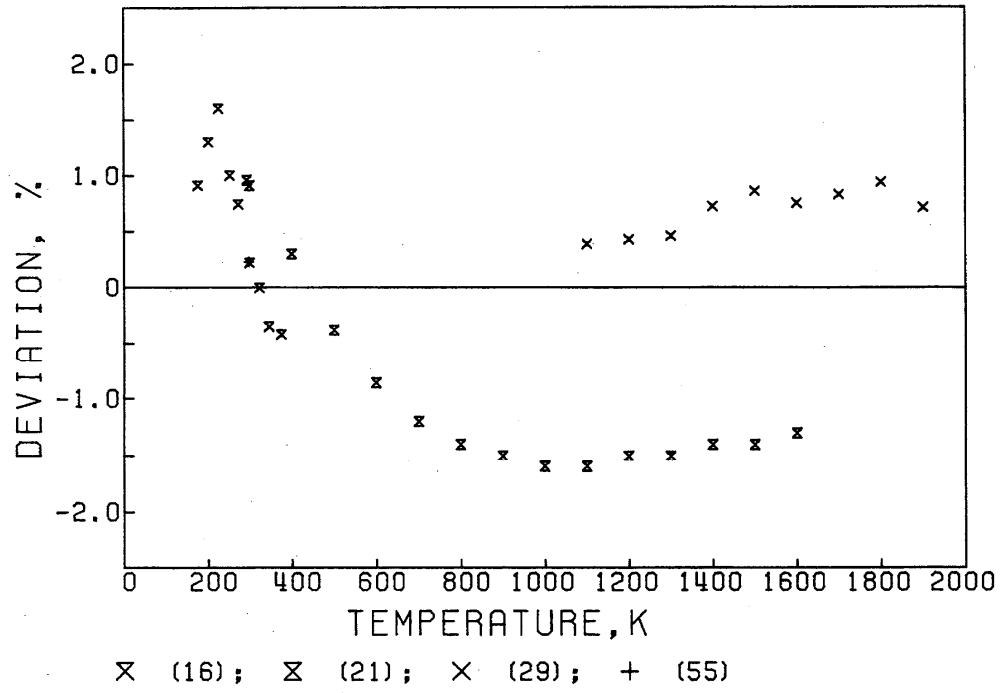

FIG. D33. Deviation plot for the viscosity of Xe. Secondary data.

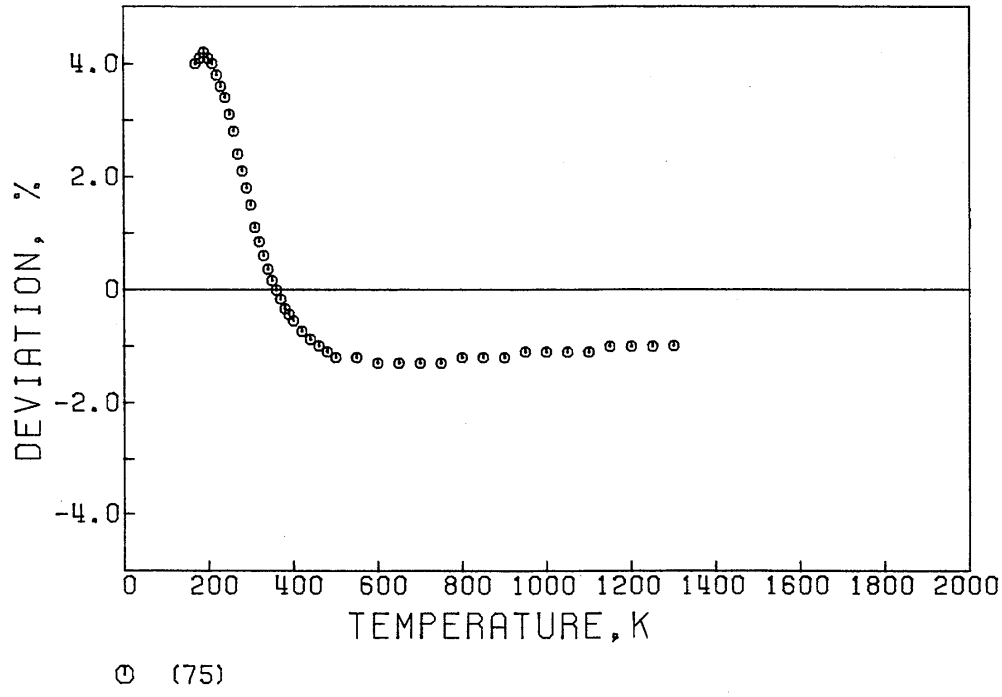

FIG. D34. Deviation plot for the viscosity of Xe. Data from [75] by Rabinovich.

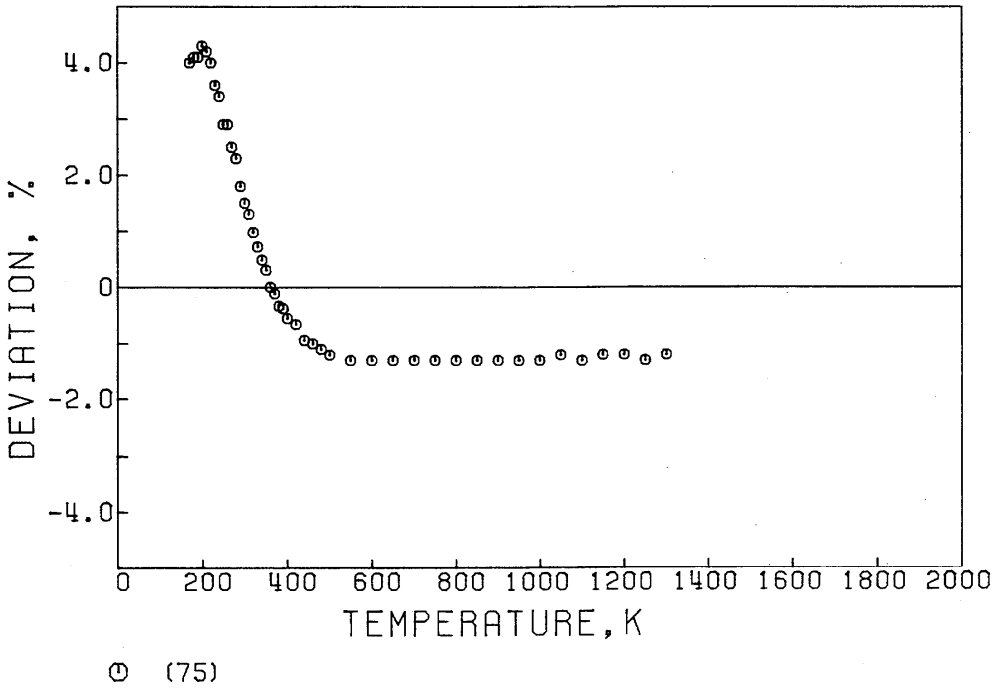

FIG. D35. Deviation plot for the thermal conductivity of Xe. Secondary data.

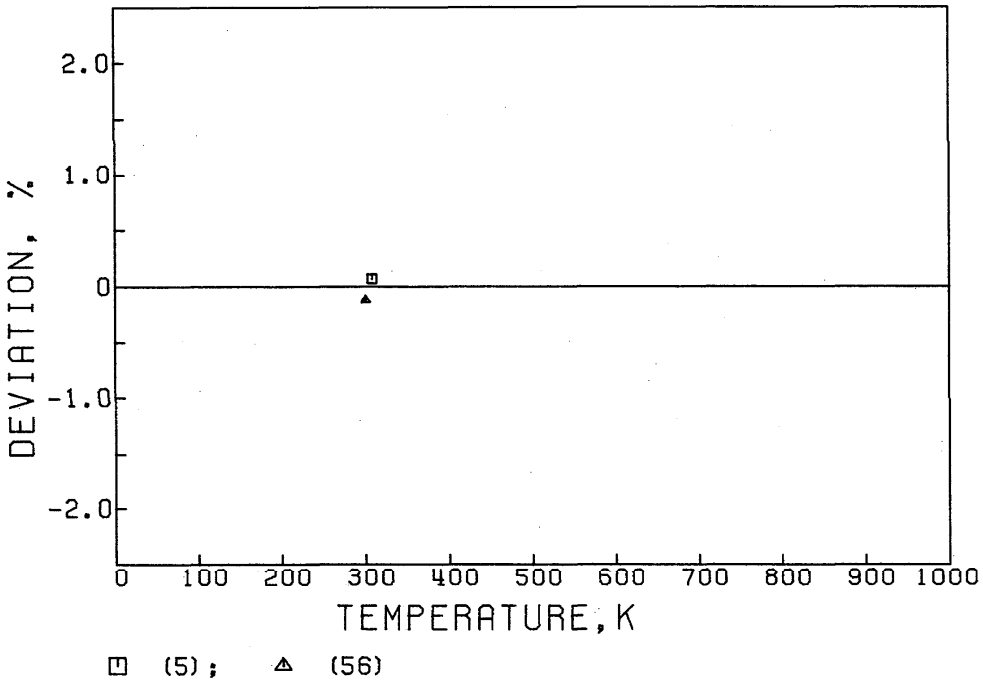

FIG. D36. Deviation plot for the thermal conductivity of Xe. Data from [75] by Rabinovich.

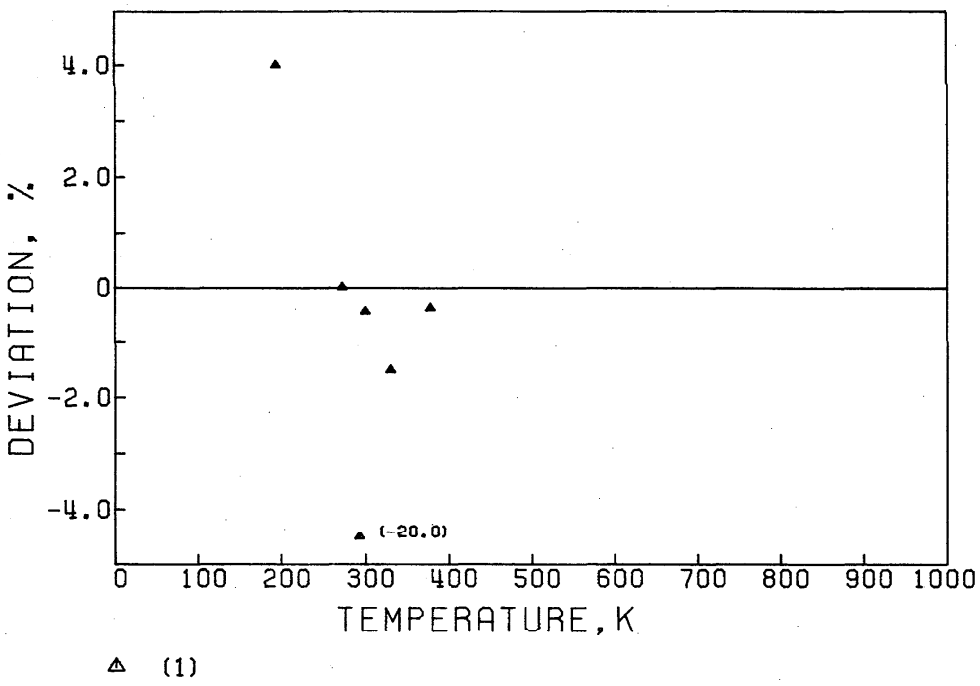

FIG. D37. Deviation plot for the self-diffusion coefficient of Xe. Secondary data.

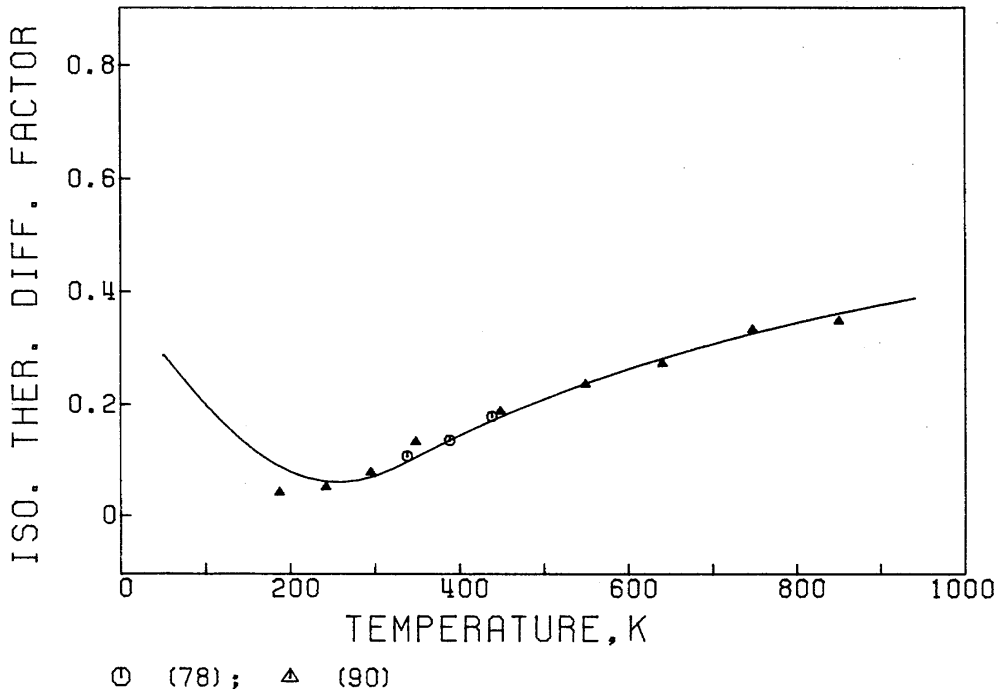

FIG. D38. Isotopic thermal diffusion factor of Xe. Secondary data.

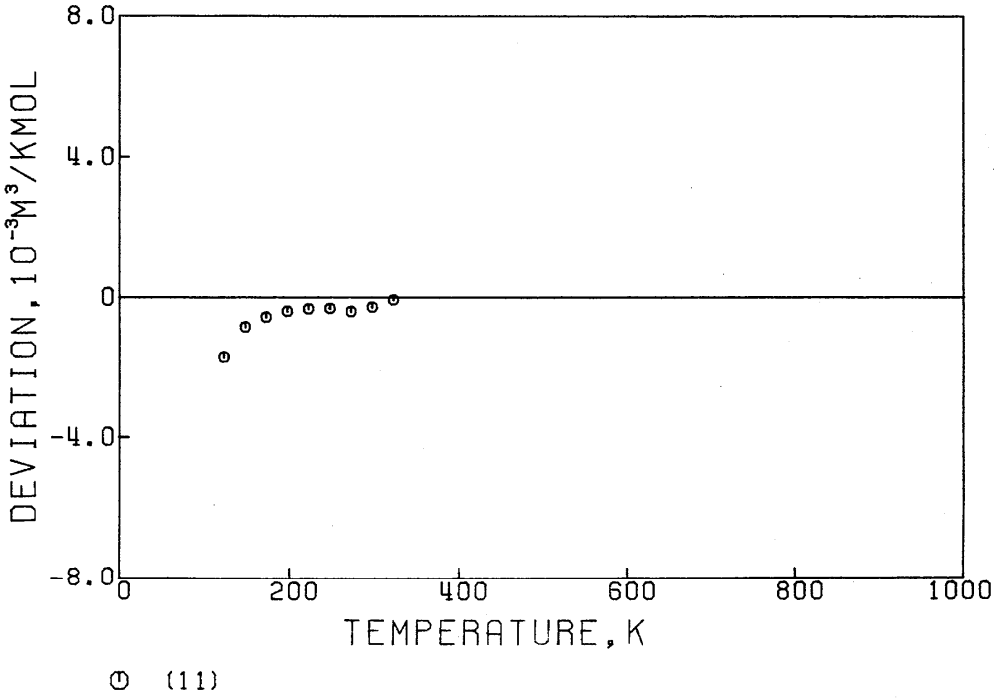

FIG. D39. Deviation plot for the interaction second virial coefficient of He–Ne. Primary data.

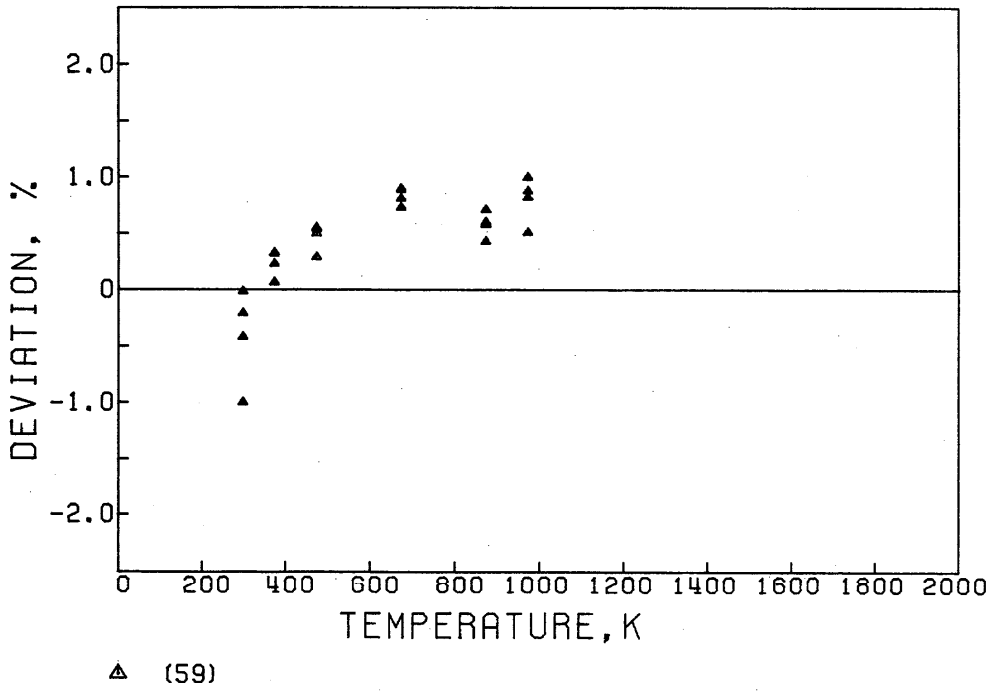

FIG. D40. Deviation plot for the viscosity of He–Ne. Primary data.

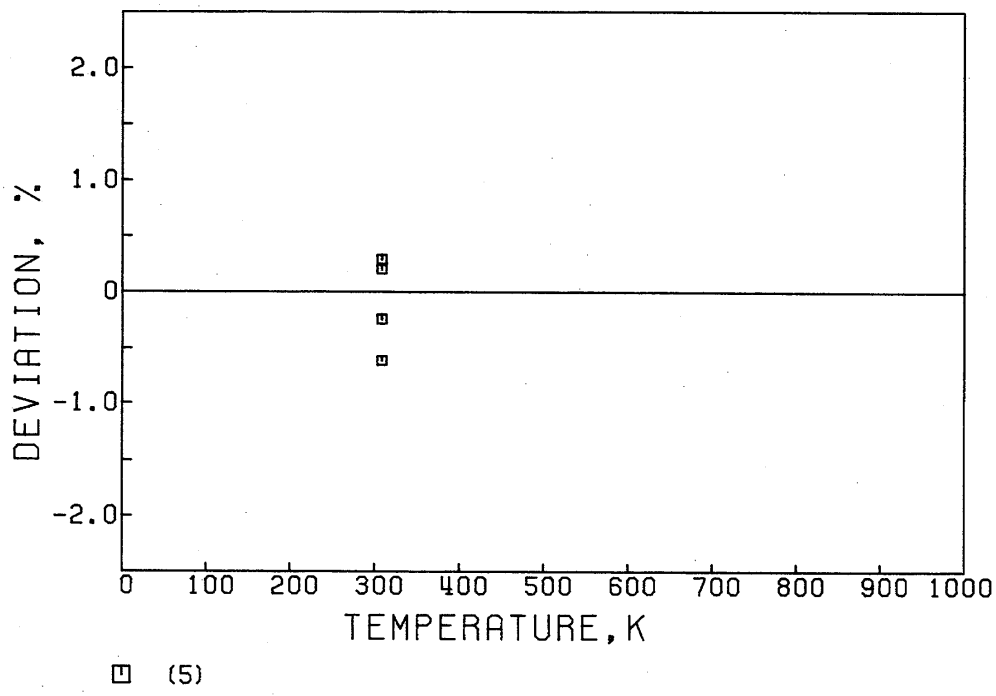

FIG. D41. Deviation plot for the thermal conductivity of He–Ne. Secondary data.

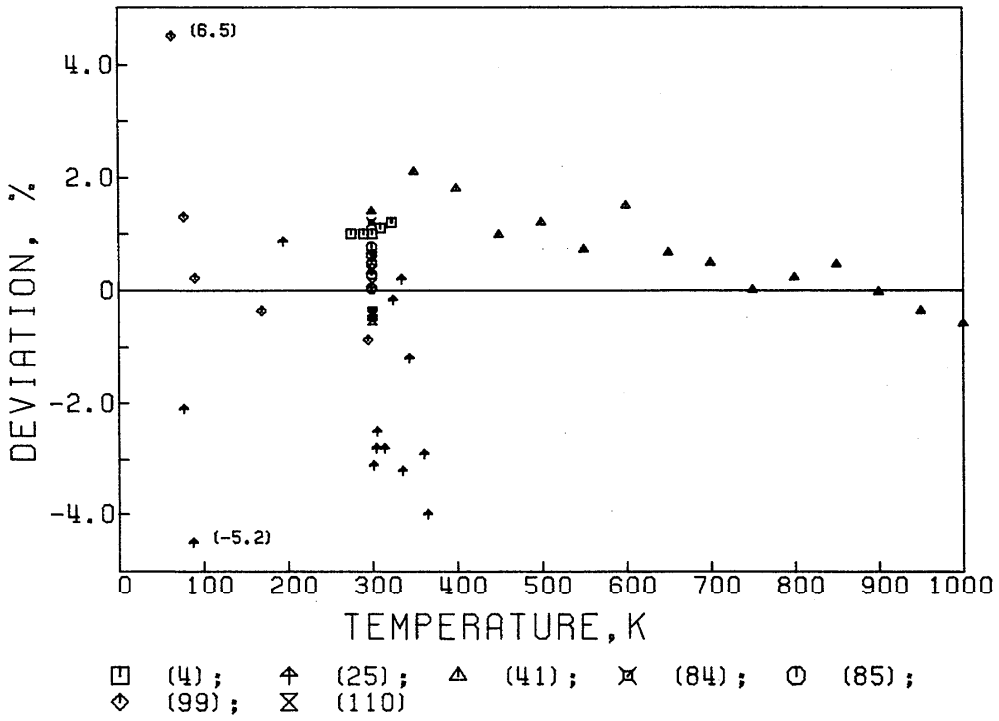

FIG. D42. Deviation plot for the binary diffusion coefficient of He–Ne. [4], [41], [84], [85], [99], [110]—primary data; [25]—secondary data.

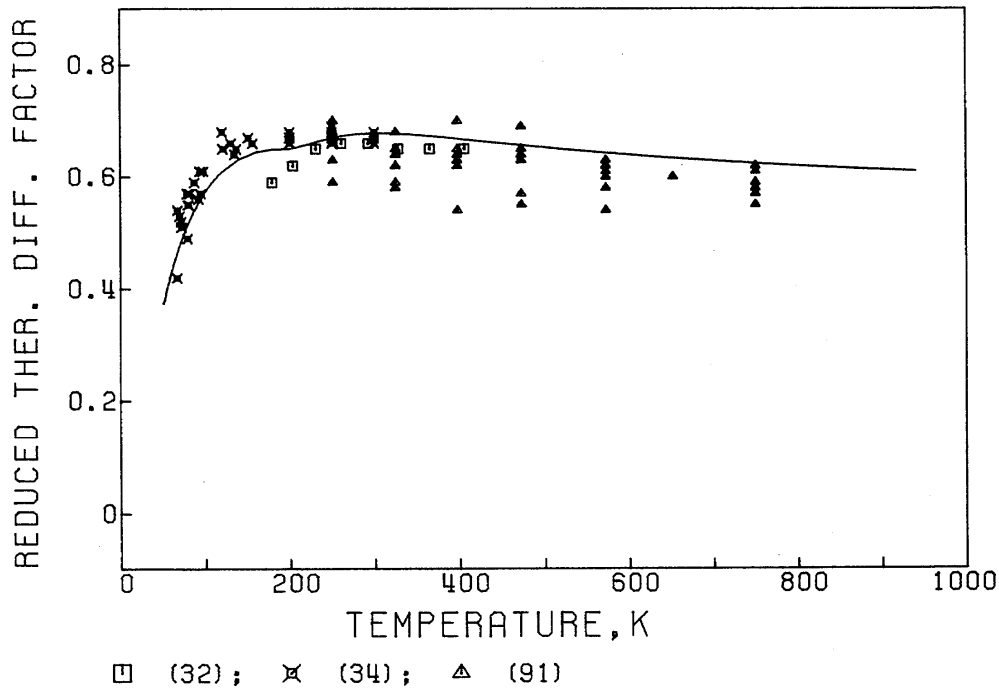

FIG. D43. Reduced thermal diffusion factor of He–Ne. Secondary data.
This is defined as

$$\alpha_T\left[\frac{x_1S_1 - x_2S_2}{x_1^2Q_1 + x_2^2Q_2 + x_1x_2Q_{12}}\right]^{-1} = (6C_{12}^* - 5)(1 + \kappa_2).$$

The solid line represents the calculated function.

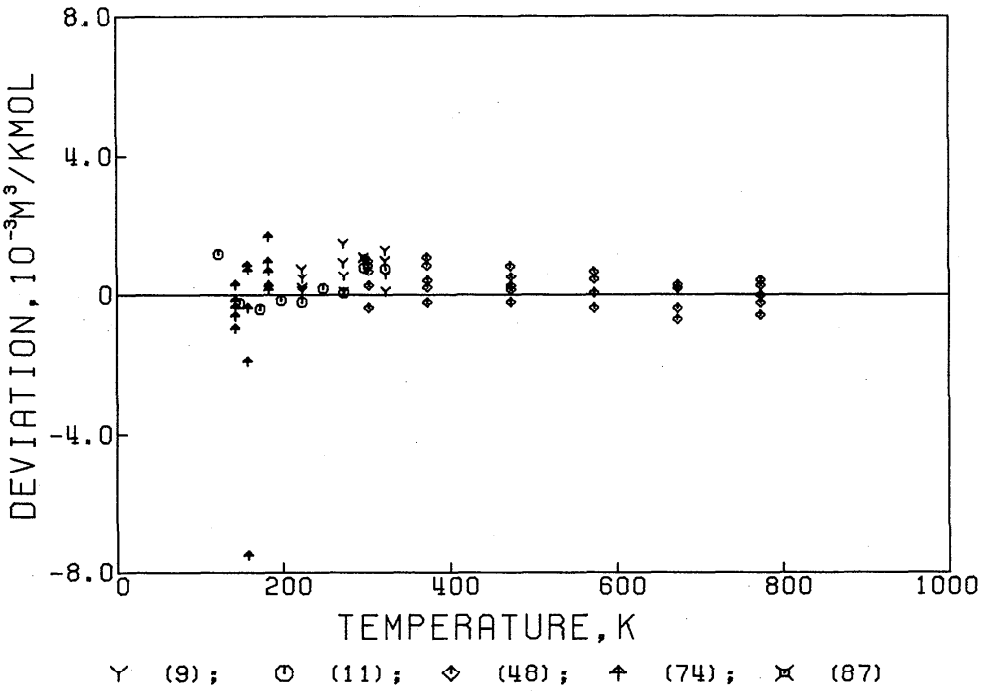

FIG. D44. Deviation plot for the second virial coefficient of He–Ar. [11]—primary data; [9], [48], [74], [87]—secondary data. [9], [48], and [74] contain second virial coefficient of mixtures, B_{mix}, and [11] and [87] contain interaction second virial coefficient B_{12}.

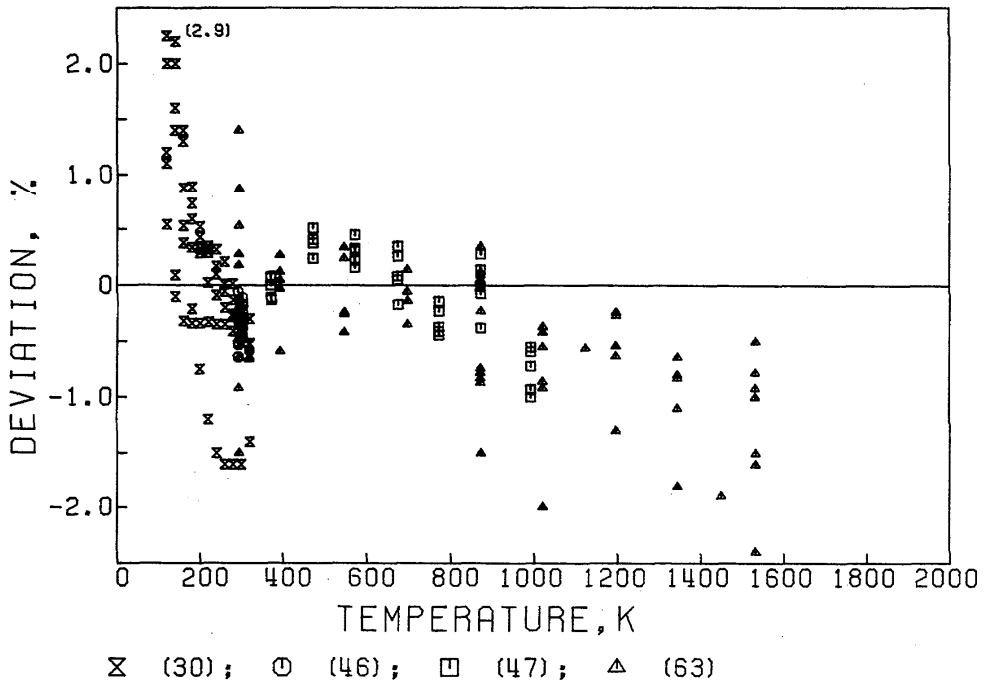

FIG. D45. Deviation plot for the viscosity of He–Ar. [30], [47], [63]—primary data; [46]—secondary data.

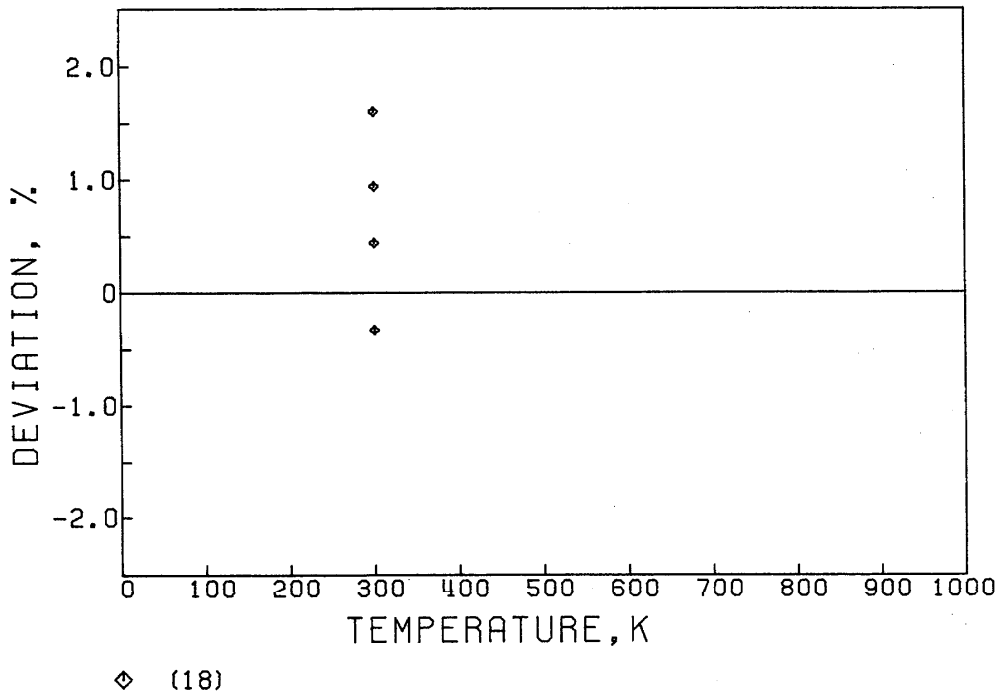

FIG. D46. Deviation plot for the thermal conductivity of He–Ar. Secondary data.

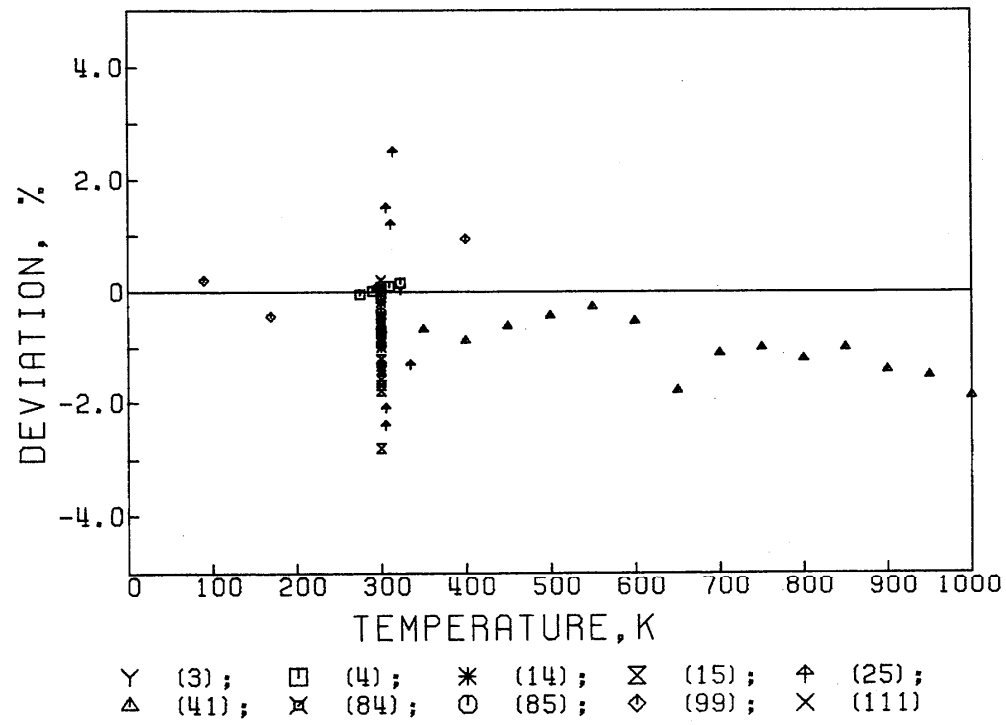

FIG. D47. Deviation plot for the binary diffusion coefficient of He–Ar. [3], [4], [14], [15], [41], [84], [85], [99], [111]—primary data; [25]—secondary data.

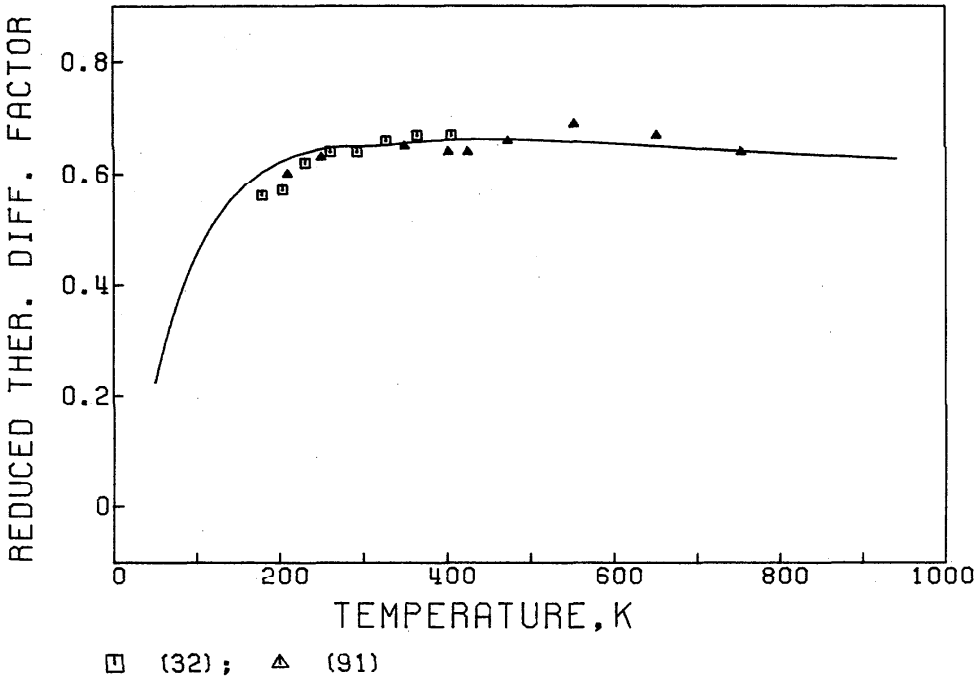

FIG. D48. Reduced thermal diffusion factor of He–Ar. Secondary data.
This is defined as

$$\alpha_T\left[\frac{x_1S_1 - x_1S_2}{x_1^2Q_1 + x_2^2Q_2 + x_1x_2Q_{12}}\right]^{-1} = (6C_{12}^* - 5)(1 + \kappa_2).$$

The solid line represents the calculated function.

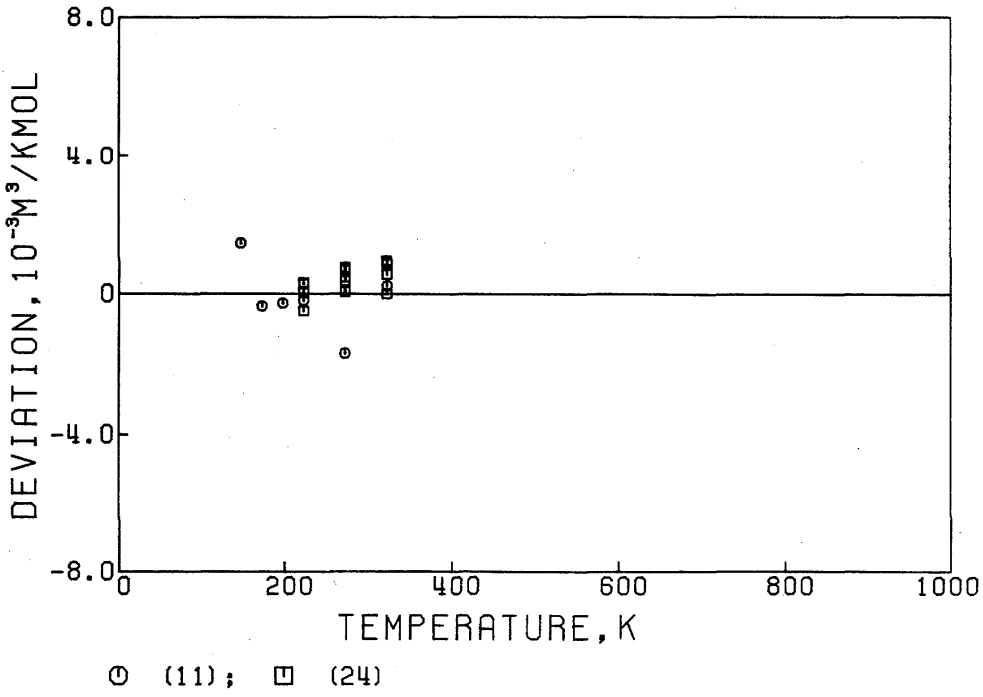

FIG. D49. Deviation plot for the second virial coefficient of He–Kr. [11]—primary data; [24]—secondary data. [11] contains second virial coefficient of mixtures B_{mix} and [24] contains interaction second virial coefficient B_{12}.

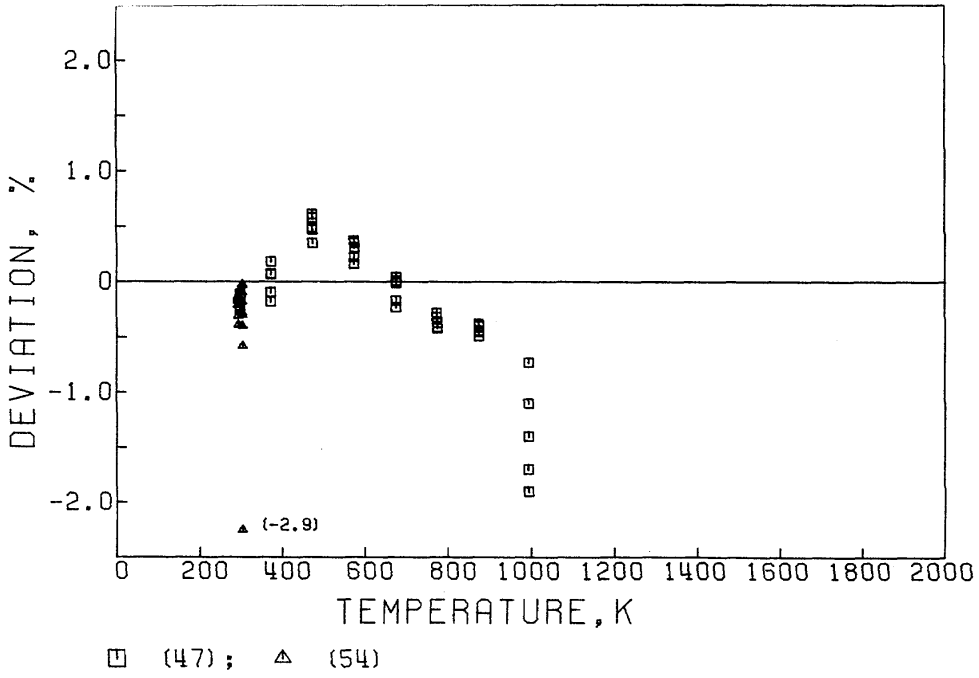

FIG. D50. Deviation plot for the viscosity of He–Kr. [47]—primary data; [54]—secondary data.

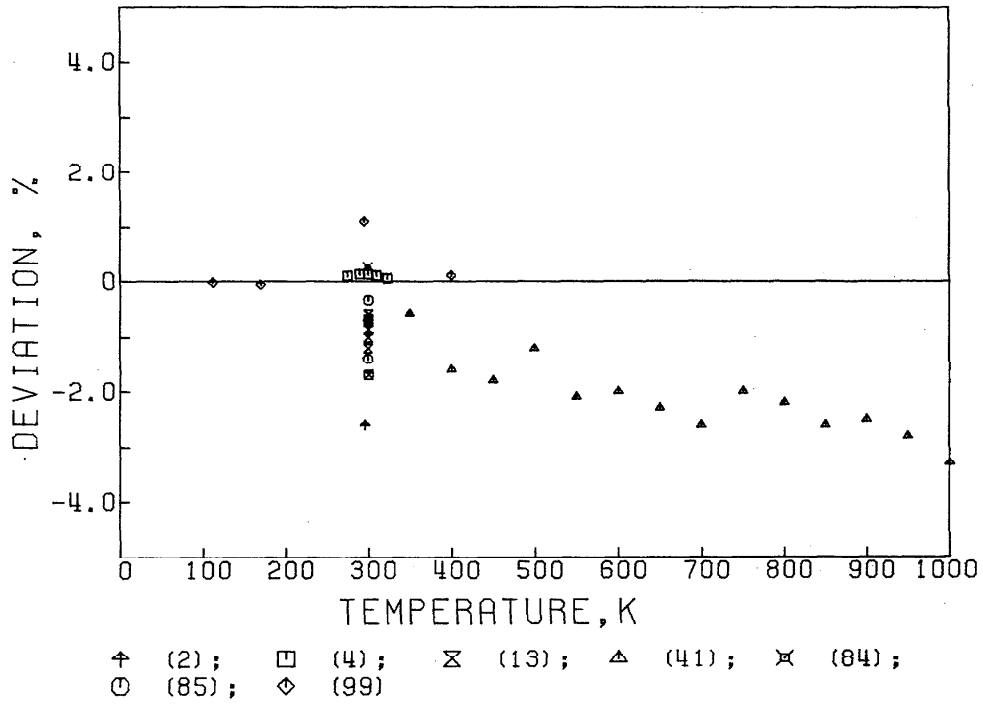

FIG. D51. Deviation plot for the binary diffusion coefficient of He–Kr. [4], [13], [41], [84], [85], [99]—primary data; [2]—secondary data.

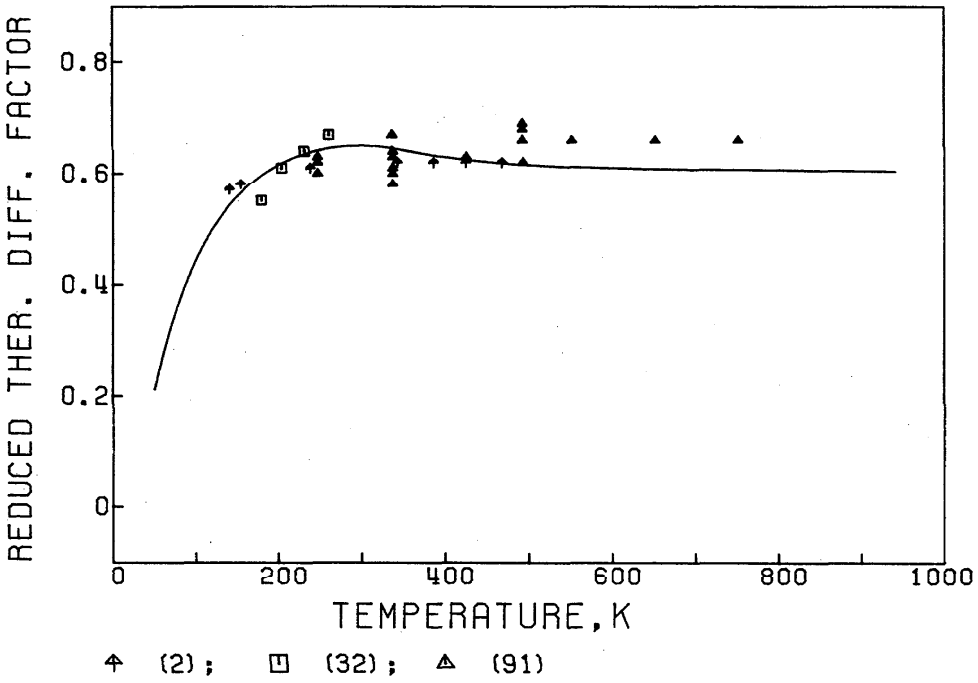

FIG. D52. Reduced thermal diffusion factor of He–Kr. Secondary data.
This is defined as

$$\alpha_T\left[\frac{x_1S_1 - x_2S_2}{x_1^2Q_1 + x_2^2Q_2 + x_1x_2Q_{12}}\right]^{-1} = (6C^*_{12} - 5)(1 + \kappa_2).$$

The solid line represents the calculated function.

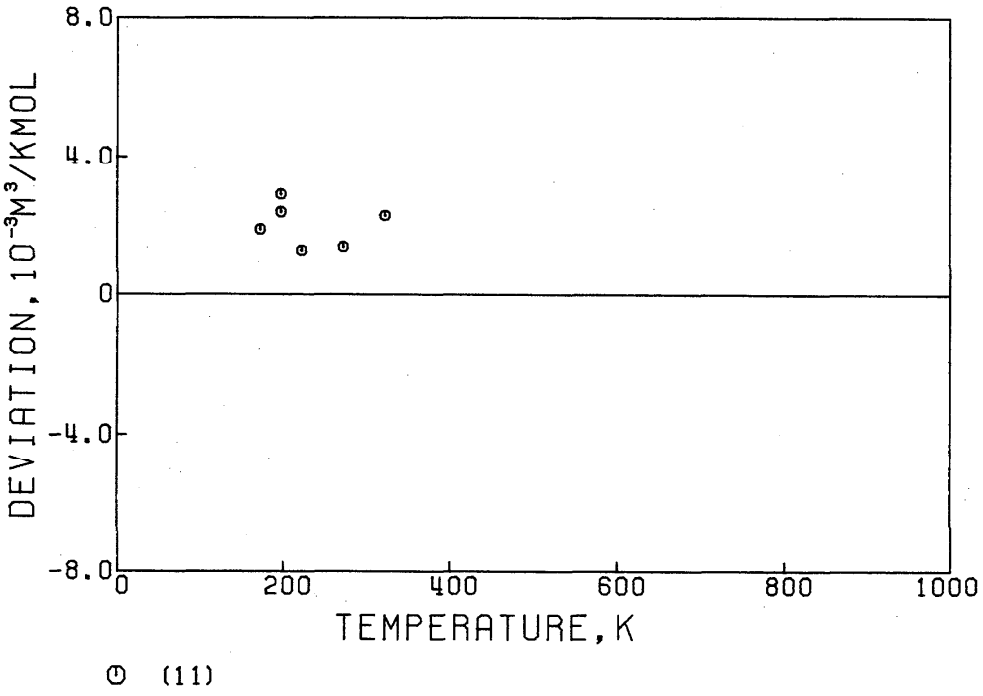

FIG. D53. Deviation plot for the interaction second virial coefficient of He–Xe. Primary data.

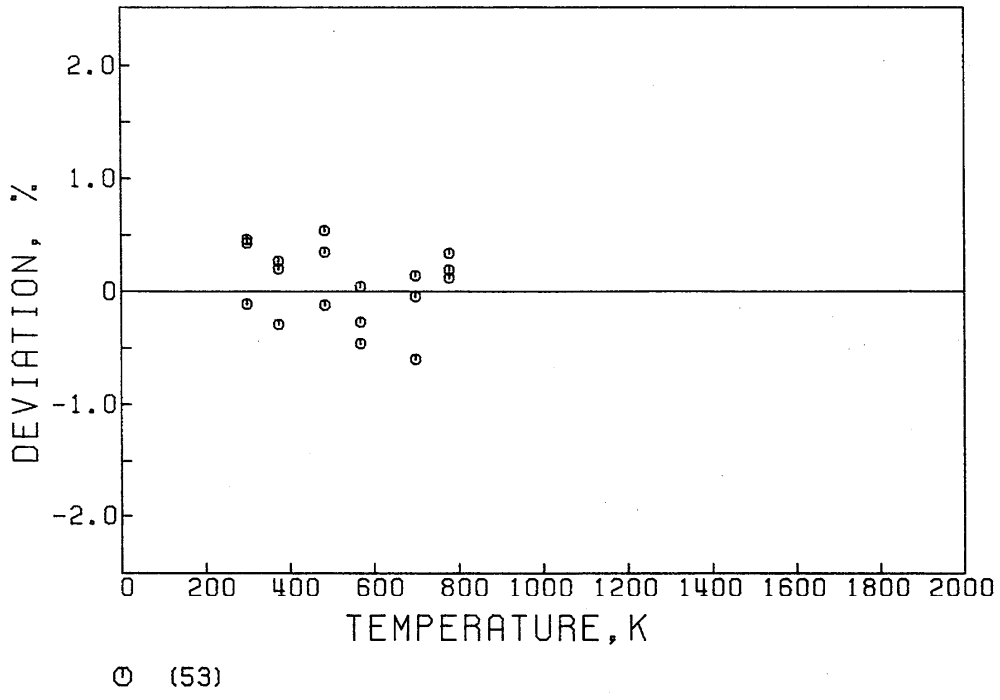

FIG. D54. Deviation plot for the viscosity of He–Xe. Primary data.

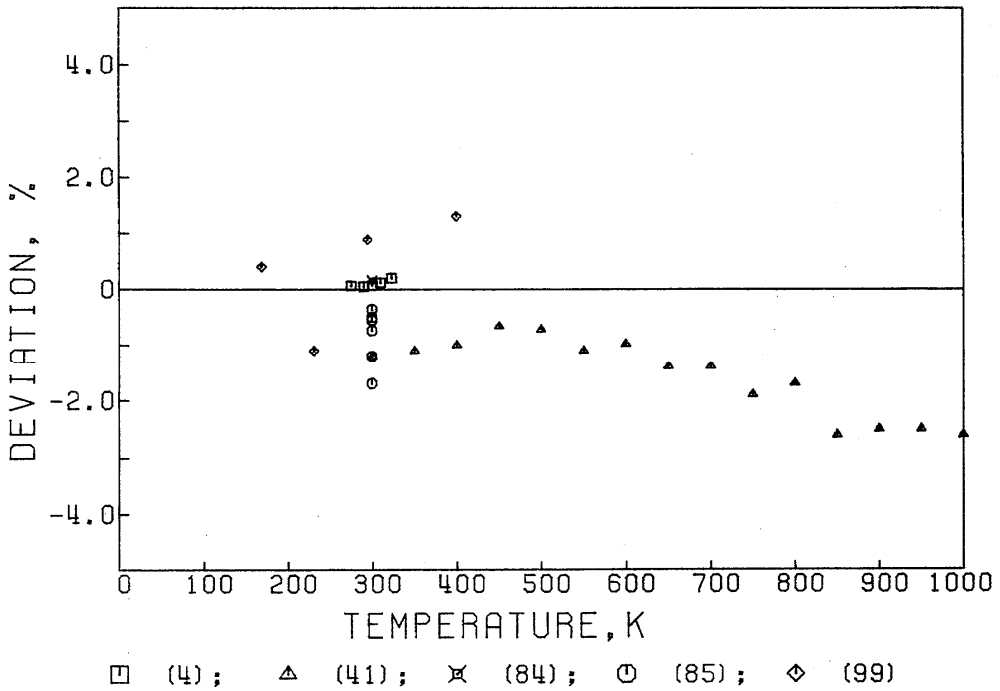

FIG. D55. Deviation plot for the binary diffusion coefficient of He–Xe. Primary data.

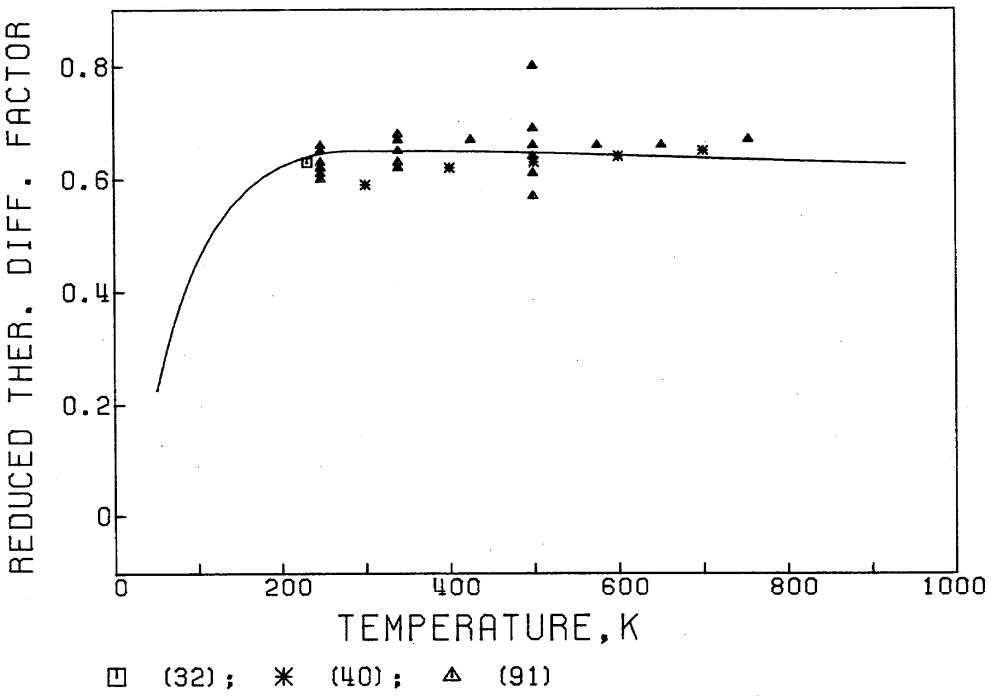

FIG. D56. Reduced thermal diffusion factor He–Xe. Secondary data.
This is defined as

$$\alpha_T\left[\frac{x_1S_1 - x_2S_2}{x_1^2Q_1 + x_2^2Q_2 + x_1x_2Q_{12}}\right]^{-1} = (6C_{12}^* - 5)(1 + \kappa_2).$$

The solid line represents the calculated function.

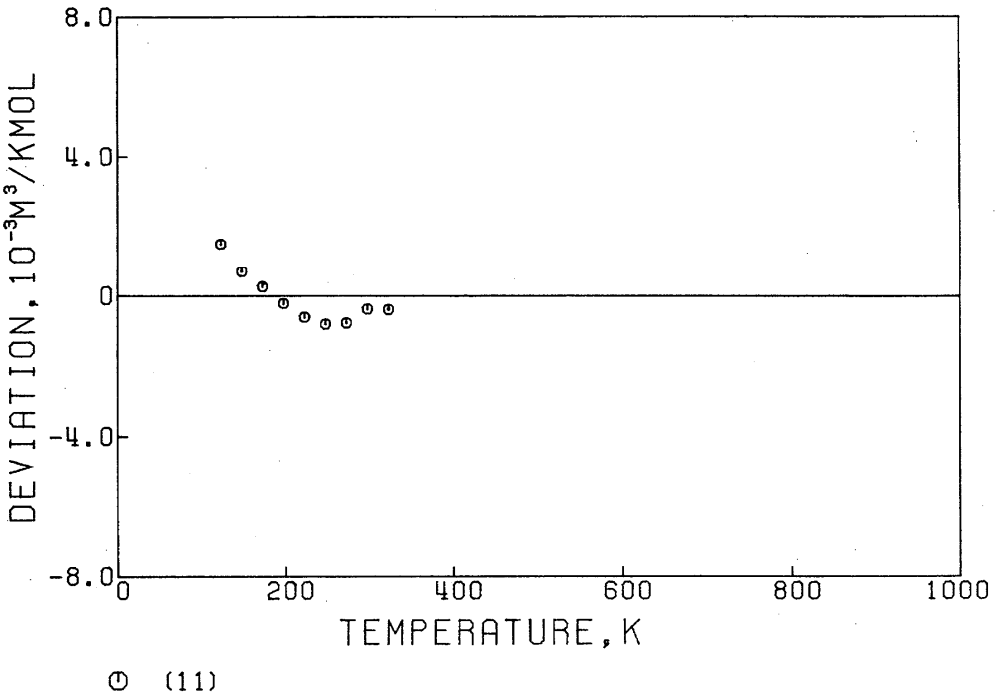

FIG. D57. Deviation plot for the interaction second virial coefficient of Ne–Ar. Primary data.

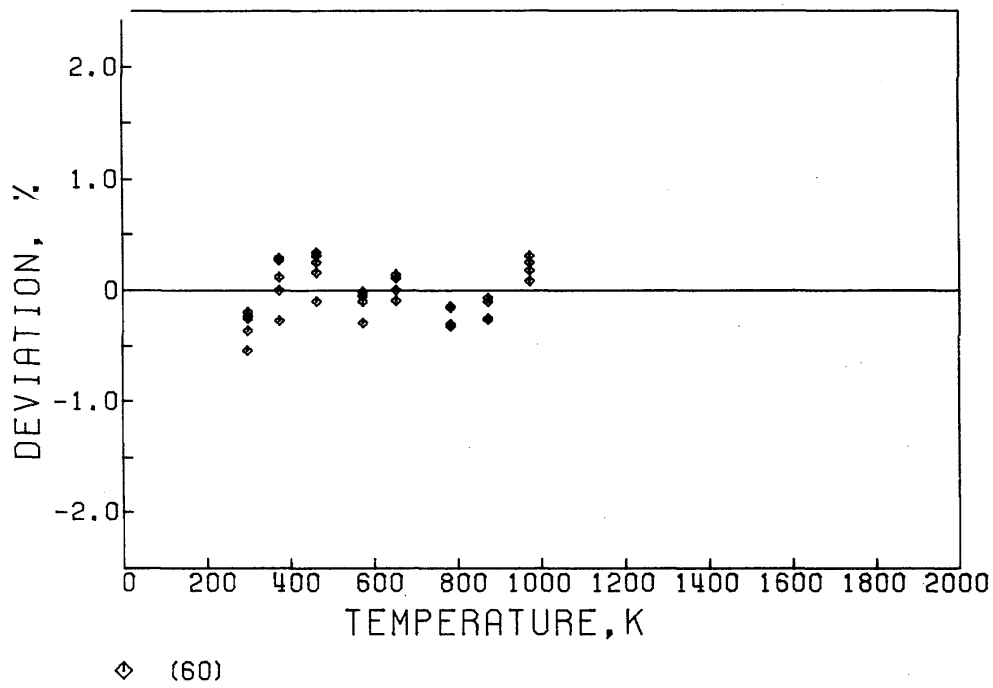

FIG. D58. Deviation plot for the viscosity of Ne–Ar. Primary data.

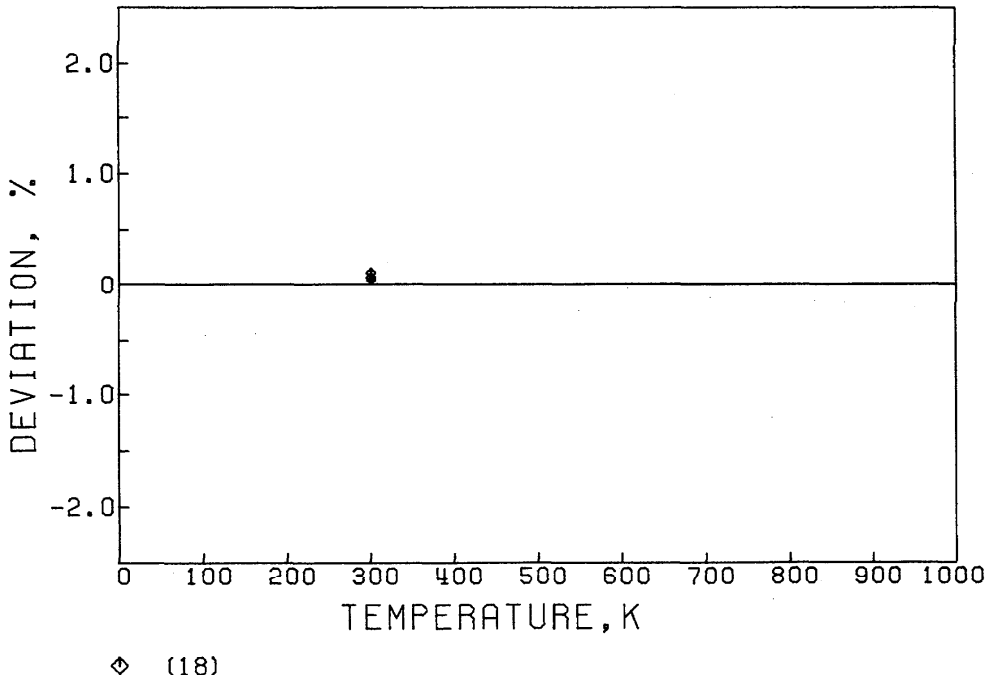

FIG. D59. Deviation plot for the thermal conductivity of Ne–Ar. Secondary data.

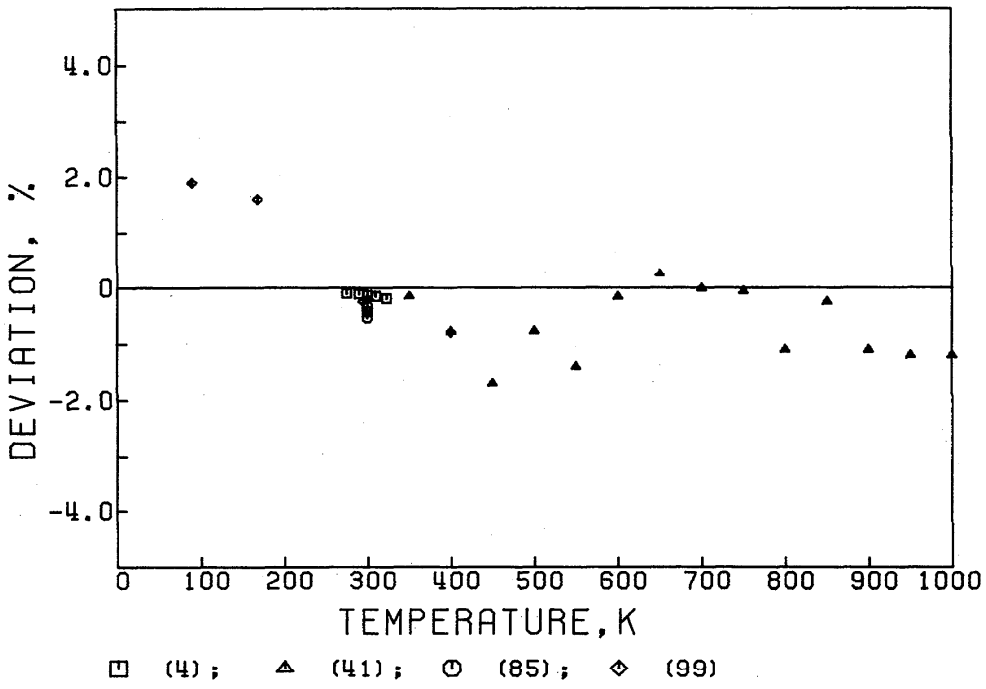

FIG. D60. Deviation plot for the binary diffusion coefficient of Ne–Ar. Primary data.

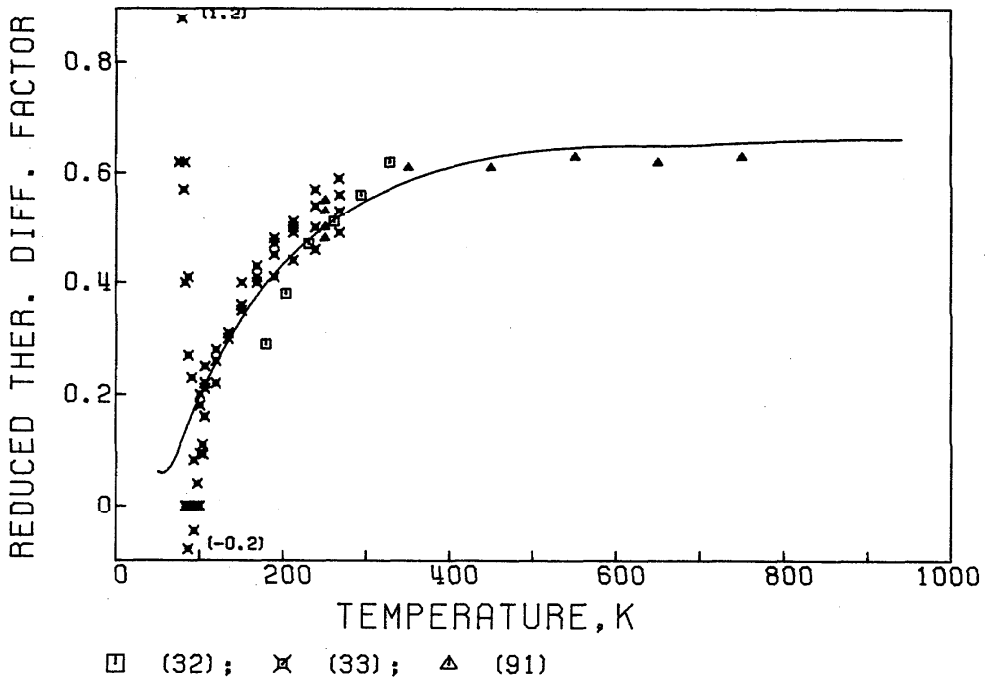

FIG. D61. Reduced thermal diffusion factor of Ne–Ar. Secondary data.
This is defined as

$$\alpha_T\left[\frac{x_1S_1 - x_2S_2}{x_1^2Q_1 + x_2^2Q_2 + x_1x_2Q_{12}}\right]^{-1} = (6C_{12}^* - 5)(1 + \kappa_2).$$

The solid line represents the calculated function.

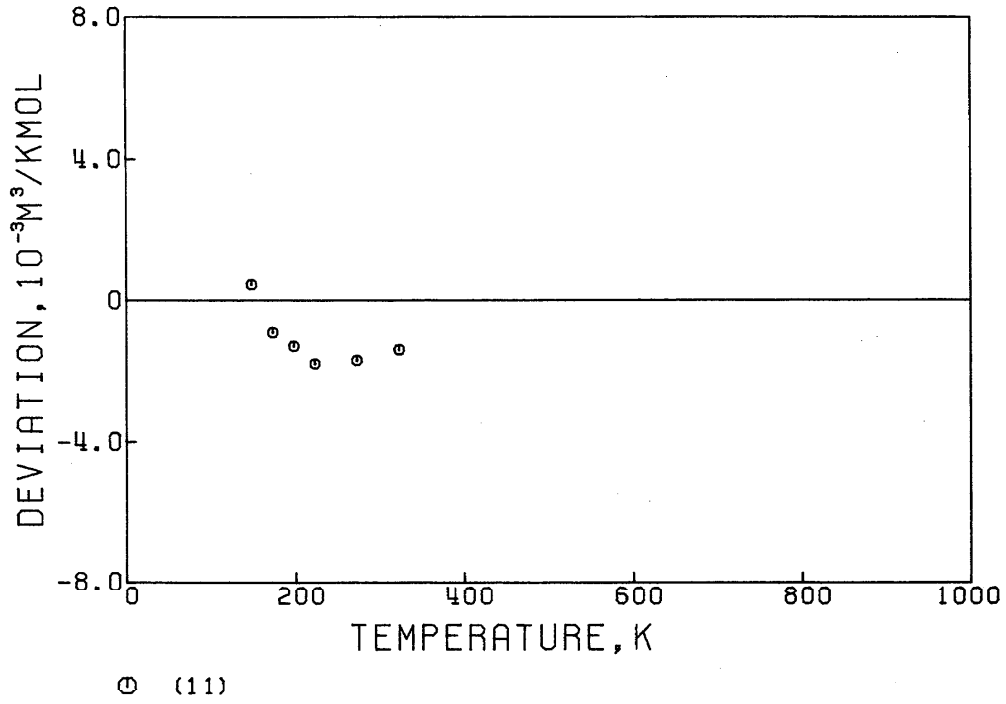

FIG. D62. Deviation plot for the interaction second virial coefficient of Ne–Kr. Primary data.

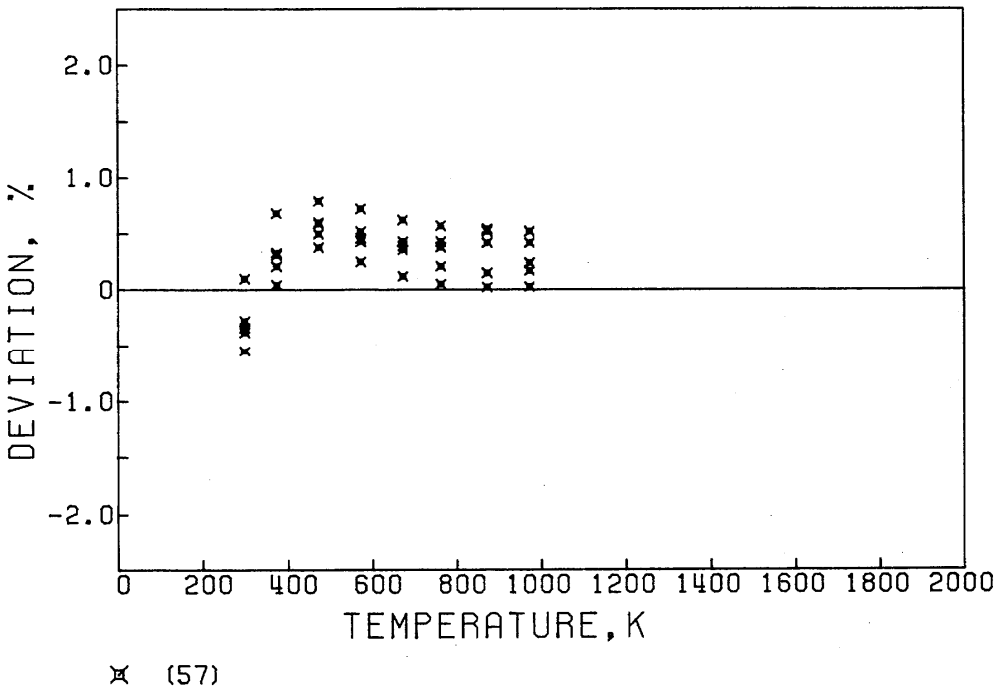

FIG. D63. Deviation plot for the viscosity of Ne–Kr. Primary data.

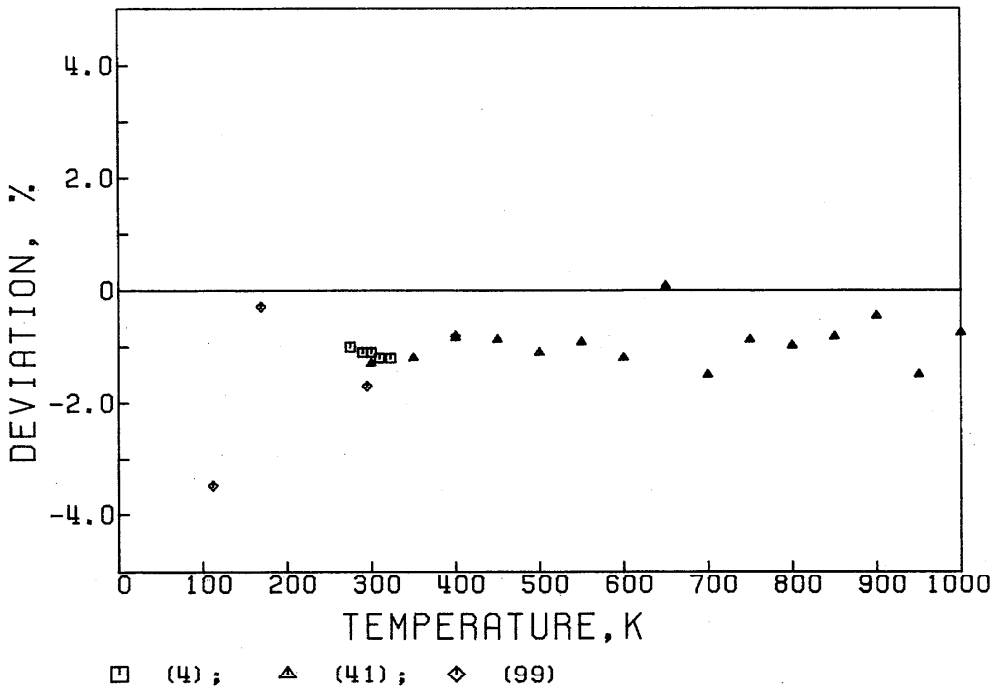

FIG. D64. Deviation plot for the binary diffusion coefficient of Ne–Kr. Primary data.

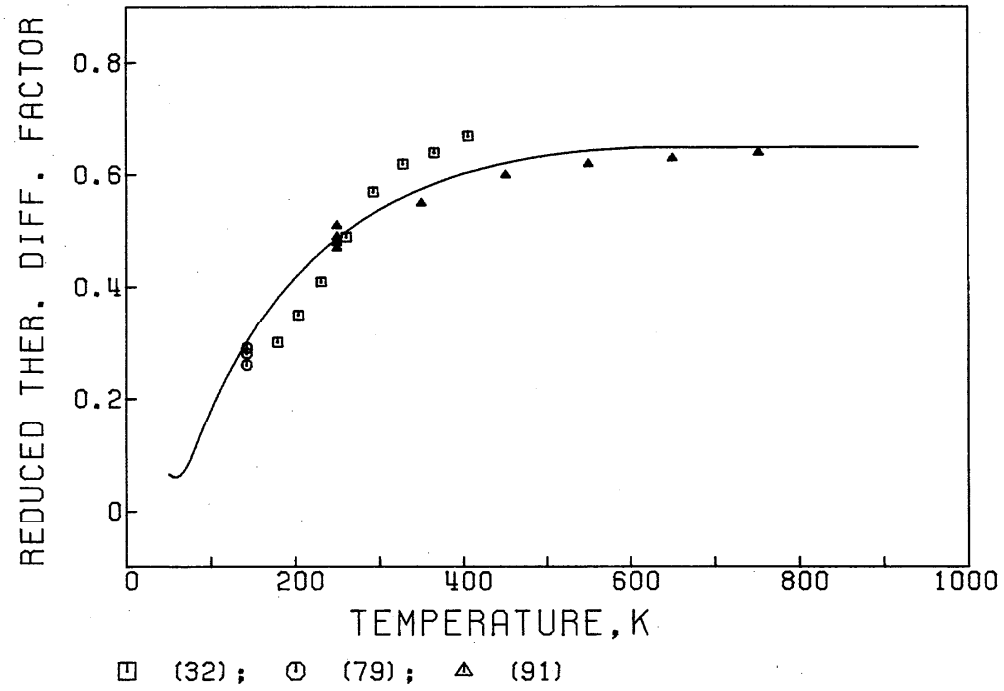

FIG. D65. Reduced thermal diffusion factor of Ne–Kr. Secondary data.
This is defined as

$$\alpha_T\left[\frac{x_1S_1 - x_2S_2}{x_1^2Q_1 + x_2^2Q_2 + x_1x_2Q_{12}}\right]^{-1} = (6C_{12}^* - 5)(1 + \kappa_2).$$

The solid line represents the calculated function.

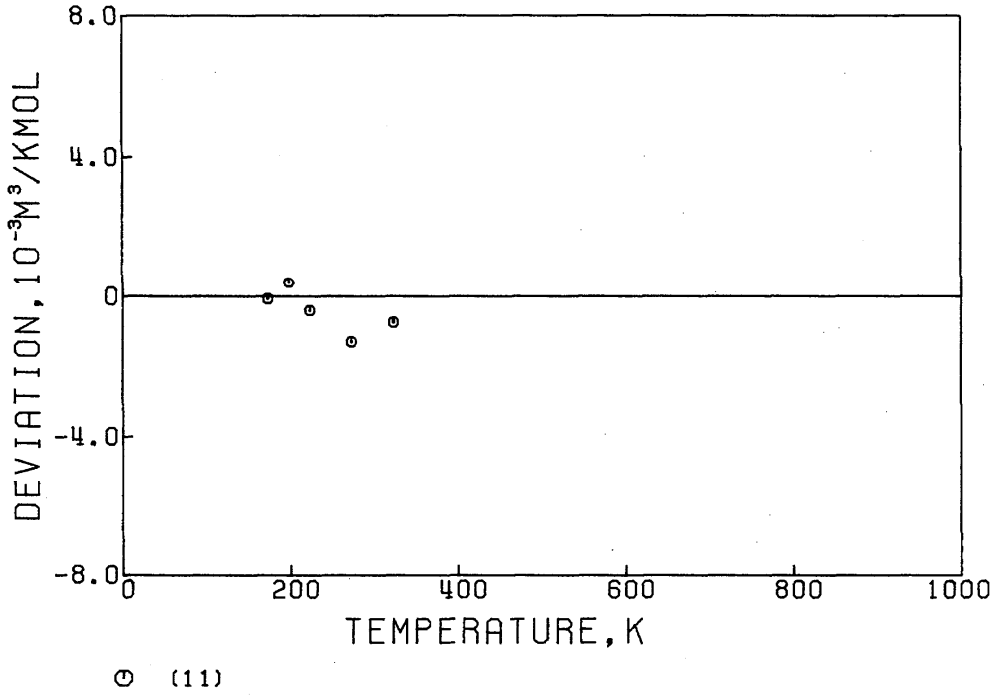

FIG. D66. Deviation plot for the interaction second virial coefficient of Ne–Xe. Primary data.

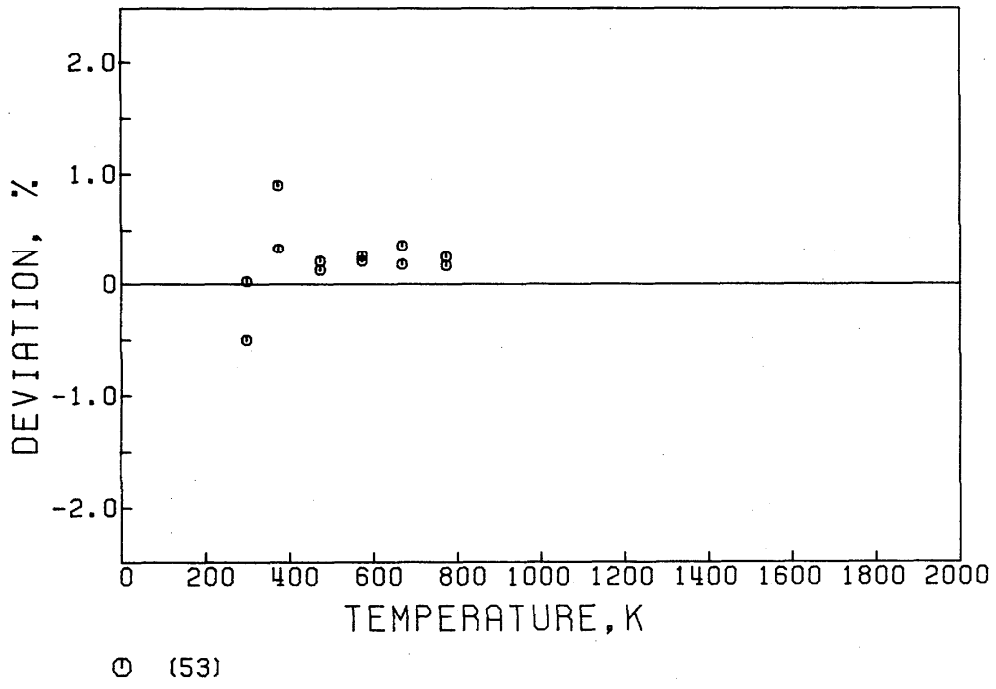

FIG. D67. Deviation plot for the viscosity of Ne–Xe. Primary data.

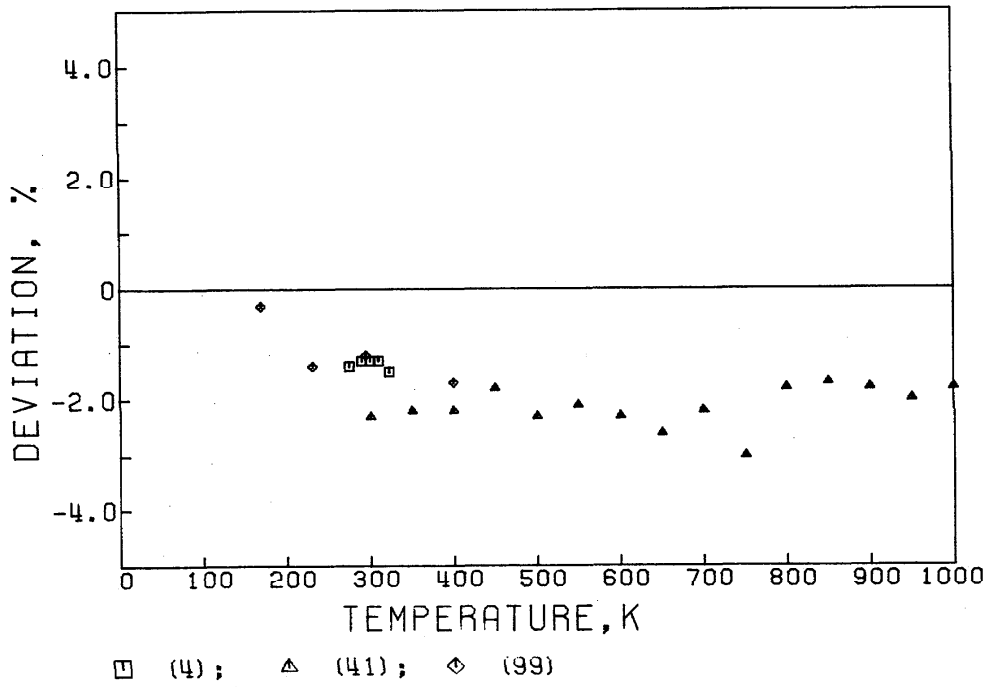

FIG. D68. Deviation plot for the binary diffusion coefficient of Ne–Xe. Primary data.

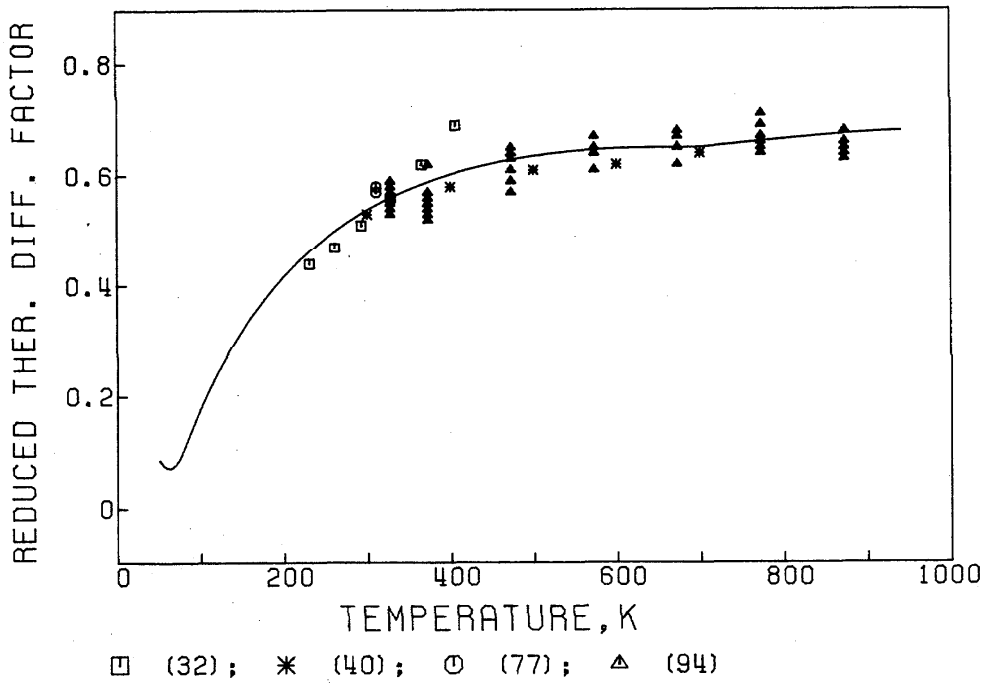

FIG. D69. Reduced thermal diffusion factor of Ne–Xe. Secondary data.
This is defined as

$$\alpha_T\left[\frac{x_1S_1 - x_2S_2}{x_1^2Q_1 + x_2^2Q_2 + x_1x_2Q_{12}}\right]^{-1} = (6C_{12}^* - 5)(1 + \kappa_2).$$

The solid line represents the calculated function.

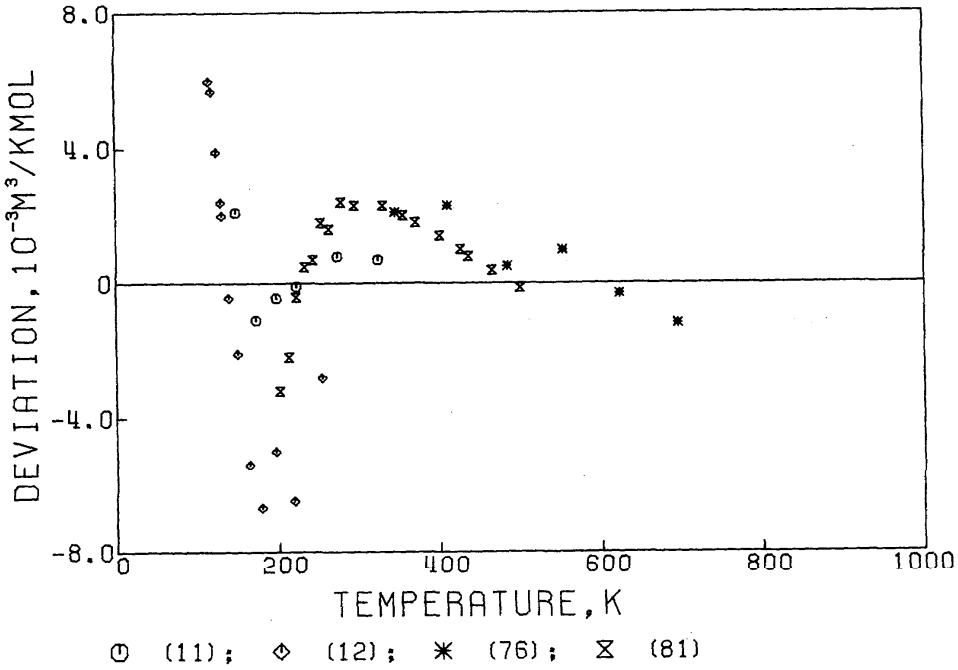

FIG. D70. Deviation plot for the interaction second virial coefficient of Ar–Kr. [11]—primary data; [12], [76], [81]—secondary data.

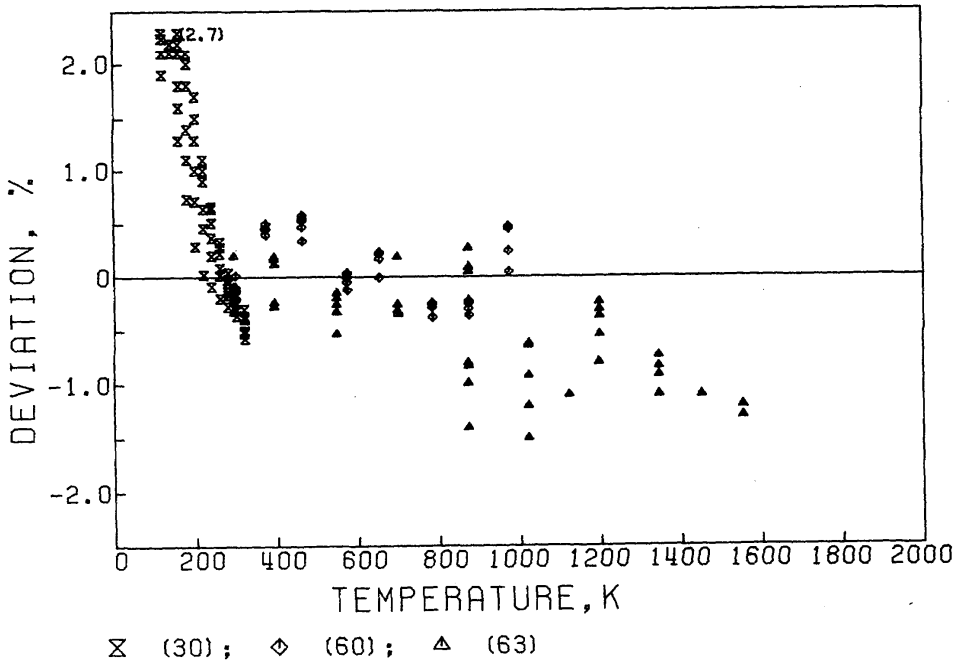

FIG. D71. Deviation plot for the viscosity of Ar–Kr. Primary data.

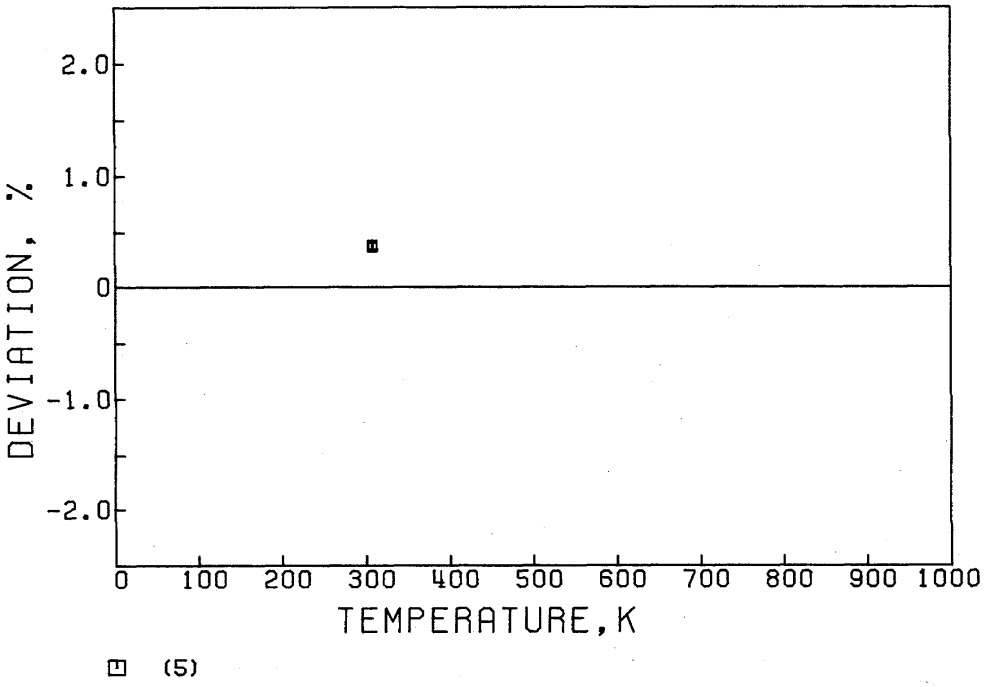

FIG. D72. Deviation plot for the thermal conductivity of Ar–Kr. Secondary data.

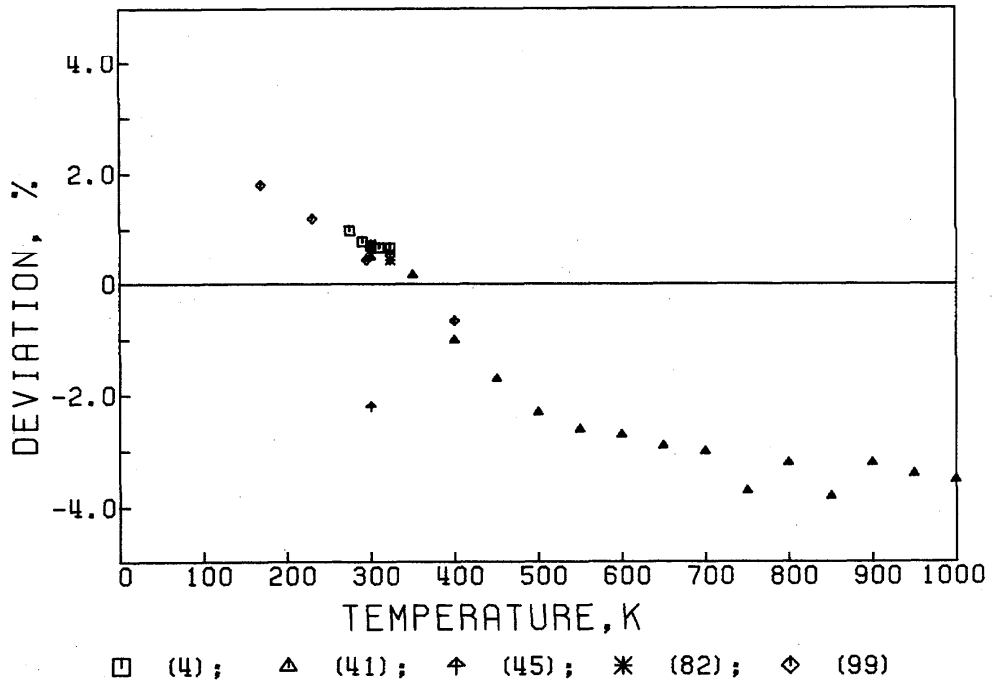

FIG. D73. Deviation plot for the binary diffusion coefficient of Ar–Kr. [4], [41], [82], [99]—primary data; [45]—secondary data.

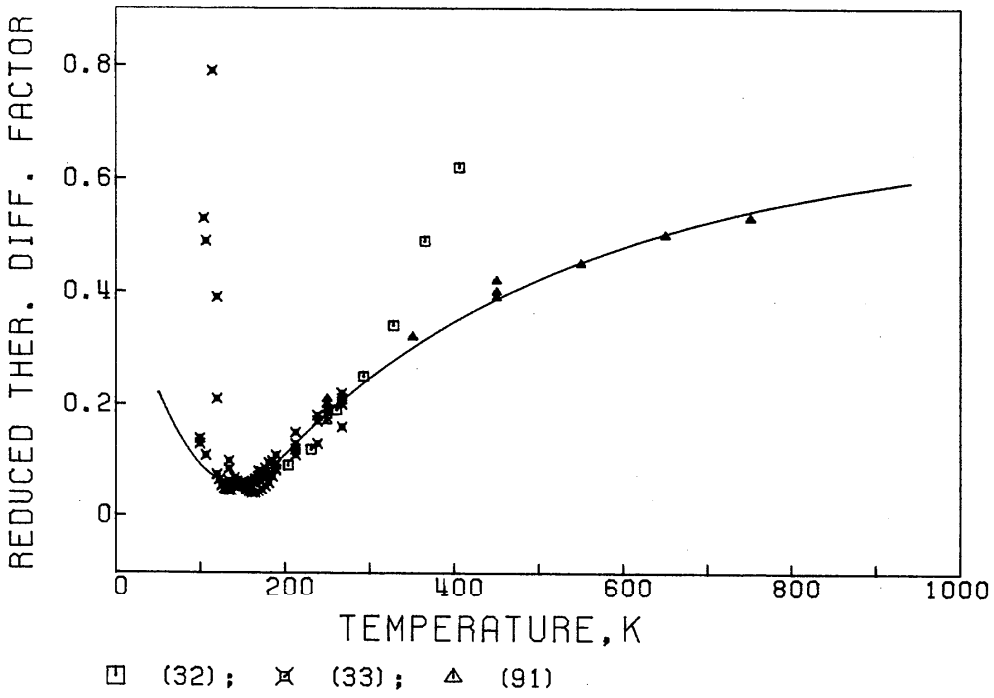

FIG. D74. Reduced thermal diffusion factor of Ar–Kr. Secondary data.
This is defined as

$$\alpha_T\left[\frac{x_1S_1 - x_2S_2}{x_1^2Q_1 + x_2^2Q_2 + x_1x_2Q_{12}}\right]^{-1} = (6C_{12}^* - 5)(1 + \kappa_2).$$

The solid line represents the calculated function.

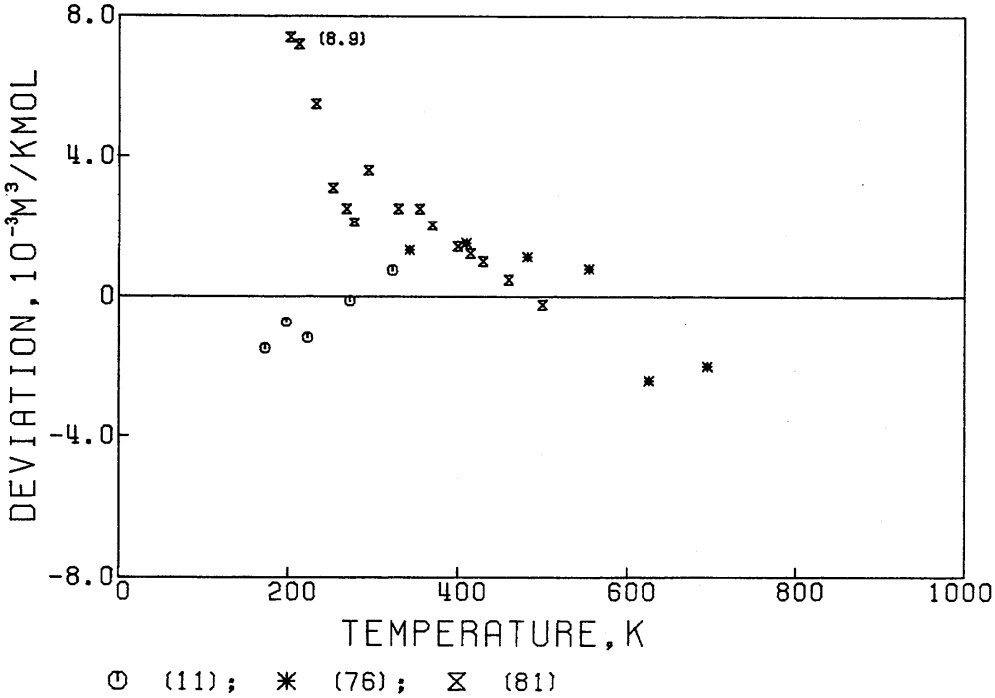

FIG. D75. Deviation plot for the interaction second virial coefficient of Ar–Xe. [11]—primary data; [76], [81]—secondary data.

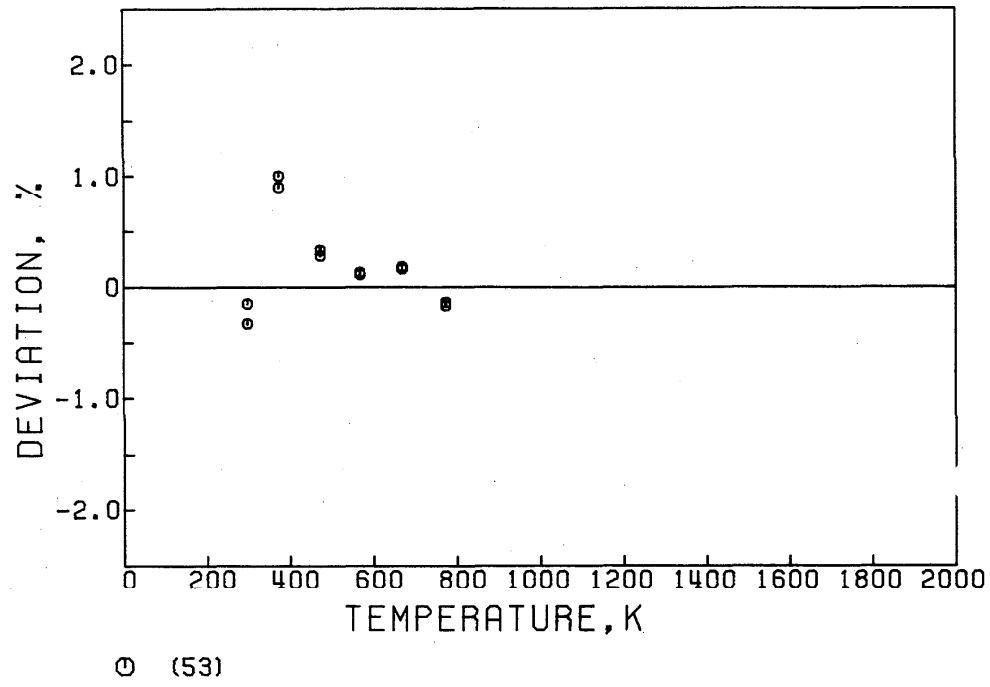

FIG. D76. Deviation plot for the viscosity of Ar–Xe. Primary data.

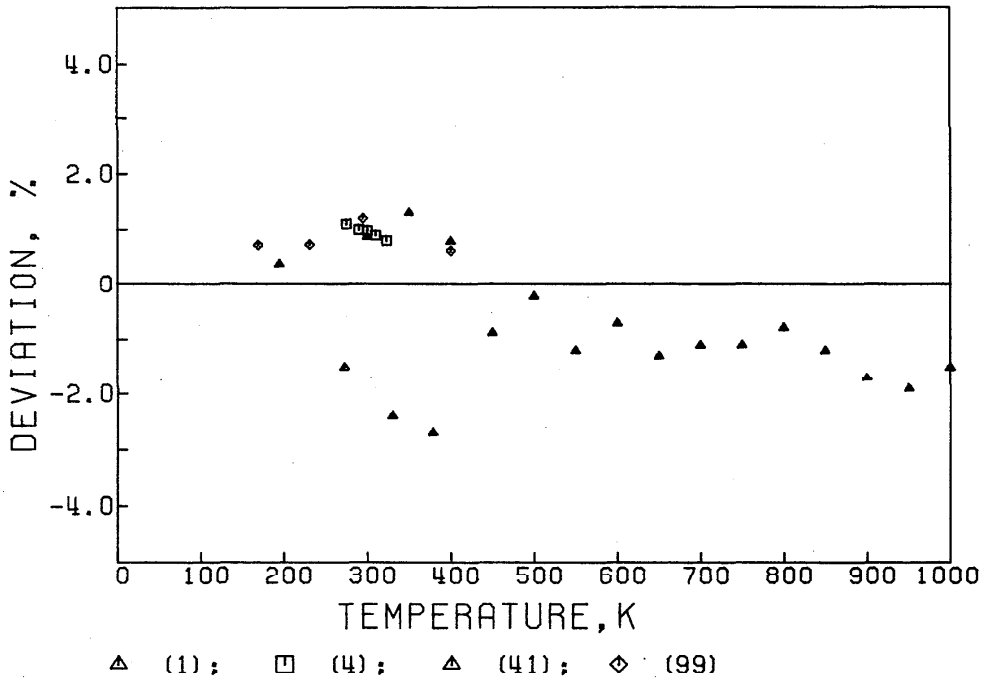

FIG. D77. Deviation plot for the binary diffusion coefficient of Ar–Xe. [4], [41], [99]—primary data; [1]—secondary data.

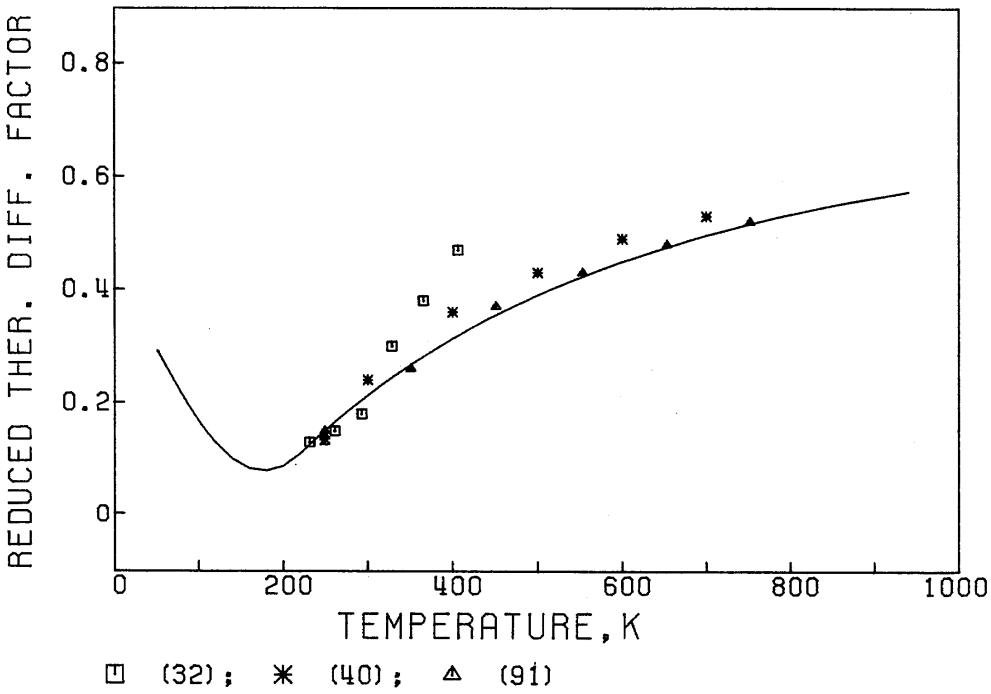

FIG. D78. Reduced thermal diffusion factor of Ar–Xe. Secondary data.
This is defined as

$$\alpha_T\left[\frac{x_1S_1 - x_2S_2}{x_1^2Q_1 + x_2^2Q_2 + x_1x_2Q_{12}}\right]^{-1} = (6C_{12}^* - 5)(1 + \kappa_2).$$

The solid line represents the calculated function.

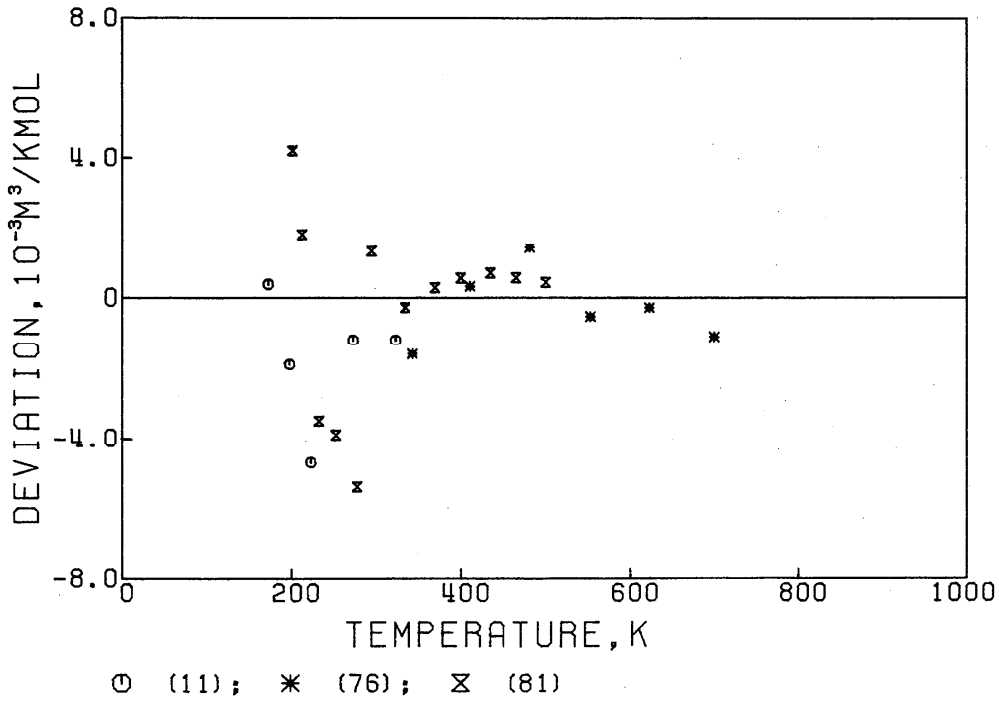

FIG. D79. Deviation plot for the interaction second virial coefficient of Kr–Xe. [11]—primary data; [76], [81]—secondary data.

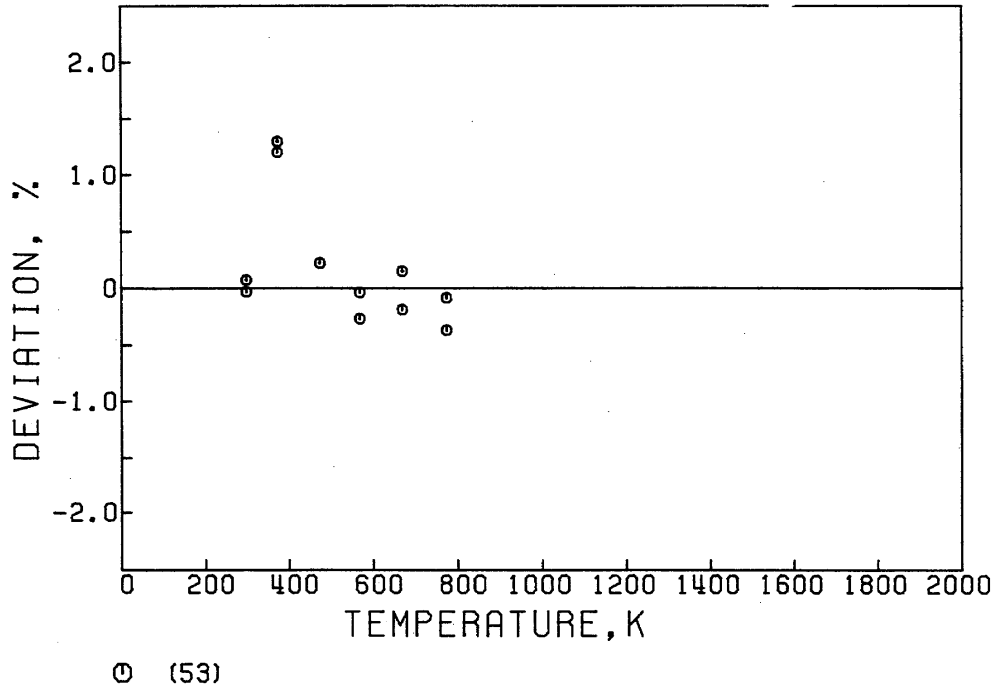

FIG. D80. Deviation plot for the viscosity of Kr–Xe. Primary data.

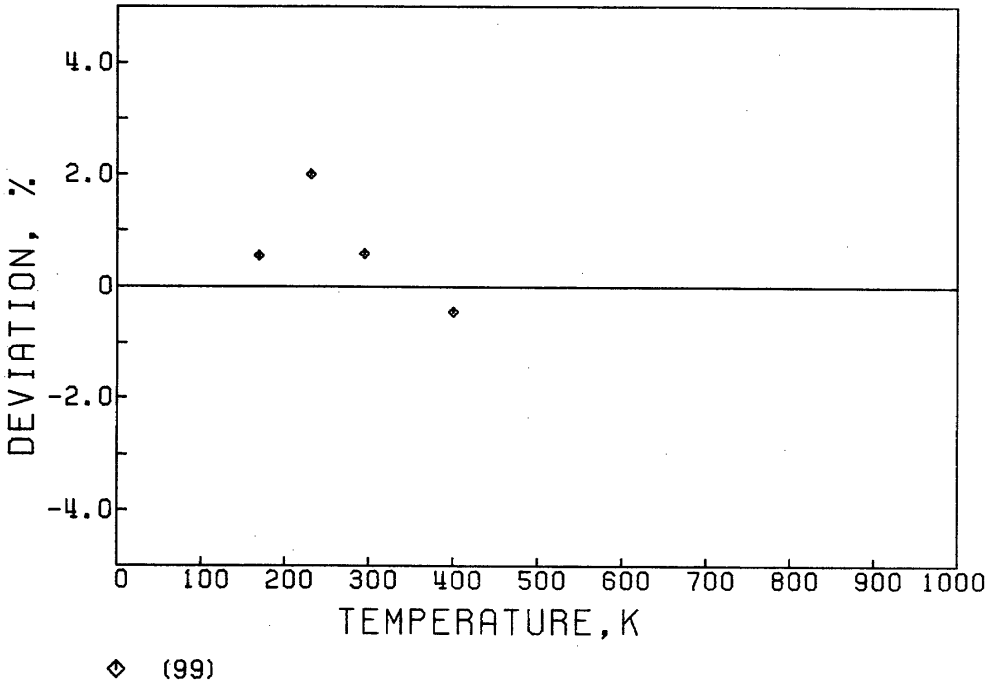

FIG. D81. Deviation plot for the binary diffusion coefficient of Kr–Xe. Primary data.

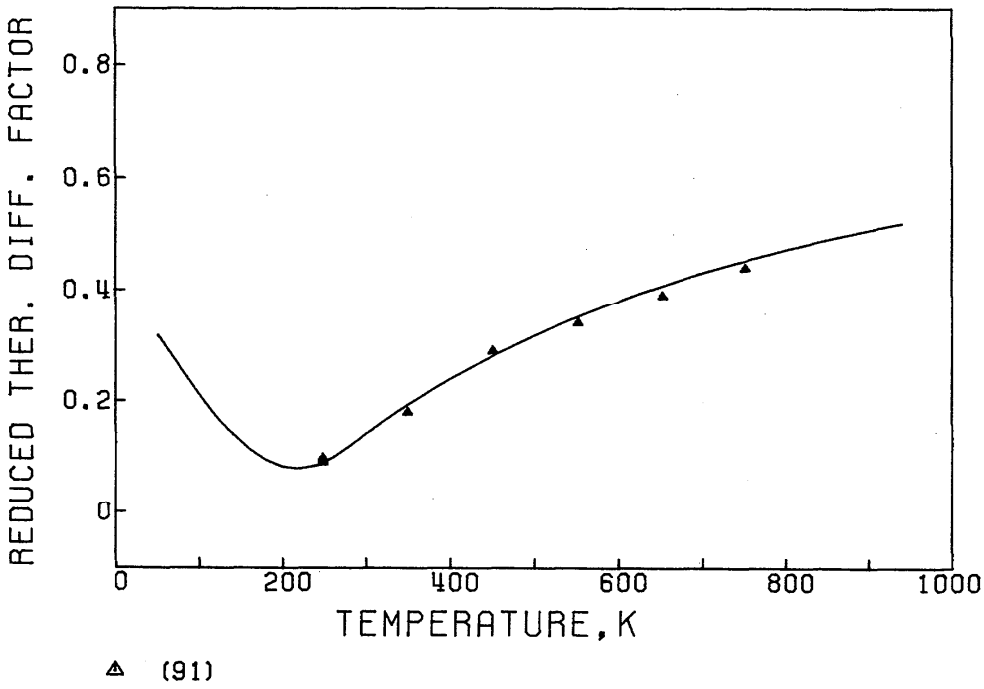

FIG. D82. Reduced thermal diffusion factor of Kr–Xe. Secondary data.
This is defined as

$$\alpha_T\left[\frac{x_1S_1 - x_1S_2}{x_1^2Q_1 + x_2^2Q_2 + x_1x_2Q_{12}}\right]^{-1} = (6C_{12}^* - 5)(1 + \kappa_2).$$

The solid line represents the calculated function.

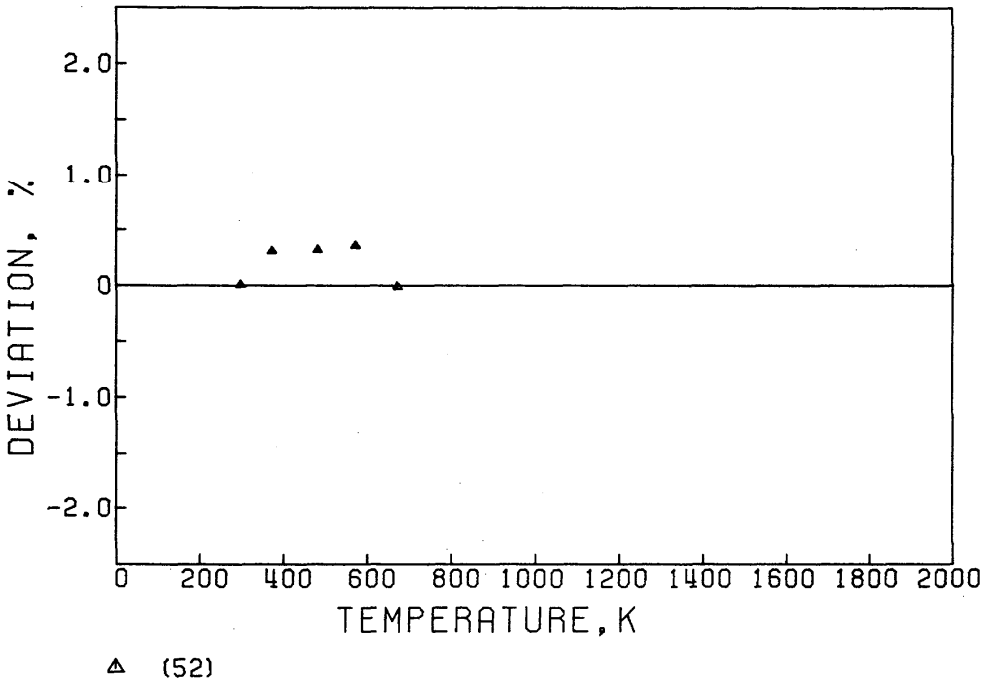

FIG. D83. Deviation plot for the viscosity of He–Ne–Kr. Secondary data.

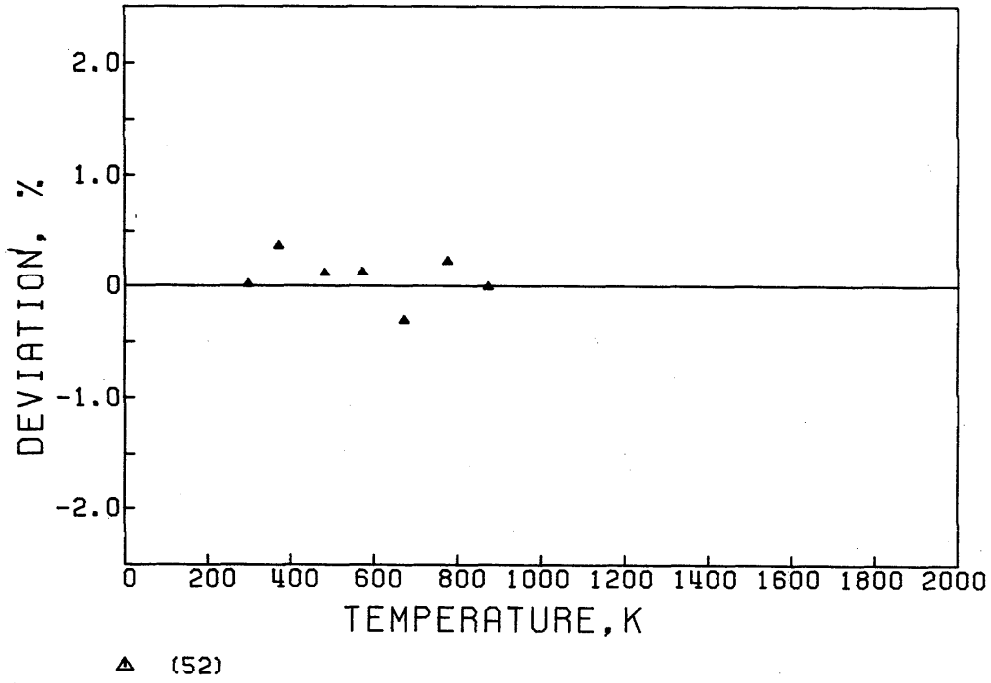

FIG. D84. Deviation plot for the viscosity of He–Ar–Kr. Secondary data.

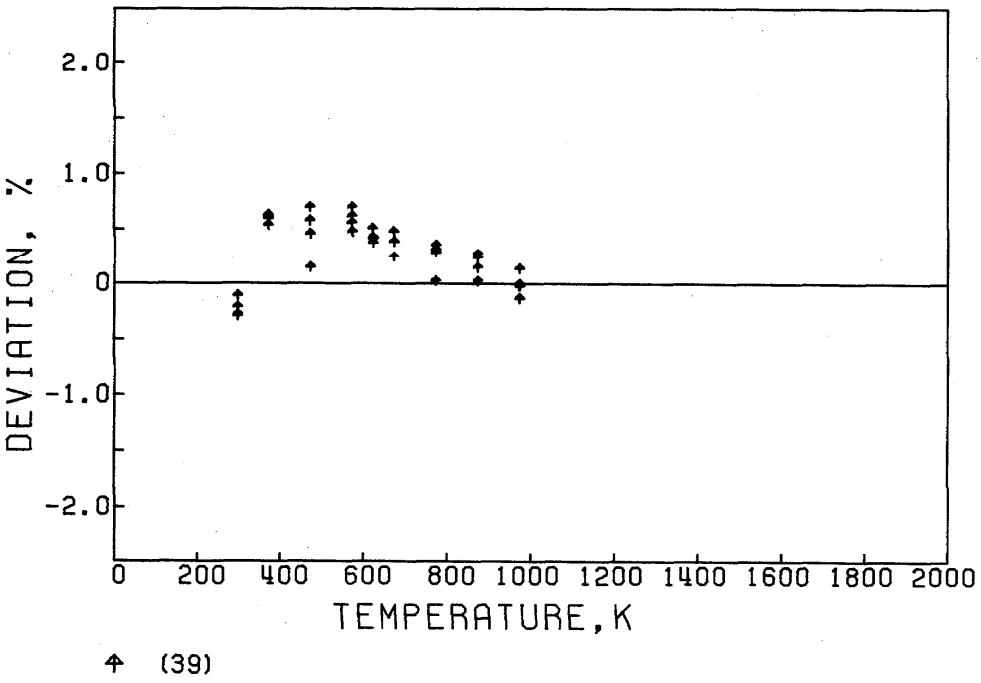

FIG. D85. Deviation plot for the viscosity of Ne–Ar–Kr. Secondary data.

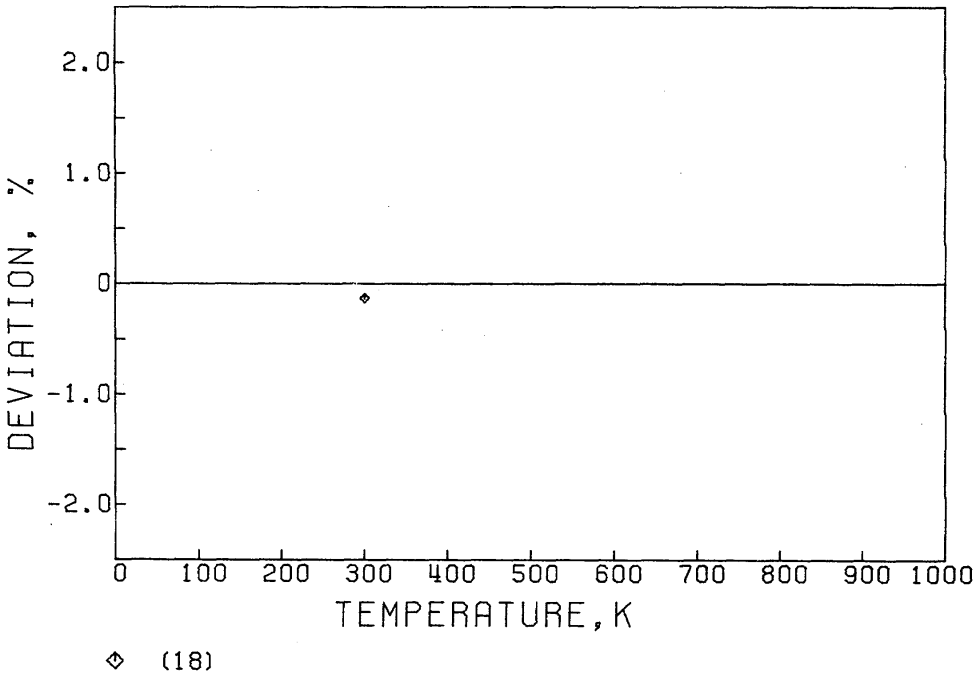

FIG. D86. Deviation plot for the thermal conductivity of Ne–Ar–Kr. Secondary data.

Appendix E. Bibliography

This bibliography lists references of Class 1 and Class 2. References containing material of Class 1 are marked with an asterisk.

[1]I. Amdur and T. F. Schatzki, J. Chem. Phys. **27**, 1049 (1957).
[2]B. K. Annis, A. E. Humphreys, and E. A. Mason, Phys. Fluids **11**, 2122 (1968).
*[3]P. S. Arora and P. J. Dunlop, J. Chem. Phys. **71**, 2430 (1979).
*[4]P. S. Arora, H. L. Robjohns, and P. J. Dunlop, Physica **95A**, 561 (1979).
[5]M. J. Assael, M. Dix, A. Lucas, and W. A. Wakeham, J. Chem. Soc. Faraday Trans. 1 **77**, 439 (1981).
[6]J. A. Beattie, R. J. Barriault, and J. S. Brierley, J. Chem. Phys. **19**, 1222 (1951).
[7]J. A. Beattie, J. S. Brierley, and R. J. Barriault, J. Chem. Phys. **20**, 1615 (1952).
[8]P. J. Bendt, Phys. Rev. **110**, 85 (1958).
[9]A. L. Blancett, K. R. Hall, and F. B. Canfield, Physica **47**, 75 (1970).
[10]M. E. Boyd, S. Y. Larsen, and H. Plumb, J. Res. Natl. Bur. Stand. Sect. A **72**, 155 (1968).
*[11]J. Brewer, Air Force Office of Scientific Research Department No. 67-2795, 1967. J. Brewer and G. W. Vaughn, J. Chem. Phys. **50**, 2960 (1969).
[12]M. A. Byrne, M. R. Jones, and L. A. K. Staveley, Trans. Faraday Soc. **64**, 1747 (1968).
*[13]P. J. Carson and P. J. Dunlop, Chem. Phys. Lett. **14**, 377 (1972).
*[14]P. J. Carson, P. J. Dunlop, and T. N. Bell, J. Chem. Phys. **56**, 531 (1972).
*[15]P. J. Carson, M. A. Yabsley, and P. J. Dunlop, Chem. Phys. Lett. **15**, 436 (1972).
[16]A. G. Clarke and E. B. Smith, J. Chem. Phys. **48**, 3988 (1968).
[17]A. G. Clarke and E. B. Smith, J. Chem. Phys. **51**, 4156 (1969).
[18]A. A. Clifford, R. Fleeter, J. Kestin, and W. A. Wakeham, Physica **98A**, 467 (1979).
[19]R. W. Crain, Jr. and R. E. Sonntag, Adv. Cryog. Eng. **11**, 379 (1966).
[20]C. A. Crommelin, J. P. Martinez, and H. Kamerlingh Onnes, Commun. Phys. Lab. Univ. Leiden **154a**, 1 (1919).
[21]R. A. Dawe and E. B. Smith, J. Chem. Phys. **52**, 693 (1970).
[22]C. A. N. de Castro and H. M. Roder, J. Res. Natl. Bur. Stand. **86**, 293 (1981).
[23]M. DePaz, M. Turi, and M. L. Klein, Physica **36**, 127 (1967).
[24]D. D. Dillard, M. Waxman, and R. L. Robinson, Jr., J. Chem. Eng. Data **23**, 269 (1978).
[25]G. A. DuBro and S. Weissman, Phys. Fluids **13**, 2682 (1970).
*[26]J. H. Dymond and E. B. Smith, *The Virial Coefficients of Gases* (Oxford University, London, 1969). See also new edition, 1980.
[27]K. Fokkens, W. Vermeer, K. W. Taconis, and R. DeBruyn Ouboter, Physica **30**, 2153 (1964).
[28]M. Goldblatt, F. A. Guevara, B. B. McInteer, Phys. Fluids **13**, 2873 (1970).
[29]M. Goldblatt and W. E. Wageman, Phys. Fluids **14**, 1024 (1971).
*[30]D. W. Gough, G. P. Matthews, and E. B. Smith, J. Chem. Soc. Faraday Trans. 1 **72**, 645 (1976).
[31]J. A. Gracki, G. P. Flynn, and J. Ross, J. Chem. Phys. **51**, 3856 (1969).
[32]K. E. Grew, Proc. R. Soc. London Ser. A **189**, 402 (1947).
[33]K. E. Grew and W. A. Wakeham, J. Phys. B **4**, 1548 (1971).
[34]K. E. Grew and W. A. Wakeham, J. Phys. B **11**, 2045 (1978).
[35]F. A. Guevara, B. B. McInteer, and W. E. Wageman, Phys. Fluids **12**, 2493 (1969).
[36]F. A. Guevara and G. Stensland, Phys. Fluids **14**, 746 (1971).
[37]J. W. Haarman, AIP Conf. Proc. **11**, 193 (1973).
[38]K. R. Hall and F. B. Canfield, Physica **47**, 219 (1970).
[39]J. M. Hellemans, J. Kestin, and S. T. Ro, Physica **71**, 1 (1974).
[40]D. Heymann and J. Kistemaker, Physica **25**, 556 (1959).
*[41]W. Hogervorst, Physica **51**, 59 (1971).
[42]L. Holborn and J. Otto, Z. Phys. **33**, 1 (1925).
[43]L. Holborn and J. Otto, Z. Phys. **38**, 359 (1926).
[44]A. E. Hoover, F. B. Canfield, R. Kobayashi, and T. W. Leland, Jr., J. Chem. Eng. Data **9**, 568 (1964).
[45]A. E. Humphreys and E. A. Mason, Phys. Fluids **13**, 65 (1970).
[46]H. Iwasaki and J. Kestin, Physica **29**, 1345 (1963).
*[47]A. S. Kalelkar and J. Kestin, J. Chem. Phys. **52**, 4248 (1970).
[48]N. K. Kalfoglou and J. G. Miller, J. Phys. Chem. **71**, 1256 (1967).
[49]W. H. Keesom and W. K. Walstra, Physica **13**, 225 (1947).
[50]W. E. Keller, Phys. Rev. **97**, 1 (1955).
[51]W. E. Keller, Phys. Rev. **98**, 1571 (1955).

[52]J. Kestin, H. E. Khalifa, and W. A. Wakeham, J. Chem. Phys. **67**, 4254 (1977).
*[53]J. Kestin, H. E. Khalifa, and W. A. Wakeham, Physica **90A**, 215 (1978).
[54]J. Kestin, Y. Kobayashi, and R. T. Wood, Physica **32**, 1065 (1966).
[55]J. Kestin and W. Leidenfrost, Physica **25**, 1033 (1959).
[56]J. Kestin, R. Paul, A. A. Clifford, and W. A. Wakeham, Physica **100A**, 349 (1980).
*[57]J. Kestin, S. T. Ro, and W. A. Wakeham, J. Chem. Phys. **56**, 4086 (1972).
*[58]J. Kestin, S. T. Ro, and W. A. Wakeham, J. Chem. Phys. **56**, 4119 (1972).
*[59]J. Kestin, S. T. Ro, and W. A. Wakeham, J. Chem. Phys. **56**, 5837 (1972).
*[60]J. Kestin, W. A. Wakeham, and K. Watanabe, J. Chem. Phys. **53**, 3773 (1970).
[61]J. Kestin and J. H. Whitelaw, Physica **29**, 335 (1963).
[62]P. S. Ku and B. F. Dodge, J. Chem. Eng. Data **12**, 158 (1967).
*[63]G. C. Maitland and E. B. Smith, J. Chem. Soc. Faraday Trans. 1 **70**, 1191 (1974).
[64]A. Michels, J. M. Levelt, and W. de Graaf, Physica **24**, 659 (1958).
[65]A. Michels, T. Wassenaar, and P. Louwerse, Physica **20**, 99 (1954).
[66]A. Michels, T. Wassenaar, and P. Louwerse, Physica **26**, 539 (1960).
[67]A. Michels, H. Wijker, and H. K Wijker, Physica **15**, 627 (1949).
[68]A. Michels and H. Wouters, Physica **8**, 923 (1941).
[69]G. A. Nicholson and W. G. Schneider, Can. J. Chem. **33**, 589 (1955).
[70]R. Paul, A. J. Howard, and W. W. Watson, J. Chem. Phys. **43**, 1622 (1965).
[71]W. C. Pfefferle, Jr., J. A. Goff, and J. G. Miller, J. Chem. Phys. **23**, 509 (1955).
[72]R. A. H. Pool, G. Saville, T. M. Herrington, B. D. C. Shields, and L. A. K. Staveley, Trans. Faraday Soc. **58**, 1692 (1962).
[73]G. A. Pope, P. S. Chappelear, and R. Kobayashi, J. Chem. Phys. **59**, 423 (1973).
[74]J. A. Provine and F. B. Canfield, Physica **52**, 79 (1971).
[75]*Thermophysical Properties of Neon, Argon, Krypton, and Xenon*, edited by V. A. Rabinovich (Izd. Standartov, Moscow, 1976).
[76]H. P. Rentschler and B. Schramm, Ber. Bunsenges. Phys. Chem. **81**, 319 (1977).
[77]W. M. Rutherford, J. Chem. Phys. **54**, 4542 (1971).
[78]W. M. Rutherford, J. Chem. Phys. **58**, 1613 (1973).
[79]C. M. Santamaria, J. M. Savirón, and J. C. Yarza, Physica **78**, 165 (1974).
[80]W. G. Schneider and J. A. H. Duffie, J. Chem. Phys. **17**, 751 (1949).
[81]B. Schramm, H. Schmiedel, R. Gehrmann, and R. Bartl, Ber. Bunsenges. Phys. Chem. **81**, 316 (1977).
*[82]I. R. Shankland and P. J. Dunlop, Physica **100A**, 64 (1980).
[83]I. H. Silberberg, K. A. Kobe, and J. J. McKetta, J. Chem. Eng. Data **4**, 314 (1959).
*[84]G. R. Staker and P. J. Dunlop, Chem. Phys. Lett. **42**, 419 (1976).
*[85]G. R. Staker, M. A. Yabsley, J. M. Symons, and P. J. Dunlop, J. Chem. Soc. Faraday Trans. 1 **70**, 825 (1974).
[86]L. Stroud, J. E. Miller, and L. W. Brandt, J. Chem. Eng. Data **5**, 51 (1960).
[87]C. C. Tanner and I. Masson, Proc. R. Soc. London Ser. A **126**, 268 (1930).
[88]W. L. Taylor, J. Chem. Phys. **58**, 834 (1973).
[89]W. L. Taylor, J. Chem. Phys. **62**, 3837 (1975).
[90]W. L. Taylor, J. Chem. Phys. **64**, 3344 (1976).
[91]W. L. Taylor, J. Chem. Phys. **72**, 4973 (1980).
[92]W. L. Taylor and S. Weissman, J. Chem. Phys. **55**, 4000 (1971).
[93]W. L. Taylor and S. Weissman, J. Chem. Phys. **59**, 1190 (1973).
[94]W. L. Taylor, S. Weissman, W. J. Haubach, and P. T. Pickett, J. Chem. Phys. **50**, 4886 (1969).
[95]W. L. Taylor and S. Weissman, J. Chem. Phys. **60**, 3684 (1974).
[96]N. J. Trappeniers, T. Wassenaar, and G. J. Wolkers, Physica **32**, 1503 (1966).
[97]J. B. Ubbink and W. J. de Haas, Physica **10**, 465 (1943).
[98]F. P. G. A. J. van Agt and H. Kamerlingh Onnes, Commun. Phys. Lab. Univ. Leiden **176 b**, 13 (1925).
*[99]R. J. J. van Heijningen, J. P. Harpe, and J. J. M. Beenakker, Physica **38**, 1 (1968).
[100]H. F. Vugts, A. J. H. Boerboom, and J. Los, Physica **44**, 219 (1969).
[101]W. W. Watson, A. J. Howard, N. E. Miller, and R. M. Shiffrin, Z. Naturforsch. **18a**, 242 (1963).
[102]R. D. Weir, I. W. Jones, J. S. Rowlinson, and G. Saville, Trans. Faraday Soc. **63**, 1320 (1967).
[103]S. Weissman, Phys. Fluids **16**, 1425 (1973).
[104]S. Weissman and G. A. DuBro, Phys. Fluids **13**, 2689 (1970).
[105]E. Whalley, Y. Lupien, and W. G. Schneider, Can. J. Chem. **31**, 722 (1953).
[106]E. Whalley, Y. Lupien, and W. G. Schneider, Can. J. Chem. **33**, 633 (1955).
[107]E. Whalley and W. G. Schneider, Trans. Am. Soc. Mech. Eng. **76**, 1001 (1954).
[108]D. White, T. Rubin, P. Camky, and H. L. Johnston, J. Phys. Chem. **64**, 1607 (1960).
[109]R. J. Wintonsky and J. G. Miller, J. Am. Chem. Soc. **85**, 282 (1963).
*[110]M. A. Yabsley and P. J. Dunlop, Phys. Lett. A **38**, 247 (1972).
*[111]M. A. Yabsley and P. J. Dunlop, Physica **85A**, 160 (1976).
[112]J. L. Yntema and W. G. Schneider, J. Chem. Phys. **18**, 641 (1950).